

Modeling of cloud microphysics: from simple concepts to sophisticated parameterizations

Part I (warm-rain microphysics)

Wojciech Grabowski

National Center for Atmospheric Research, Boulder, Colorado

**Earth
in visible light**

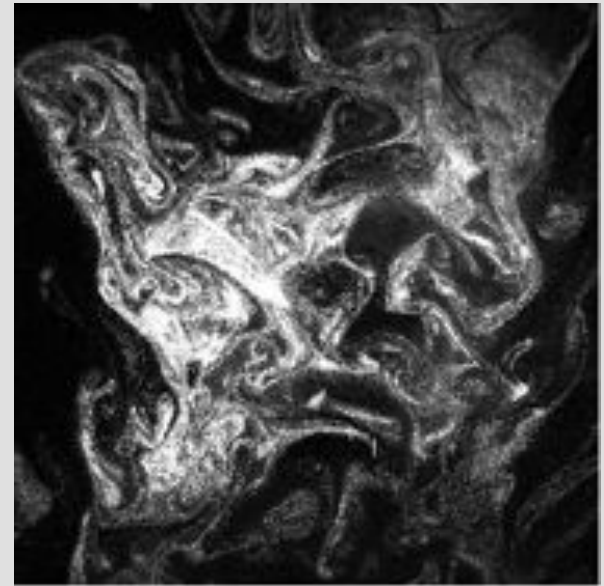


H
1,000 km

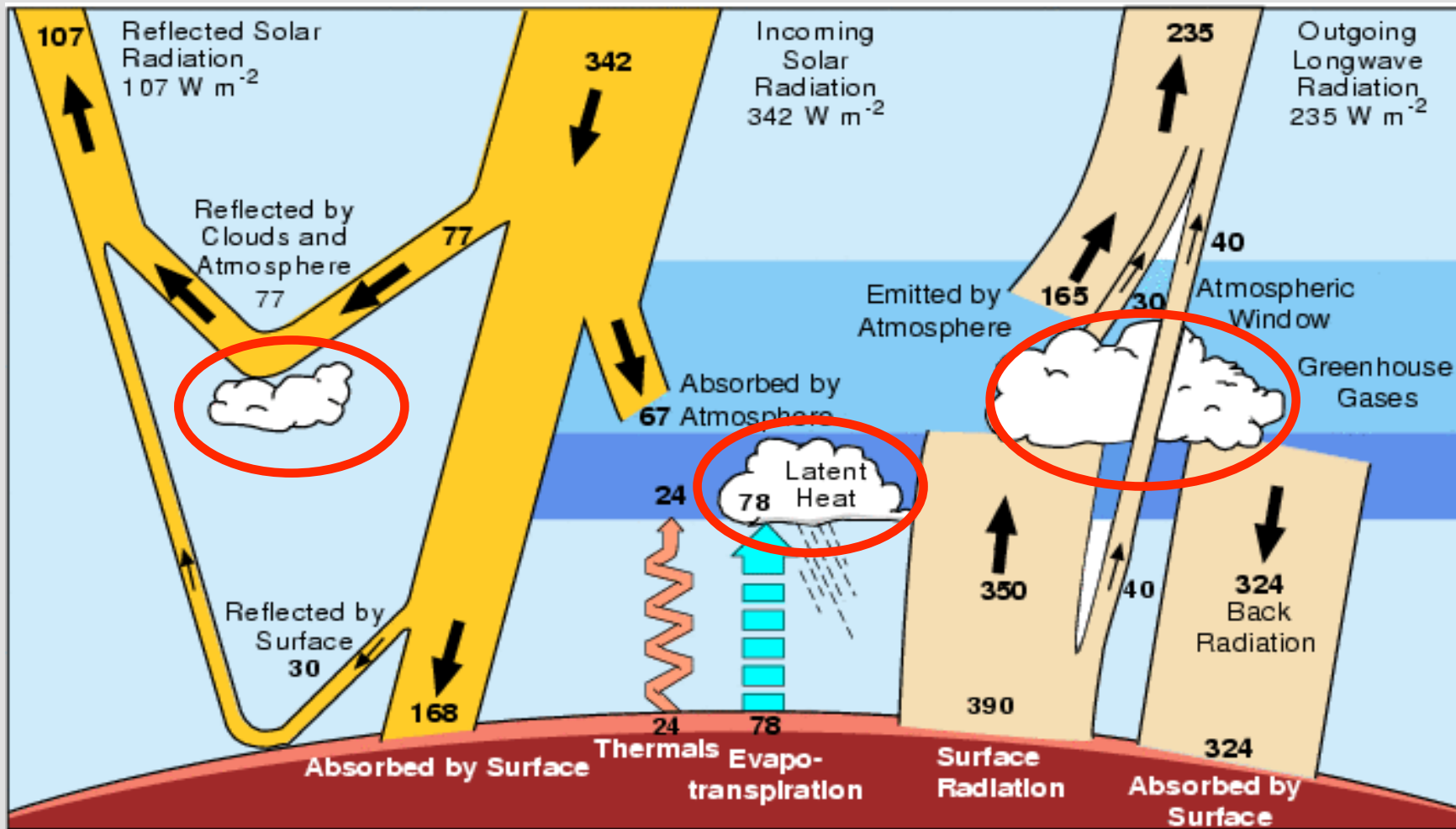
**Small cumulus
clouds**



**Mixing in laboratory
cloud chamber**



H
10 cm



Kiehl and Trenberth 1997

The Earth annual and global mean energy budget

Clouds form when the air reaches saturation (water saturation for warm clouds).

This is typically because of the vertical motion within the atmosphere.



**small Cumulus humilis clouds only
mark tops of boundary-layer eddies...**



**deeper Cumulus (mediocris or congestus)
clouds have life (dynamics) of their own...**

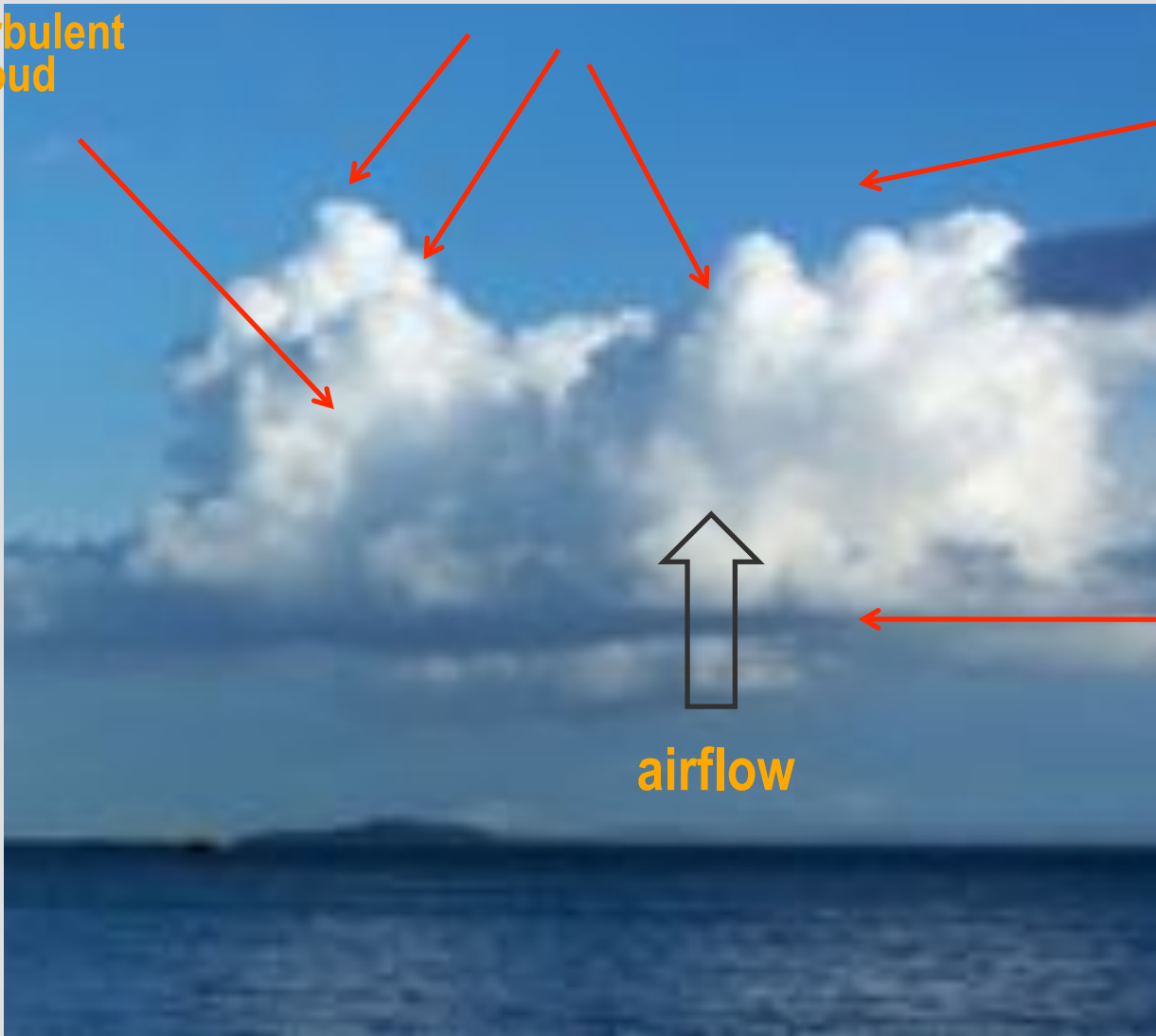
**interfacial
instabilities**

**turbulent
cloud**

**calm (low-
turbulence)
environment**

**cloud base
(activation of cloud
droplets)**

airflow





droplet spectra

vertical and along-track velocity

liquid water content

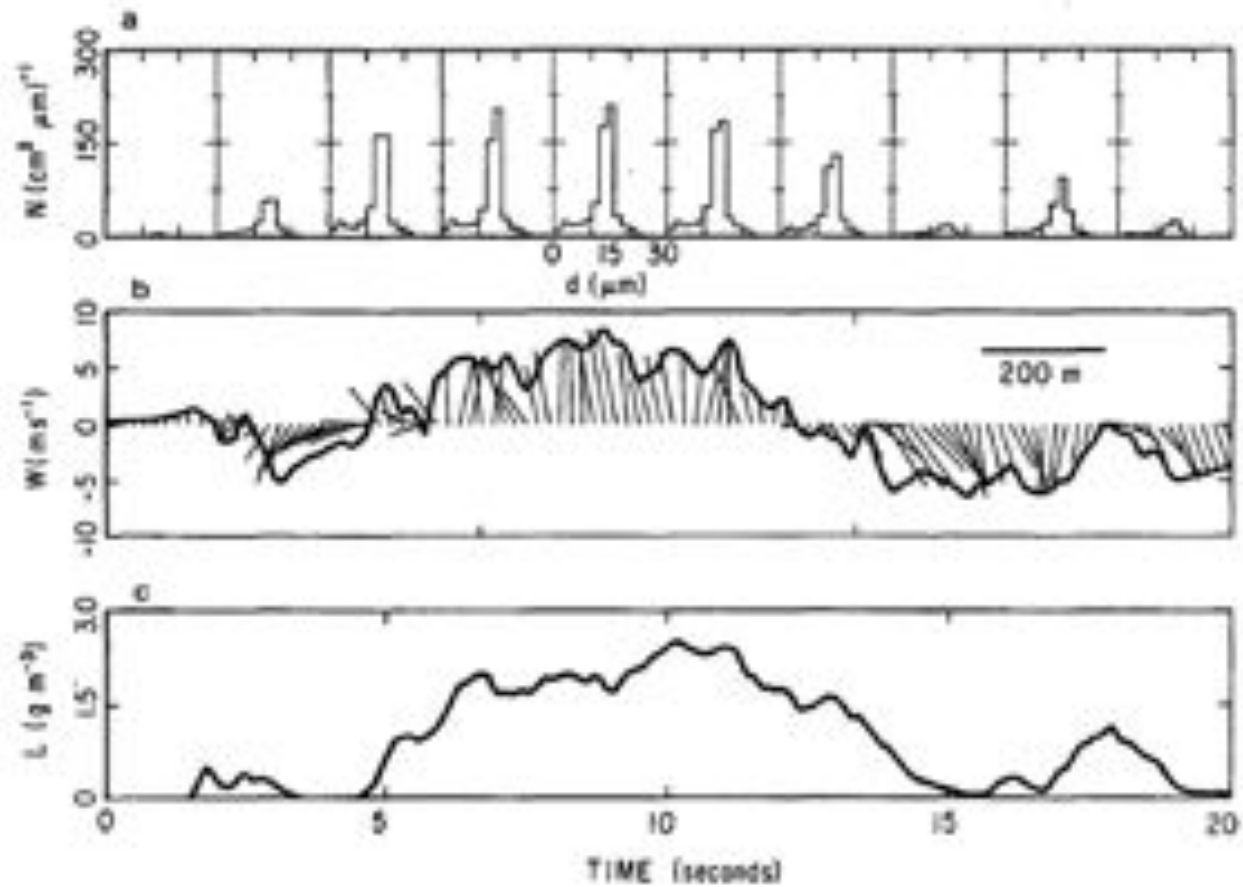


FIG. 3. Penetration at 600 mb, 6 June: (a) two-second averaged droplet spectra (sizes for diameter bins are those given by the manufacturer); (b) wind velocity, the lines represent wind vectors formed from the vertical wind and the wind along the flight path; (c) liquid water density measured by the Johnson-Williams device. All H-2 measurements.

(Austin et al. JAS 1985)

droplet spectra

vertical and along-track velocity

liquid water content

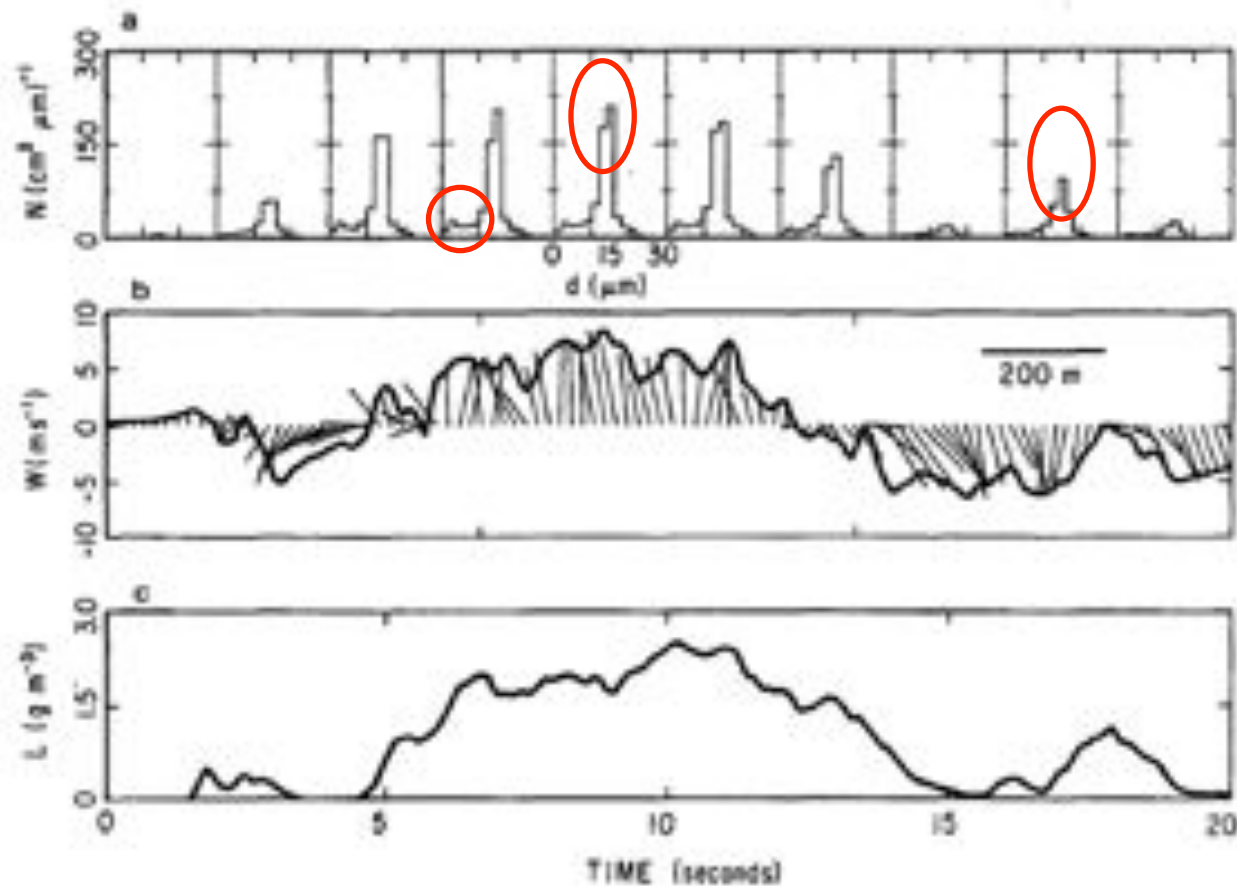


FIG. 3. Penetration at 600 mb, 6 June: (a) two-second averaged droplet spectra (sizes for diameter bins are those given by the manufacturer); (b) wind velocity, the lines represent wind vectors formed from the vertical wind and the wind along the flight path; (c) liquid water density measured by the Johnson-Williams device. All H-2 measurements.

(Austin et al. JAS 1985)

The Water Content of Cumuliform Cloud

By J. WARNER, Radiophysics Laboratory, C.S.I.R.O., Sydney

(Manuscript received April 5, 1955)

Abstract

Measurements have been made of liquid water content throughout many cumuliform clouds. The amount of water present at any level was always less than the adiabatic value, and the ratio of these two quantities decreased with height above cloud base. This ratio was found to be independent of the horizontal extent of the cloud except in the case of very small clouds. The transition between clear air and dense cloud was frequently abrupt.

I. WARNER

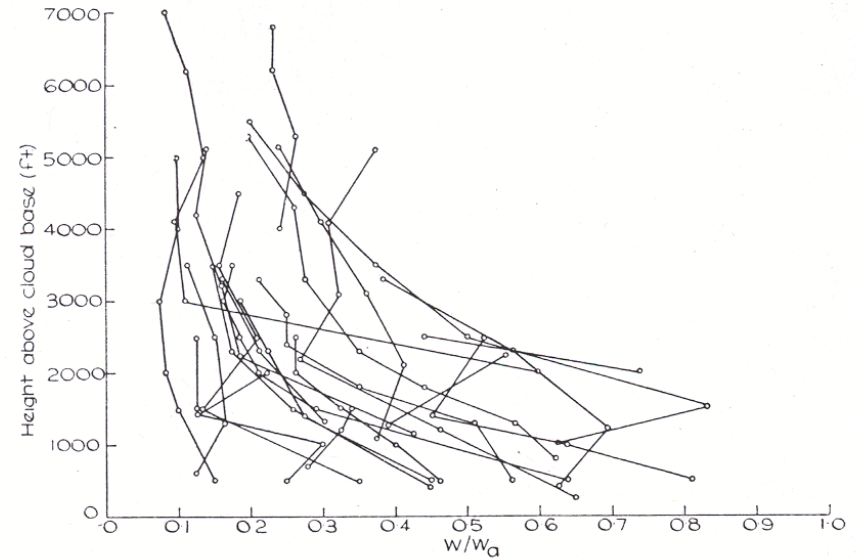


Fig. 7. Ratio of observed liquid water content to adiabatic value versus height above base.

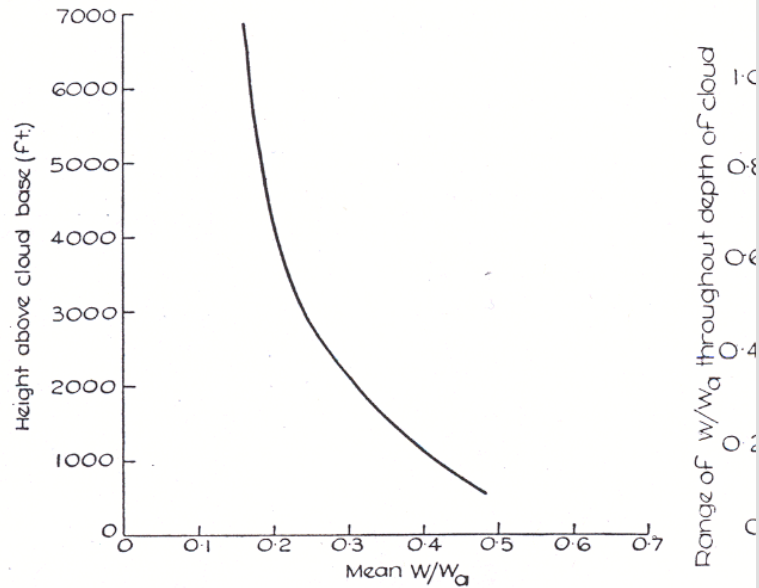


Fig. 8. Mean ratio W/W_a versus height above base.



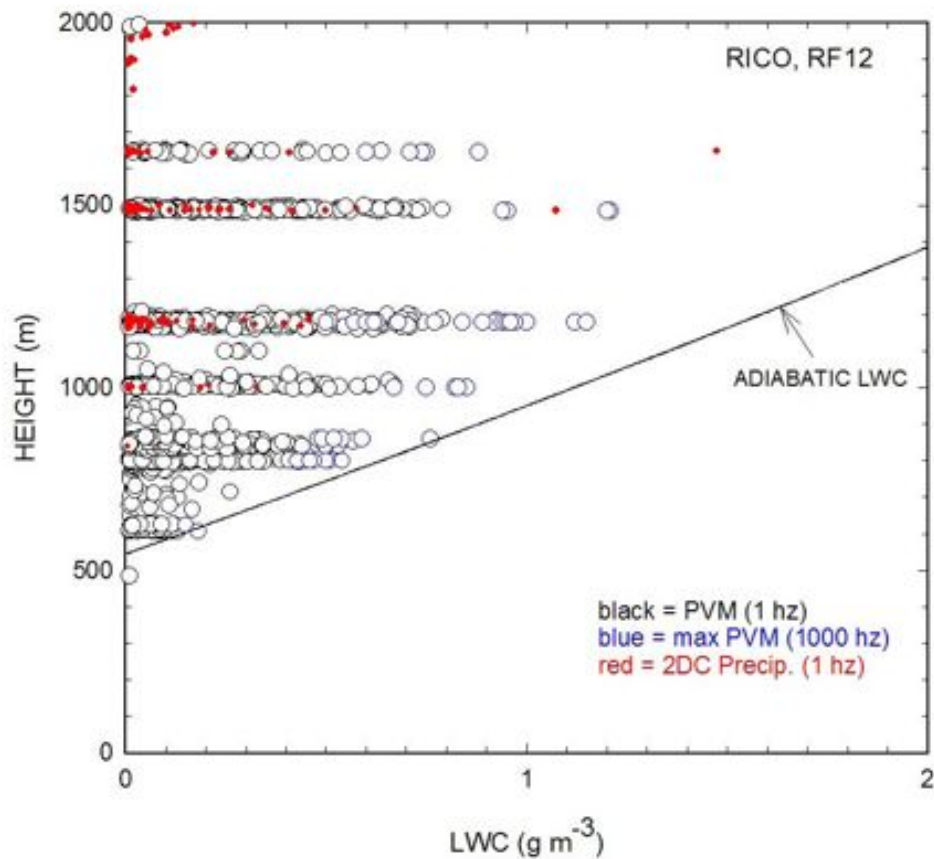


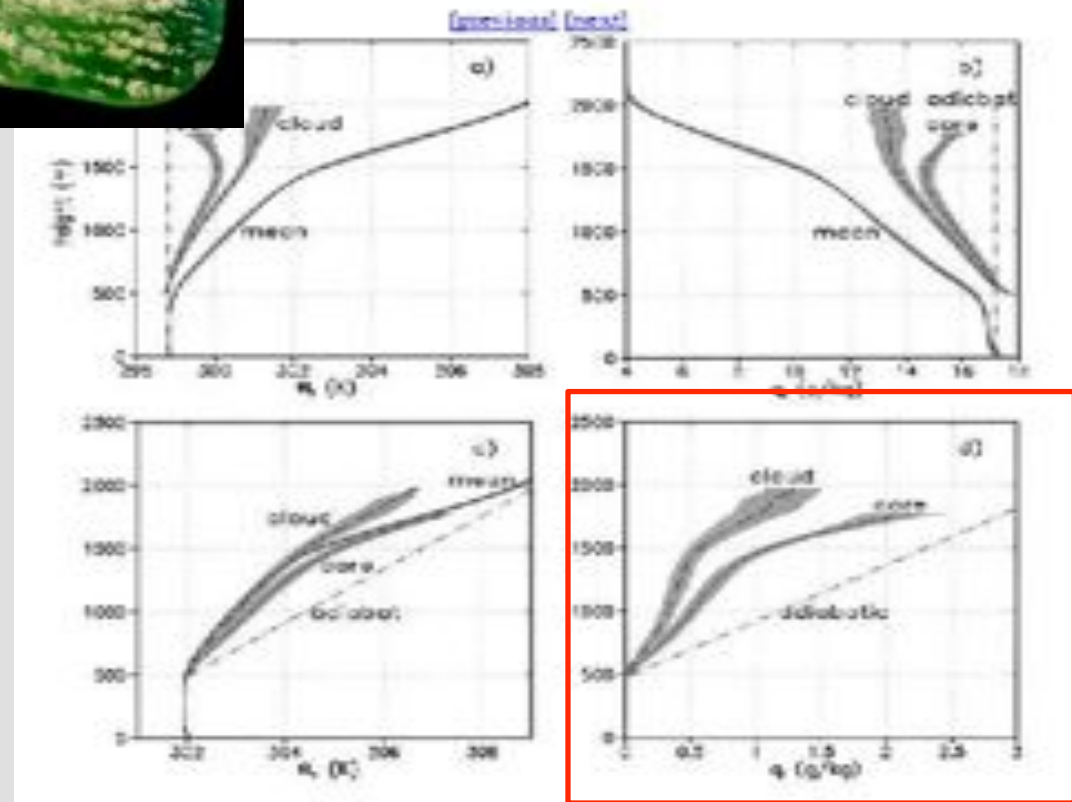
Figure 1 - 100-m resolution (1Hz), maximum 10-cm resolution (1000 Hz), and 2DC LWC for all ~ 200 Cu aircraft passes for flight RF12.



Gerber et al. (AMS Cloud Physics Conference, Madison, July 2006; published in JMSJ 2008)

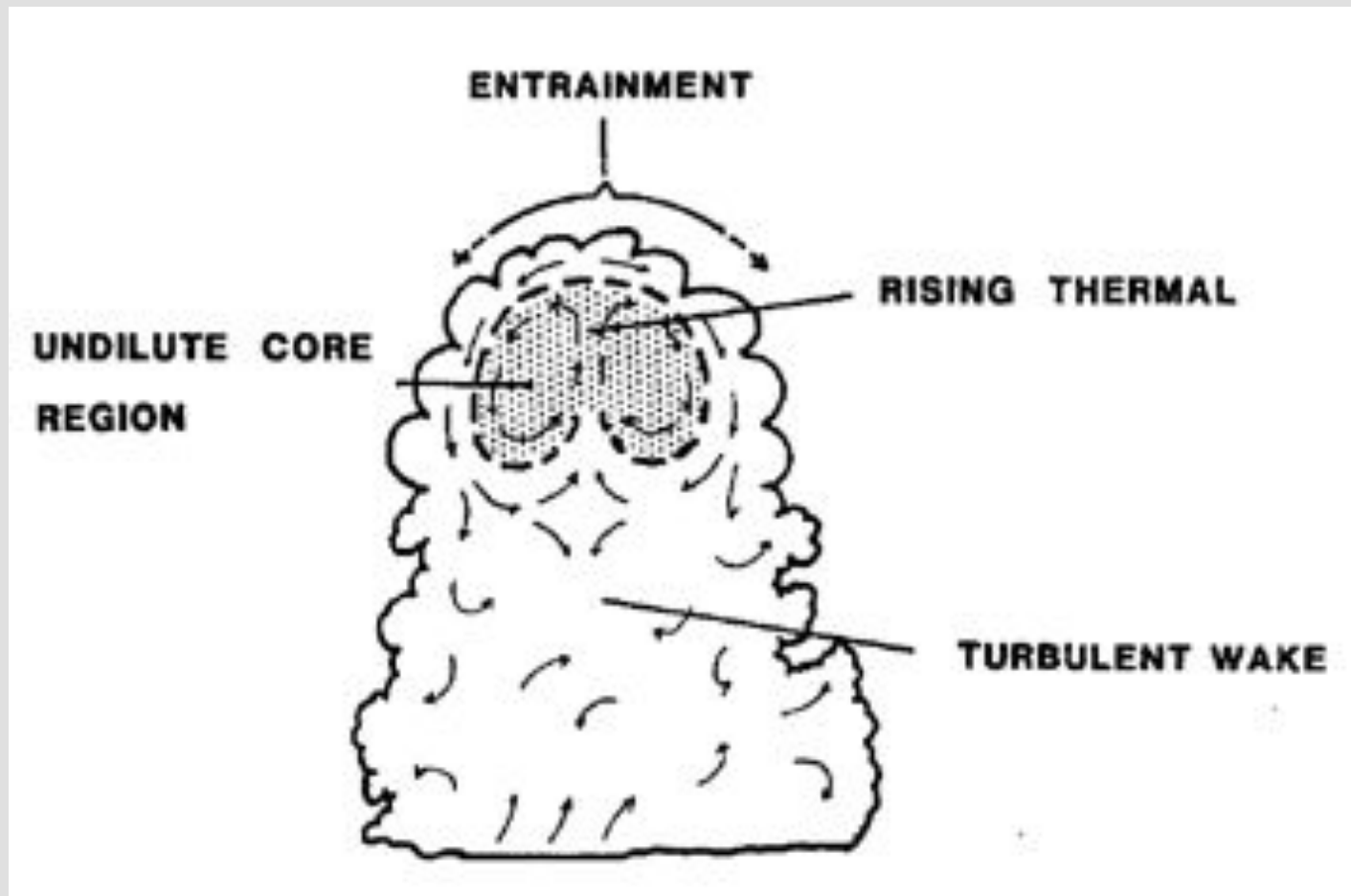
Shallow convective clouds are strongly diluted by entrainment...

Siebesma et al. JAS 2003



Turbulent entrainment is a fundamental feature of small convective clouds (and most of other clouds as well)...





Blyth et al. (JAS 1988)

Turbulent entrainment is a fundamental feature of small convective clouds (and most of other clouds as well)...

Where are these structures coming from?

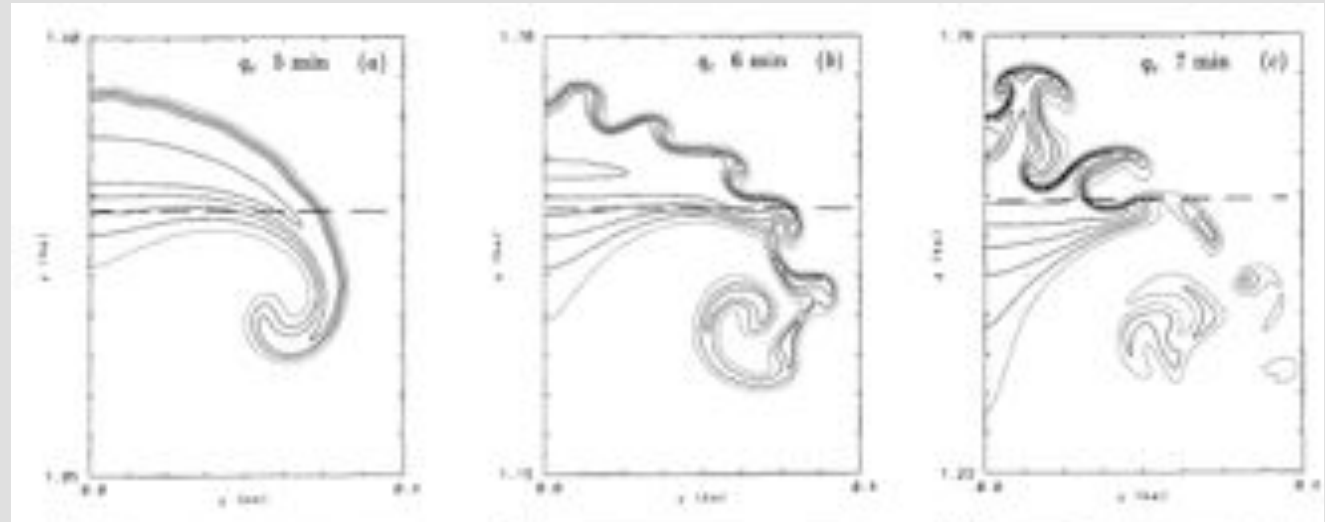


$$\text{Re} = UL/\nu \sim 10^7$$

$$U \sim 1 \text{ m s}^{-1}$$

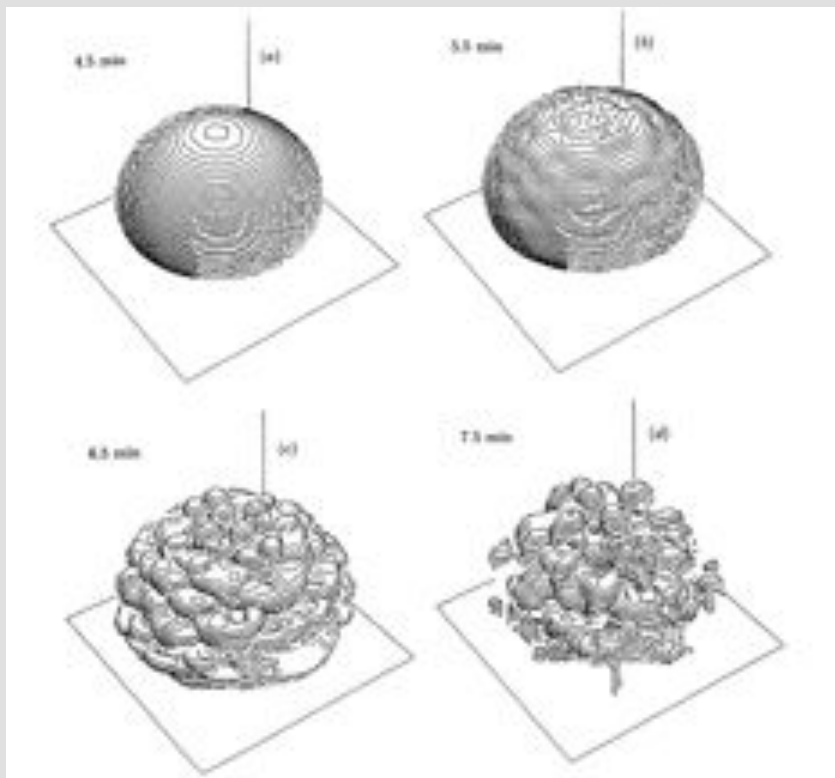
$$L \sim 100 \text{ m}$$

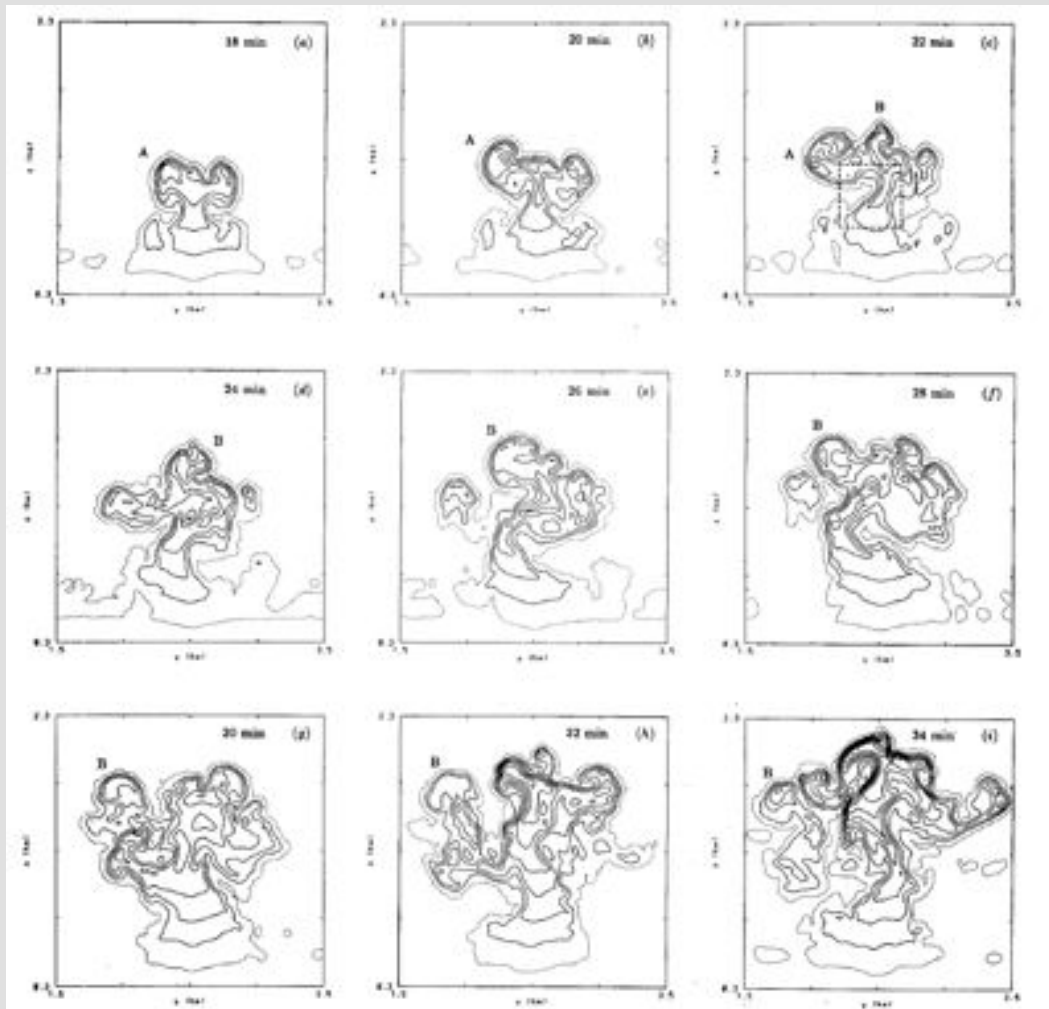
$$\nu \sim 10^{-5} \text{ m}^2 \text{ s}^{-1}$$



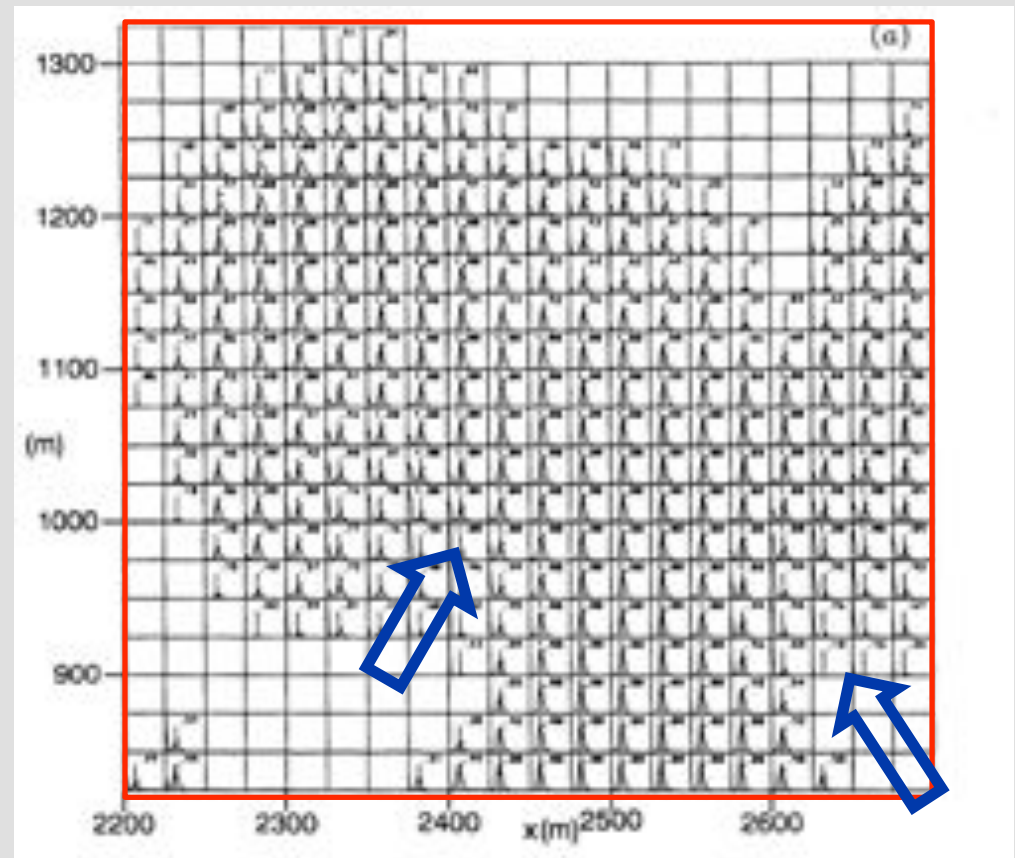
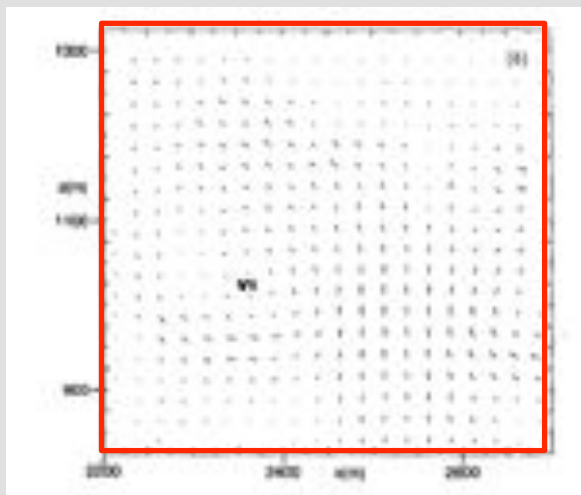
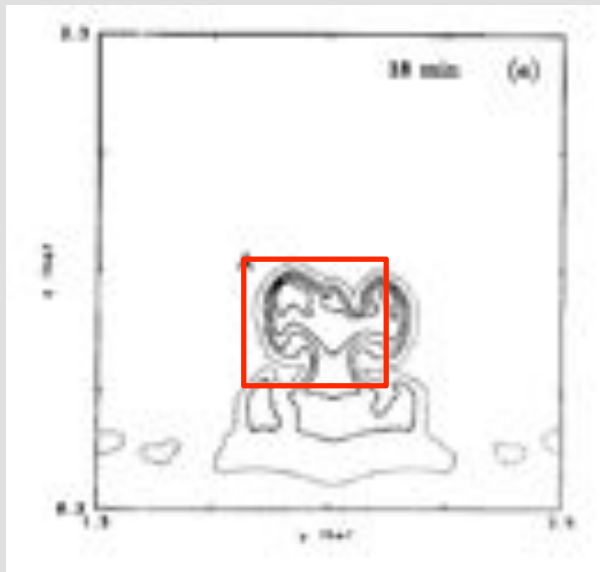
Cloud-environment interface instability

Klaassen and Clark (JAS 1984)
 Grabowski (JAS 1989)
 Grabowski and Clark (JAS 1991, 1993a, 1993b)





Brenguier and Grabowski (JAS 1993)



Brenguier and Grabowski (JAS 1993)



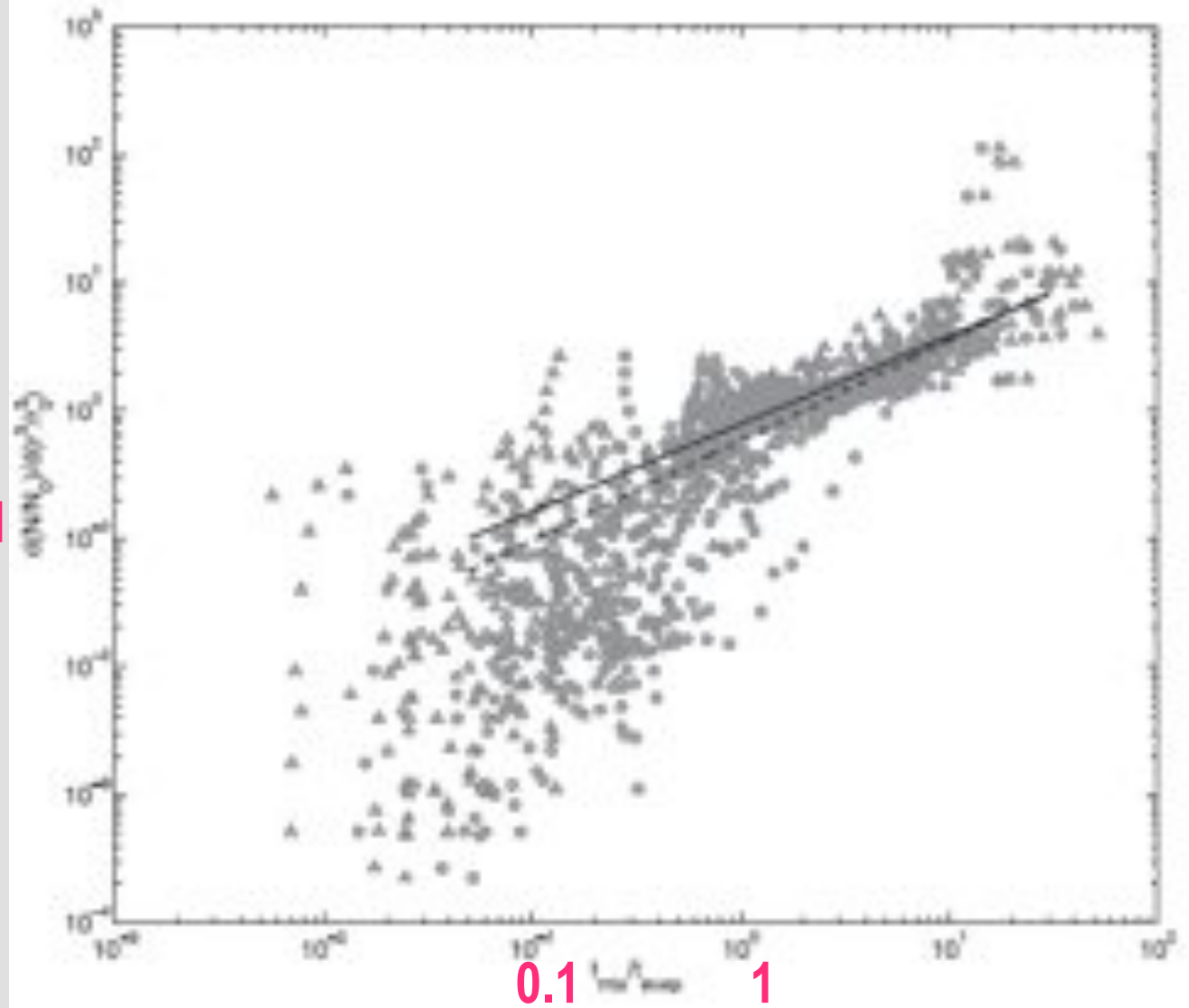
Brenguier and Grabowski (JAS 1993)

Turbulent entrainment is a fundamental feature of small convective clouds (and most of other clouds as well)...

...but its impact on the spectrum of cloud droplets is still poorly understood.



slope
10
0.1



← homogeneous

10

→ extremely inhomogeneous

$t_{\text{mix}}/t_{\text{evap}}$ (Damkholer number)

Andrejczuk et al. JAS
2009

A Large Eddy Simulation Intercomparison Study of Shallow Cumulus Convection

JAS
2003

A. PIER SIEBESMA,¹ CHRISTOPHER S. BRETHERTON,² ANDREW BROWN,² ANDREAS CHLOND,⁴ JOAN CUXART,⁶
PETER G. DUYNKERKE,^{1*} HONGLI JIANG,⁷ MARAT KHAIROUTDINOV,³ DAVID LEWELLEN,¹ CHIN-HOH MOENG,⁷
ENRIQUE SANCHEZ,³ BJORN STEVENS,¹ AND DAVID E. STEVENS^{8*}

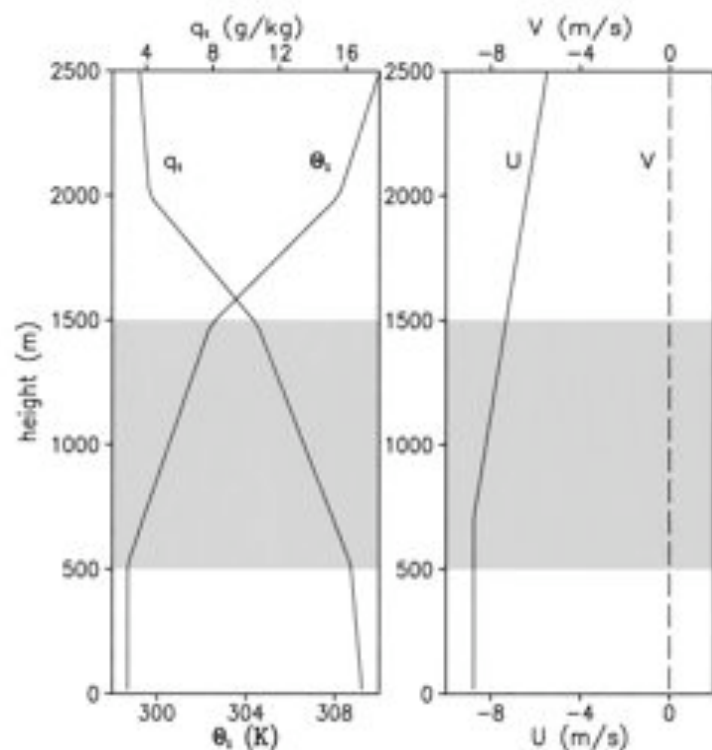
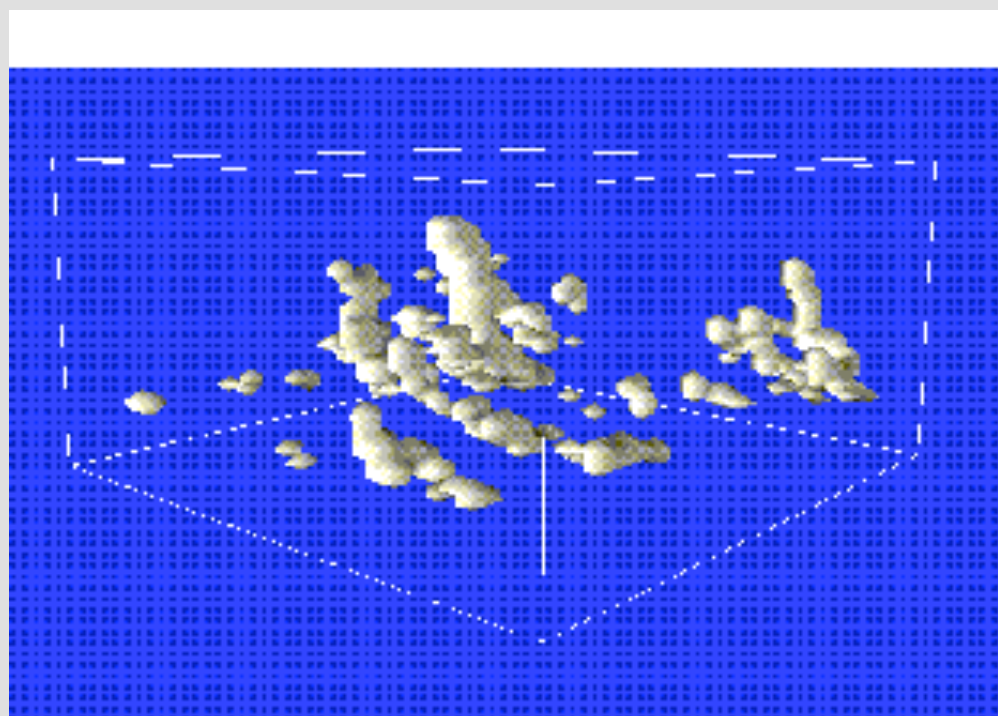
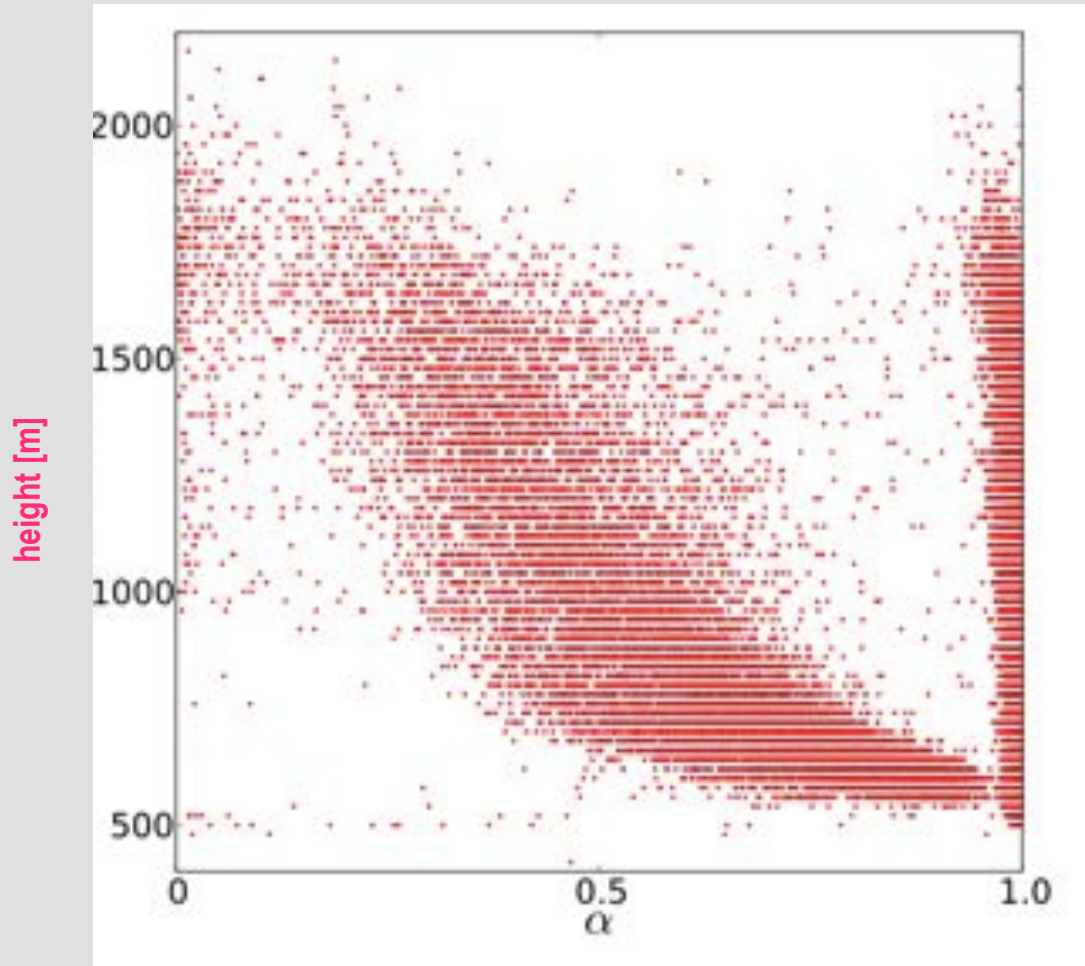


FIG. 1. Initial profiles of the total water specific humidity q_t , the liquid water potential temperature θ_l , and the horizontal wind components u and v . The shaded area denotes the conditionally unstable cloud layer.



Changes of the parameter α with height



D. Jarecka
(PhD work
in
progress)

$\alpha = 0$
homogeneous
mixing

$\alpha = 1$
extremely
inhomogeneous mixing

***Fundamentals of
(warm) cloud physics***

ELEMENTARY CLOUD PHYSICS:

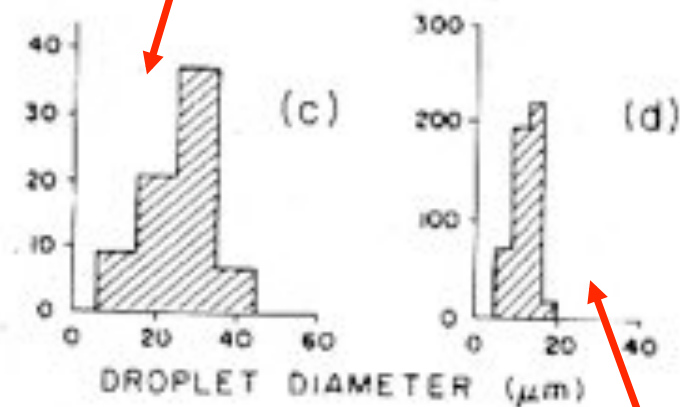
clouds form due to cooling of air (e.g., adiabatic expansion of a parcel of air rising in the atmosphere)

- *condensation*: water vapor \rightarrow cloud droplets

heterogeneous nucleation on atmospheric aerosols called Cloud Condensation Nuclei (CCN); typically highly soluble salts (sea salt, sulfates, ammonium salts, nitrates)

only a very small percentage of CCN used by clouds (i.e., water clouds form just above saturation)

Maritime cumulus



Continental cumulus

From cloud droplets and ice crystals
to precipitation:

WARM RAIN:

→ gravitational collision and coalescence between
cloud droplets

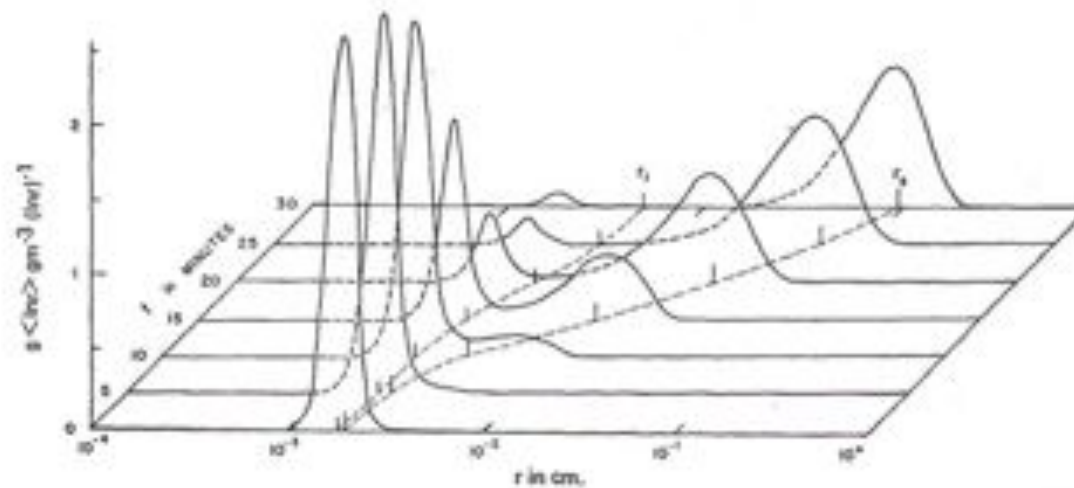


FIG. 5. Time evolution of the initial spectrum for $r_0^2 = 18 \mu\text{m}$, via $\alpha = 0.25$.

Berry and Reinhardt JAS 1974

THE DISTRIBUTION OF RAINDROPS WITH SIZE

By *J. S. Marshall and W. McK. Palmer*¹

McGill University, Montreal

(Manuscript received 26 January 1948)

$$N_D = N_0 e^{-\Delta D}$$

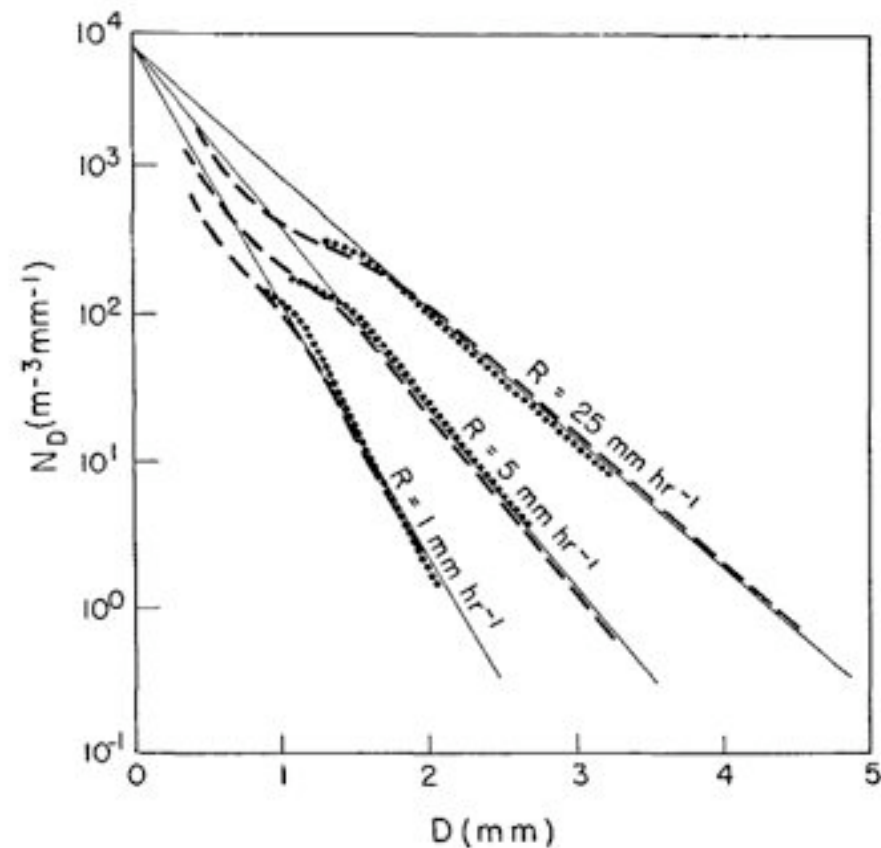


FIG. 2. Distribution function (solid straight lines) compared with results of Laws and Parsons (broken lines) and Ottawa observations (dotted lines).

Modeling moist processes in the atmosphere:

- Gas dynamics for the air with moisture (i.e., containing water vapor, suspended small cloud particles, falling larger precipitation particles);
- Thermodynamics for the air containing water vapor (i.e., phase changes, latent heating, etc).

- **Water vapor is a minor constituent:**

mass loading is typically smaller than 1%; thermodynamic properties (e.g., specific heats etc) only slightly modified;

- **Suspended small particles (cloud droplets, cloud ice):**

mass loading is typically smaller than a few tenths of 1%, particles are much smaller than the smallest scale of the flow; multiphase approach is not required, but sometimes used (e.g., DNS with suspended droplets)

- **Precipitation (raindrops, snowflakes, graupel, hail):**

mass loading can reach a few %, particles are larger than the smallest scale of the flow; multiphase approach needed only for very-small-scale modeling

Continuous medium approach: apply density as the main field variable (density of water vapor, density of cloud water, density of rainwater, etc...)

$$\frac{\partial \rho_v}{\partial t} + \nabla(\rho_v \mathbf{u}) = S \quad \text{or} \quad \frac{d\rho_v}{dt} + \rho_v \nabla \mathbf{u} = S$$

In practice, mixing ratios are typically used. Mixing ratio is the ratio between the density (of water vapor, cloud water...) and the air density.

**Mixing ratios
versus
specific
humidities...**

$$\frac{\partial \rho_a}{\partial t} + \nabla(\rho_a \mathbf{u}) = 0 \quad \text{or} \quad \frac{d\rho_a}{dt} + \rho_a \nabla \mathbf{u} = 0$$

$$\frac{\partial \rho_v}{\partial t} + \nabla(\rho_v \mathbf{u}) = S \quad \text{or} \quad \frac{d\rho_v}{dt} + \rho_v \nabla \mathbf{u} = S$$

$$\text{mixing ratio : } q = \frac{\rho_v}{\rho_a}$$

$$\frac{dq}{dt} = \frac{S}{\rho_a}$$

$$\text{specific humidity : } Q = \frac{\rho_v}{\rho_v + \rho_a}$$

$$\frac{dQ}{dt} = \frac{\rho_a}{\rho_v + \rho_a} \frac{S}{\rho_v + \rho_a}$$

Gas dynamics for the moist air:

In the spirit of the Boussinesq approximation, moisture and condensate affect gas dynamics equations only through the buoyancy term

$$\frac{d\mathbf{u}}{dt} = -\frac{1}{\rho} \nabla p - g\mathbf{k} + \dots (\text{Coriolis, turbulence, etc})$$

$$\rho = \rho_0(z) + \rho'$$

$$p = p_0(z) + p'$$

$$(\rho_0 + \rho') \frac{d\mathbf{u}}{dt} = -\frac{\partial p_0}{\partial z} - \rho_0 g - \frac{\partial p'}{\partial z} - \rho' g + \dots$$

$$\frac{d\mathbf{u}}{dt} = -\frac{1}{\rho_0} \nabla p' - g\mathbf{k} \frac{\rho'}{\rho_0} + \dots$$

For small-Mach number flows ($|\mathbf{u}| \ll c_s$; c_s - speed of sound):

$$\frac{\rho'}{\rho_0} \approx -\frac{T'}{T_0}$$

$$\frac{d\mathbf{u}}{dt} = -\frac{1}{\rho_0} \nabla p' + g\mathbf{k} \frac{T'}{T_0} + \dots$$

Density temperature T_d : the temperature dry air has to have to yield the same density as moist cloudy air

$$T_d = T \frac{1 + q/\epsilon}{1 + q + Q}$$

T - air temperature

q - water vapor mixing ratio ($\sim 10^{-3}$)

Q - condensate mixing ratio (cloud water, rain, ice, snow, etc.; $\sim 10^{-3}$)

$$\epsilon = \frac{R_d}{R_v} \approx 0.622$$

$$T_d \approx T \left[1 + \left(\frac{1}{\epsilon} - 1 \right) q - Q \right]$$

$$T_d \approx T (1 + 0.61q - Q)$$

T , q and Q –
thermodynamics
(and much more!)

Thermodynamics:

Moist air is treated as a perfect gas

Phase changes lead to the release of latent heat and formation of condensed (liquid or solid) phase of the water substance (cloud droplets, raindrops, ice crystals, snow, etc)

Condensed phase is treated as continuous medium, i.e., described as density (of cloud droplets, raindrops, etc).

First Law of Thermodynamics:

$$dq = du + p dv \quad (1)$$

dq - heat (per unit mass) added to the system

du - increase of internal energy (per unit mass)

$p dv$ - work (per unit mass) performed by the system

$$du = c_v dT, \quad pv = RT, \quad v = 1/\rho, \quad c_v + R = c_p$$

$$dq = c_p dT - \frac{RT}{p} dp \quad (2)$$

Introducing *potential temperature* as:

$$\theta = T \left(\frac{p_{\infty}}{p} \right)^{R/c_p} \quad (3)$$

where $p_{\infty} = \text{const}$ (typically 1000 mb), (1) can be written as:

$$d\theta = \frac{\theta}{c_p T} dq \quad (4)$$

$$\frac{d\theta}{dt} = \frac{\theta}{c_p T} S$$

where $S = \frac{dq}{dt}$ is the heat source per unit mass
[in $\text{J kg}^{-1} \text{s}^{-1}$]

$S = 0$ - adiabatic motions

$S \neq 0$ - motions with diabatic processes (heating due to radiative transfer, phases changes, chemical reactions, etc)

For phase changes of water substance:

$$S = L \frac{dQ}{dt}$$

where L is the latent heat (of condensation, freezing, or sublimation), and $\frac{dQ}{dt}$ is the change of corresponding water mixing ratio

If only phase changes are included, then potential temperature equation is:

$$\frac{d\theta}{dt} = \frac{L\theta}{c_p T} \frac{dq}{dt}$$

L – latent heat (of condensation, freezing, or sublimation)

$\frac{dq}{dt}$ – change of corresponding condensate mixing ratio

Modeling of cloud microphysics: solving a system of PDEs (advection/diffusion type) coupled through the source terms:

$$\frac{d\theta}{dt} = S_\theta$$

$$\frac{dq_v}{dt} = S_{q_v}$$

for $i = 1, N$:

$$\frac{dq_c^{(i)}}{dt} = S^{(i)}$$

θ - potential temperature

q_v - water vapor mixing ratio

$q_c^{(i)}$ - condensed water mixing ratios

$S^{(i)}$ - sources/sinks for condensed water (phase changes, transfer from one category to another, sedimentation, etc.)

***Modeling of warm-
rain microphysics***

BULK MODEL OF CONDENSATION:

$$\frac{d\theta}{dt} = \frac{L_v \theta}{c_p T} C_d$$

$$\frac{dq_v}{dt} = -C_d$$

$$\frac{dq_c}{dt} = C_d$$

θ - potential temperature

q_v - water vapor mixing ratio

q_c - cloud water mixing ratio

L_v - latent heat of condensation/evaporation

C_d - condensation rate

Note: θ/T function of pressure only ($\approx \theta_o/T_o$)

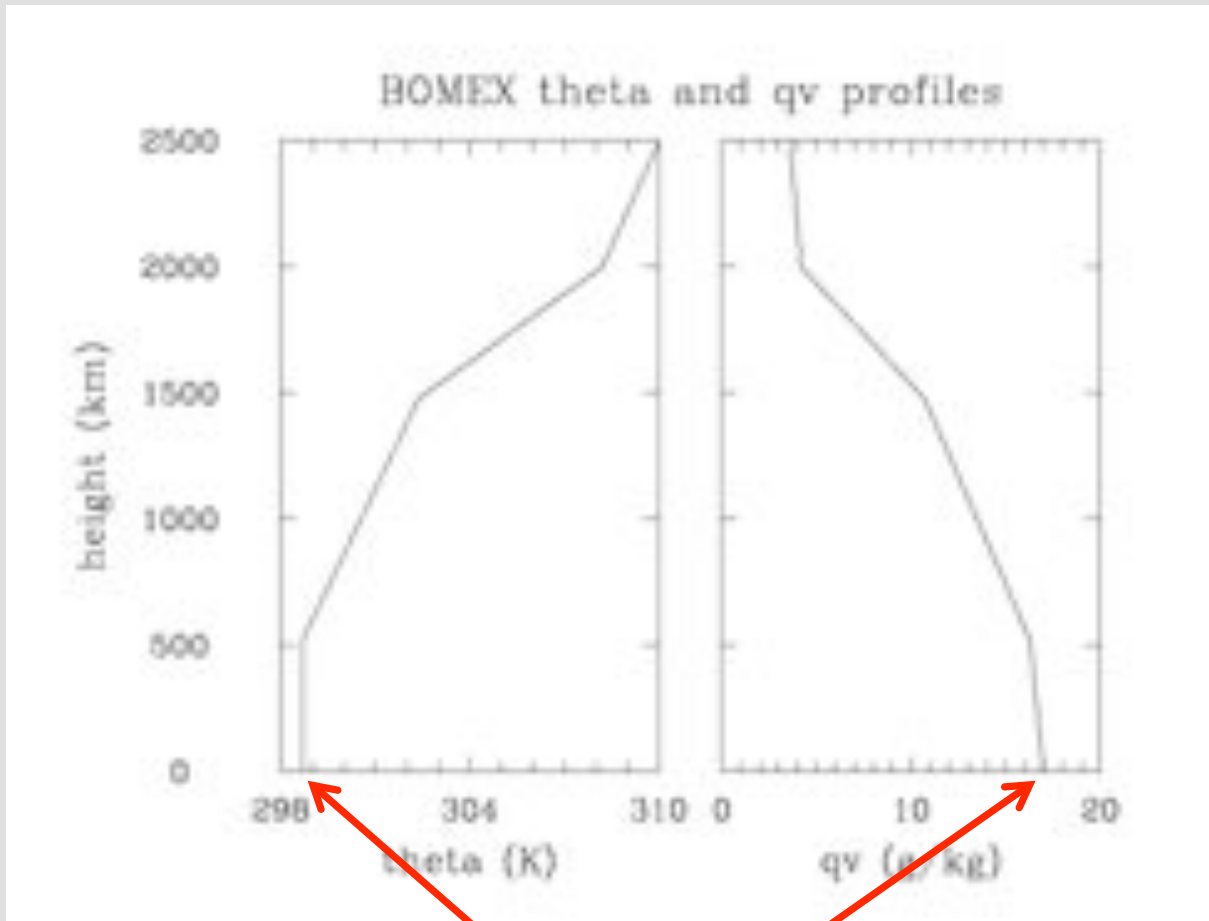
C_d is defined such that cloud is always at saturation, which is a very good approximation:

$$q_c = 0 \quad \text{if} \quad q_v < q_{vs}$$

$$q_c > 0 \quad \text{only if} \quad q_v = q_{vs}$$

where $q_{vs}(p, T) \approx 0.622 \frac{e_s(T)}{p}$ is the water vapor mixing ratio at saturation

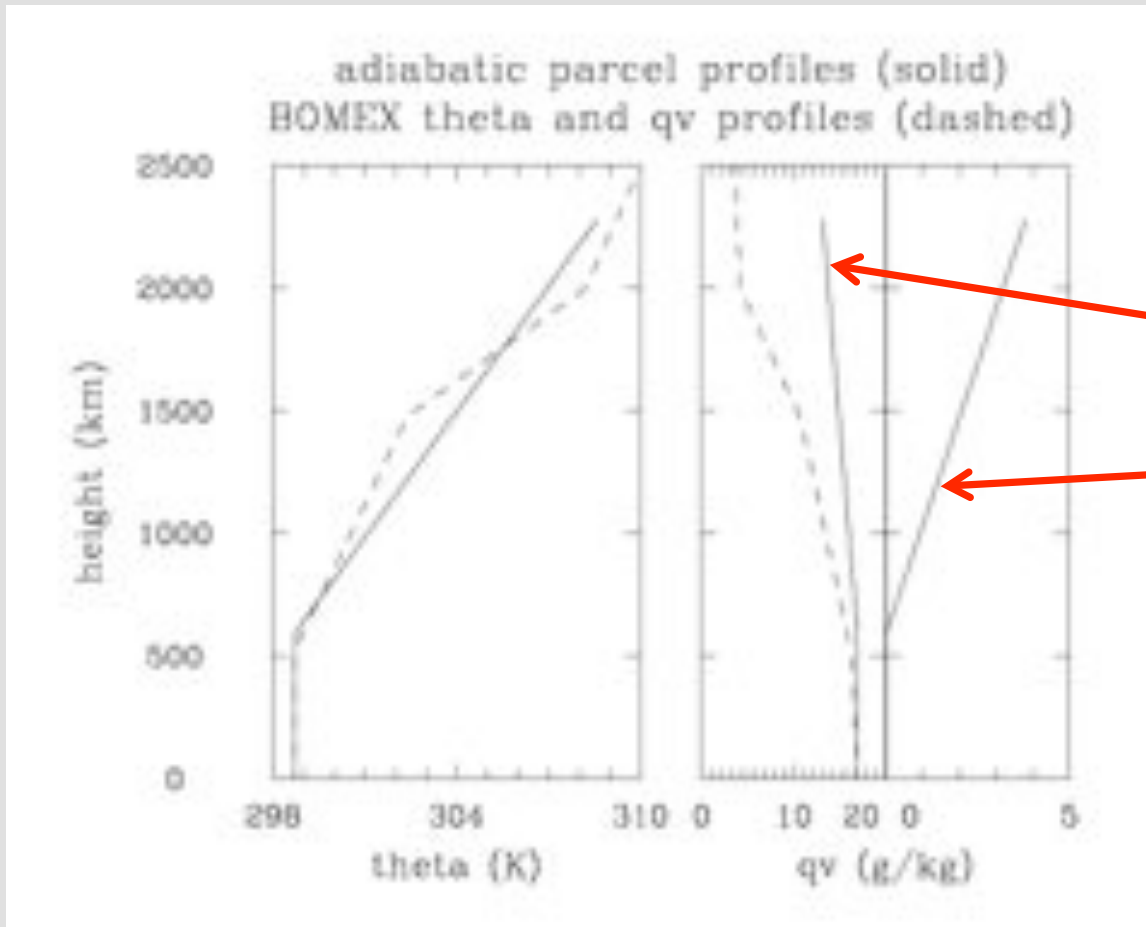
A very simple (but useful) model: rising adiabatic parcel...



Take a parcel
from the surface
and move it up...

$$\frac{d\theta}{dt} = \frac{L_v \theta}{c_p T} C_d$$
$$\frac{dq_v}{dt} = -C_d$$
$$\frac{dq_c}{dt} = C_d$$

... by solving
these equations.



Look not only on the patterns (i.e., processes), but also on specific numbers (e.g., temperature change, mixing ratios, etc).

**Invariant
variables:**

total water,

**liquid water
potential
temperature,**

**equivalent
potential
temperature.**

If $\bar{\theta}/\bar{T} = \text{const}$ (shallow convection approximation)

$$\frac{d\theta}{dt} = \frac{L_v \bar{\theta}}{c_p \bar{T}} C_d$$

$$\frac{dq_v}{dt} = -C_d$$

$$\frac{dq_c}{dt} = C_d$$

can be converted into:

$$\frac{d\theta_I}{dt} = 0$$

$$\frac{dQ}{dt} = 0$$

θ_I is one of the two:

$$\theta_c = \theta + \frac{L_v \bar{\theta}}{c_p \bar{T}} q_v - \text{equivalent potential temperature}$$

$$\theta_l = \theta - \frac{L_v \bar{\theta}}{c_p \bar{T}} q_c - \text{liquid water potential temperature}$$

$$Q = q_v + q_c - \text{total water mixing ratio}$$

Adding rain or drizzle:

WARM RAIN BULK MODEL (Kessler 1969):

$$\frac{d\theta}{dt} = \frac{L_v \theta}{c_p T} (C_d - EVAP)$$

$$\frac{dq_v}{dt} = -C_d + EVAP$$

$$\frac{dq_c}{dt} = C_d - AUT - ACC$$

$$\frac{dq_r}{dt} = \frac{1}{\rho} \frac{\partial}{\partial z} (\rho q_r v_t) + AUT + ACC - EVAP$$

θ - potential temperature

q_v - water vapor mixing ratio

q_c - cloud water mixing ratio

q_r - rain water mixing ratio

C_d - condensation rate

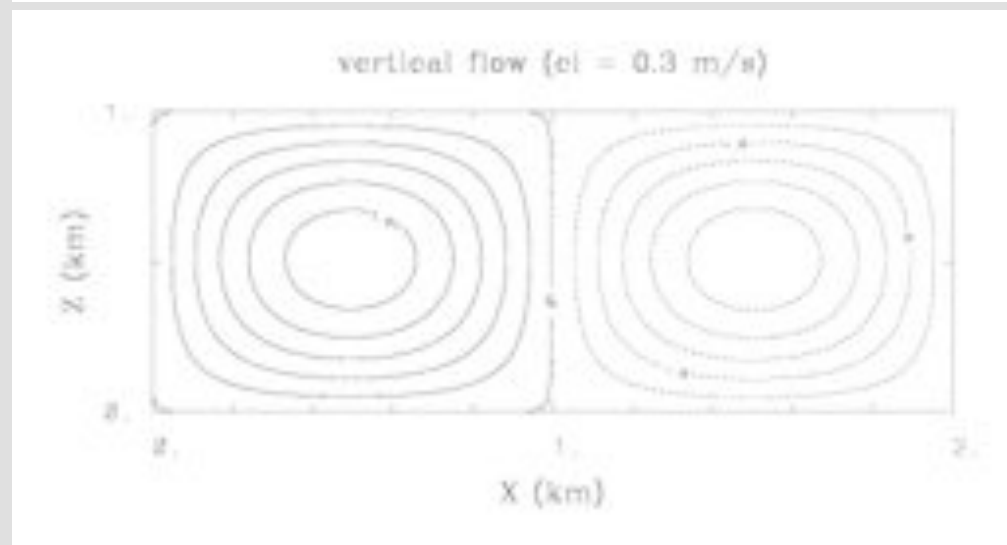
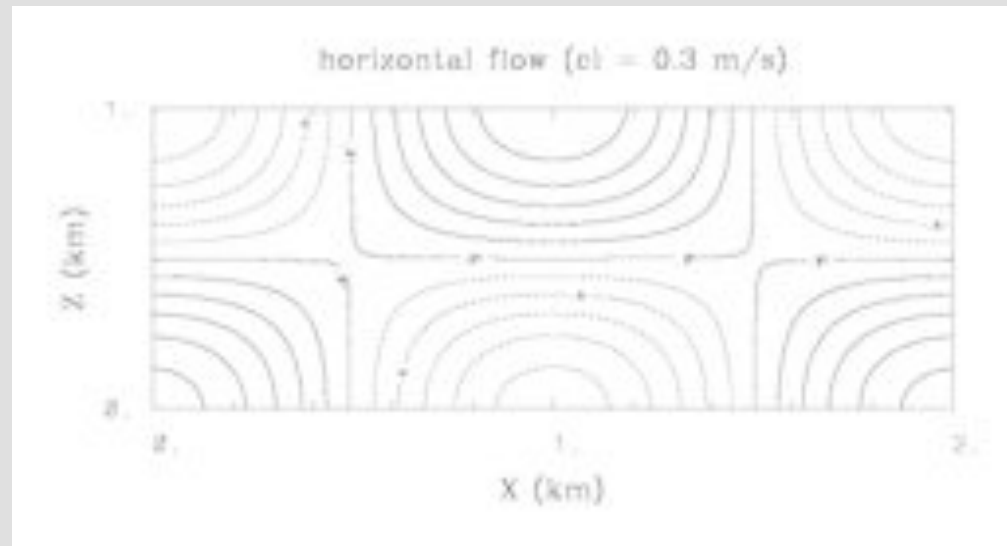
$EVAP$ - rain evaporation rate

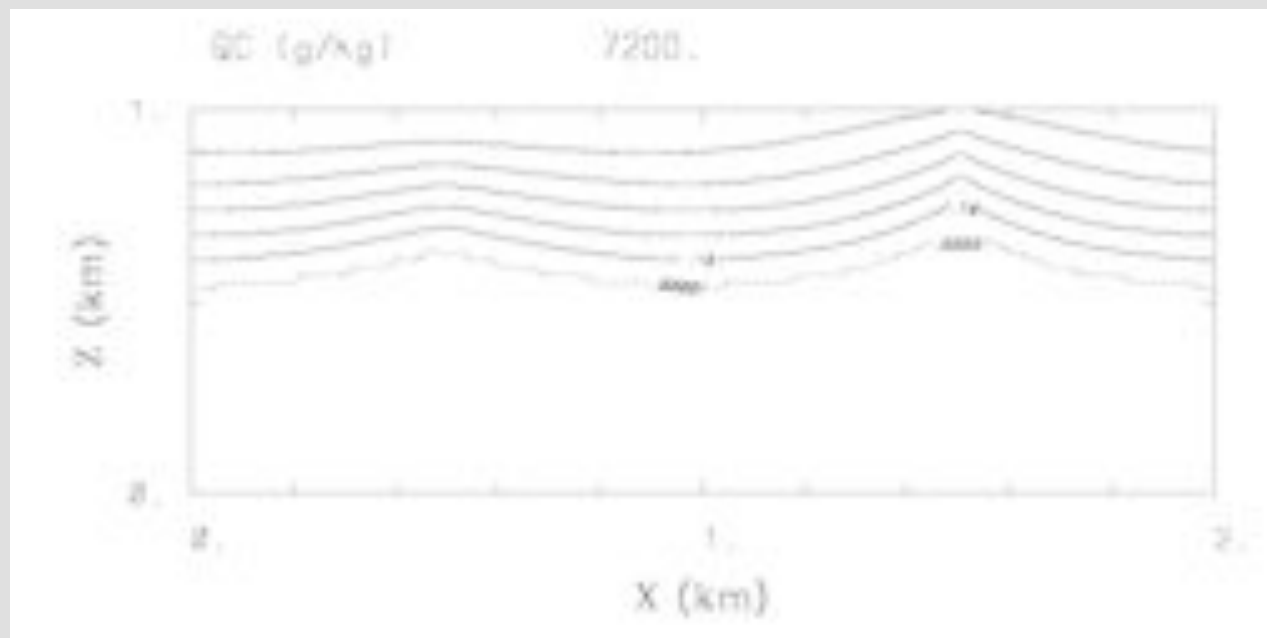
AUT - "autoconversion" rate: $q_c \rightarrow q_r$

ACC - accretion rate: $q_c, q_r \rightarrow q_r$

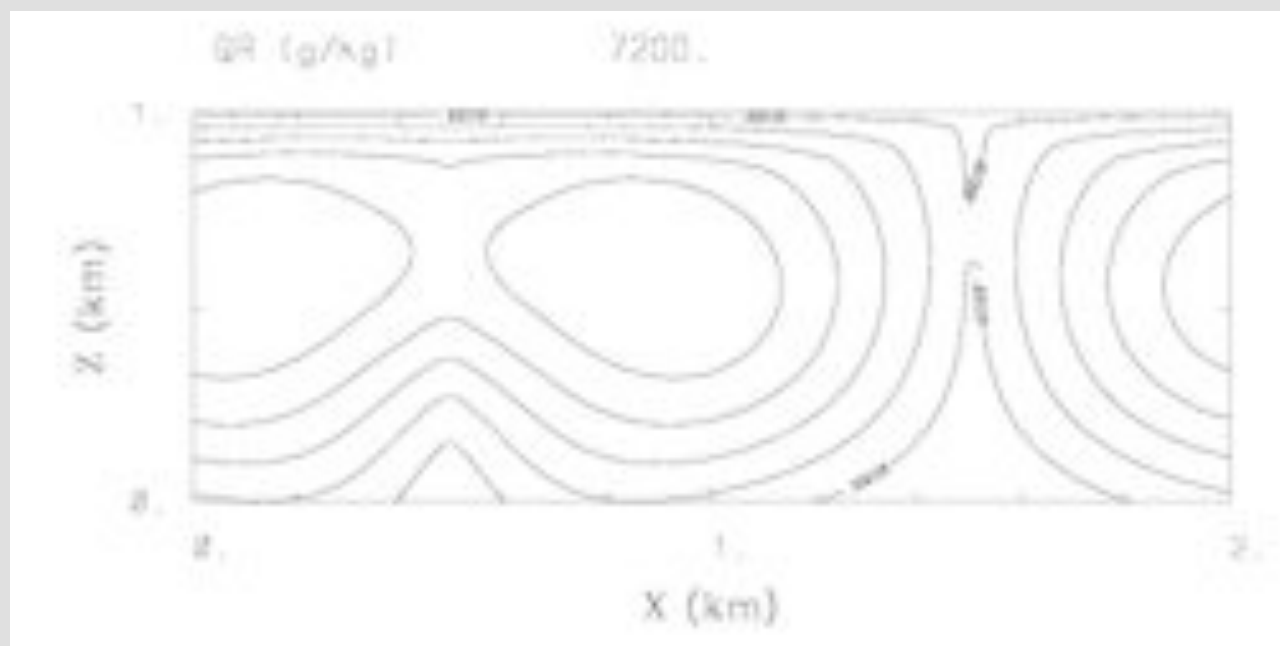
$v_t(q_r)$ - rain terminal velocity (typically derived by assuming a drop size distribution; e.g., the Marshall-Palmer distribution $N(D) = N_o \exp(-\Lambda D)$, $N_o = 10^7 \text{ m}^{-4}$).

*We need something more complicated than a rising parcel as rain has to fall out. One possibility is to use the **kinematic (prescribed flow)** framework...*



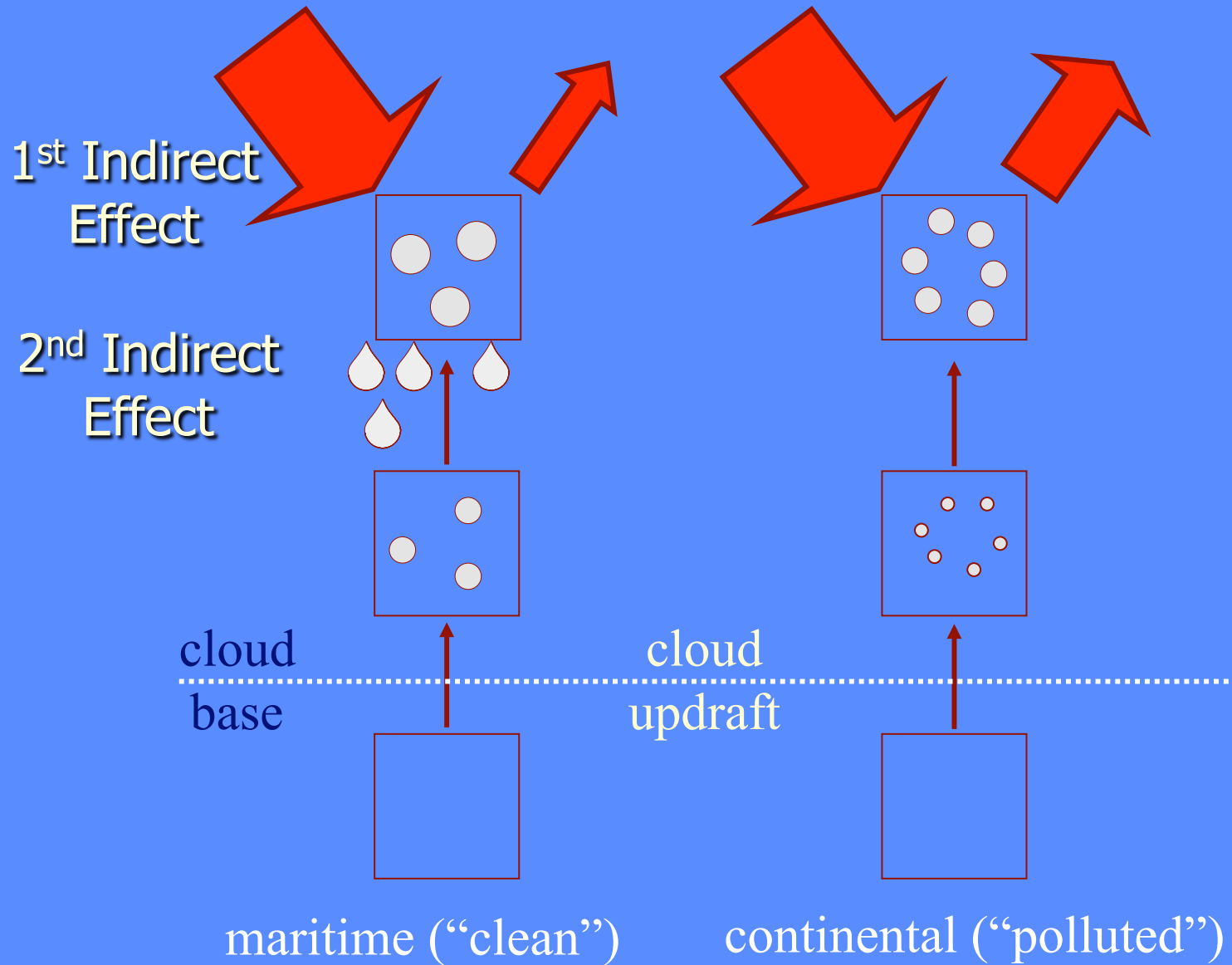


Cloud water and rain (drizzle) fields after 2 hrs (almost quasi-equilibrium...)



So far we only had information about the mass of cloud and precipitation. Do we need to know something about droplet sizes?

Indirect aerosol effects



RADIATIVE FORCING COMPONENTS

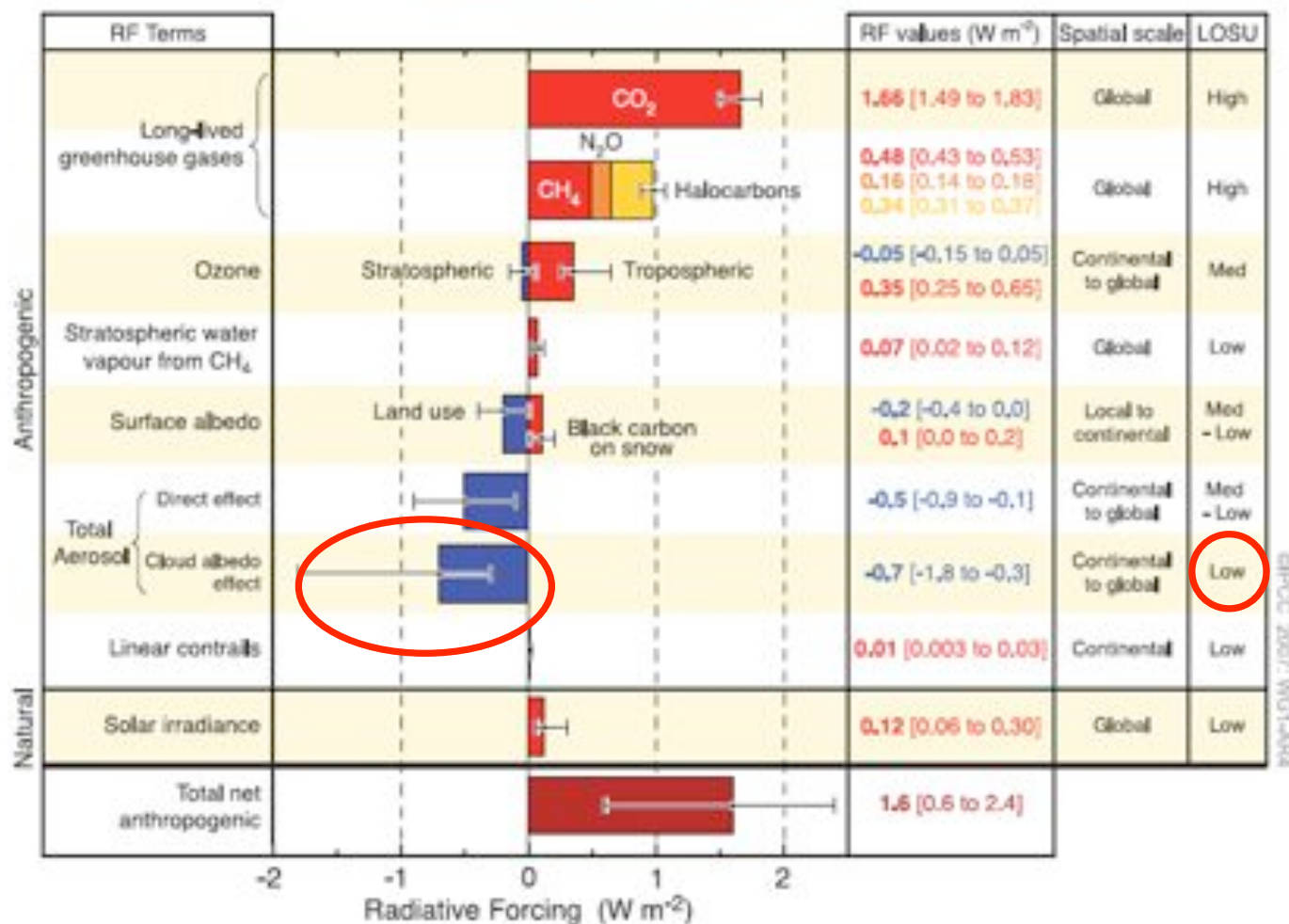


Figure SPM.2. Global average radiative forcing (RF) estimates and ranges in 2005 for anthropogenic carbon dioxide (CO₂), methane (CH₄), nitrous oxide (N₂O) and other important agents and mechanisms, together with the typical geographical extent (spatial scale) of the forcing and the assessed level of scientific understanding (LOSU). The net anthropogenic radiative forcing and its range are also shown. These require summing asymmetric uncertainty estimates from the component terms, and cannot be obtained by simple addition. Additional forcing factors not included here are considered to have a very low LOSU. Volcanic aerosols contribute an additional natural forcing but are not included in this figure due to their episodic nature. The range for linear contrails does not include other possible effects of aviation on cloudiness. (2.9, Figure 2.20)



Stratocumulus topped boundary layer

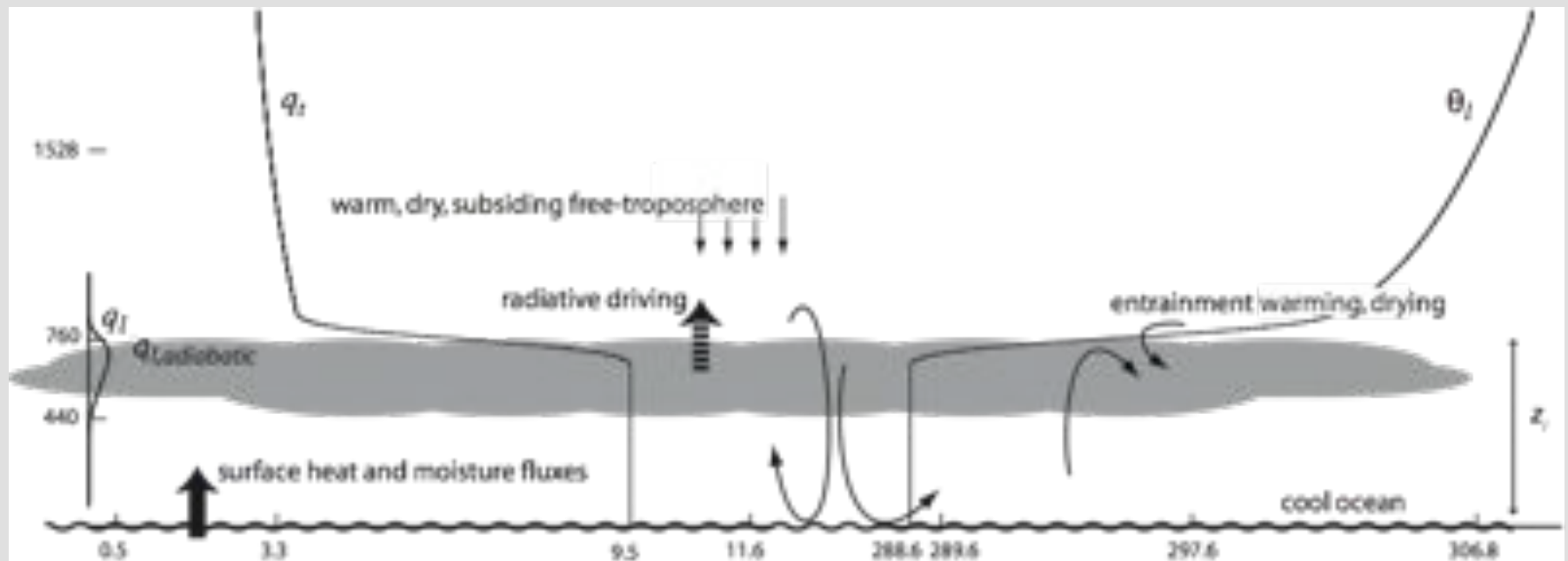


Figure from Bjorn Stevens

What determines the concentration of cloud droplets?

To answer this, one needs to understand formation of cloud droplets, that is, the activation of cloud condensation nuclei (CCN) .

This typically happens near the cloud base, when the rising air parcel approaches saturation.

Saturation ratio:

Saturated water vapor pressure over an aqueous solution droplet with radius r

Saturated water vapor pressure over plain water surface

$$\frac{e_r}{e_\infty} = 1 + \frac{a}{r} - \frac{b}{r^3}$$

Surface tension (Kelvin) effect

Solute (Raoult) effect

$$a = \frac{2\sigma}{\rho_l R_v T} \quad b = \frac{4im_s M_v}{3\pi\rho_l M_s}$$

σ - surface tension

ρ_l - water density

R_v - gas constant for water vapor

T - air temperature

i - van't Hoff factor

m_s - mass of solute

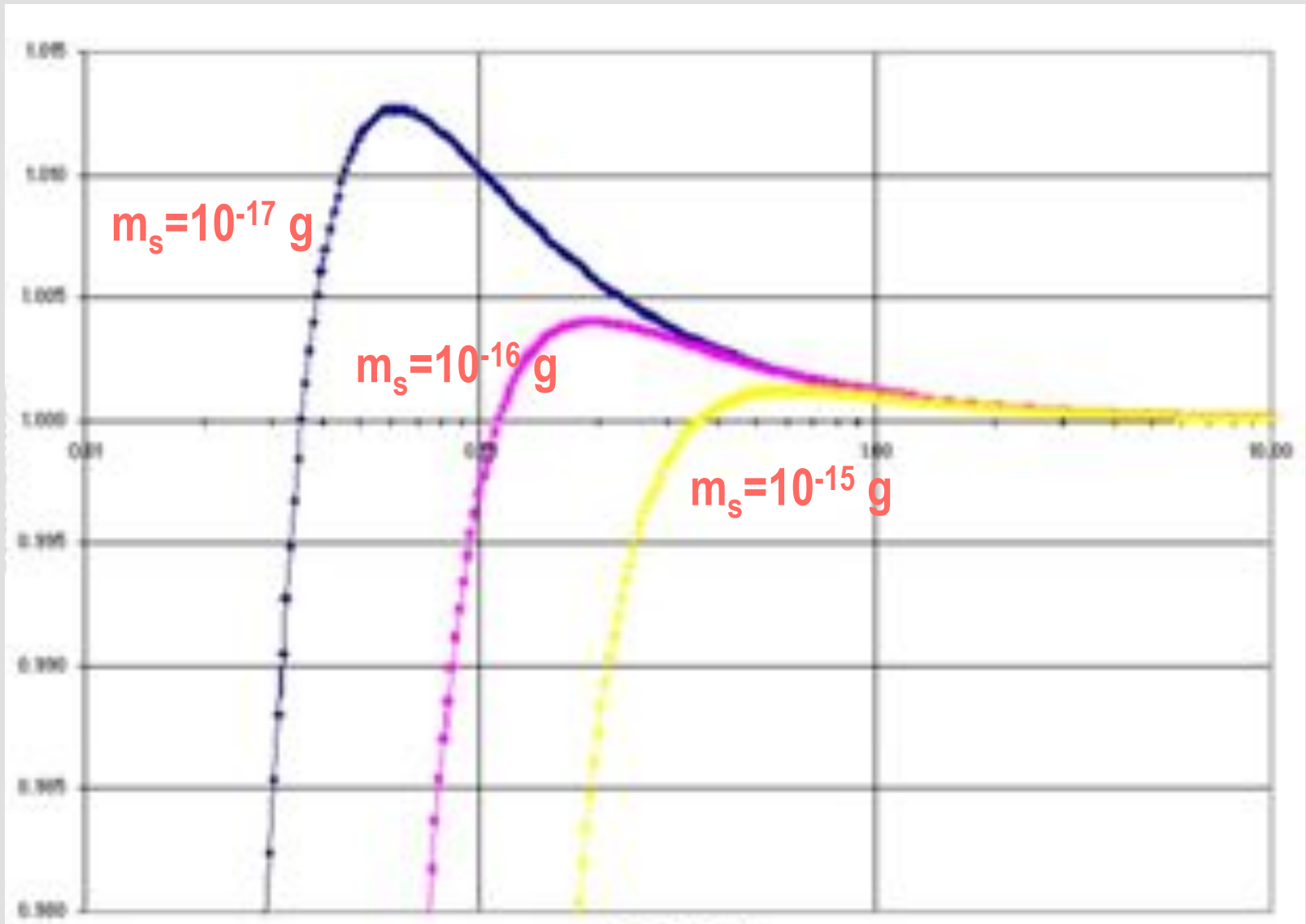
M_v - molar mass of water

M_s - molar mass of solute

Saturation ratio S

1%

-1%



.01

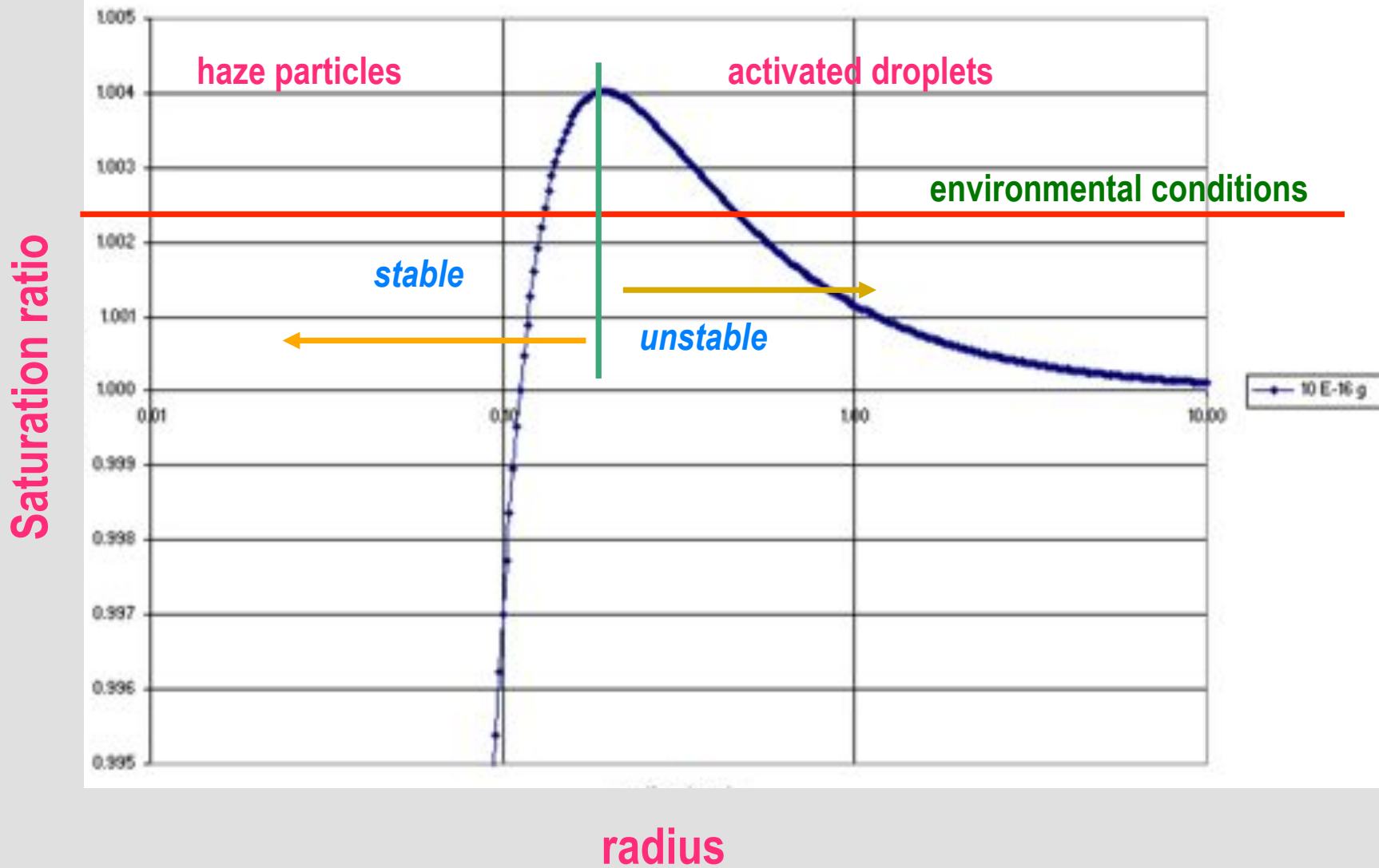
0.1

1.

10.

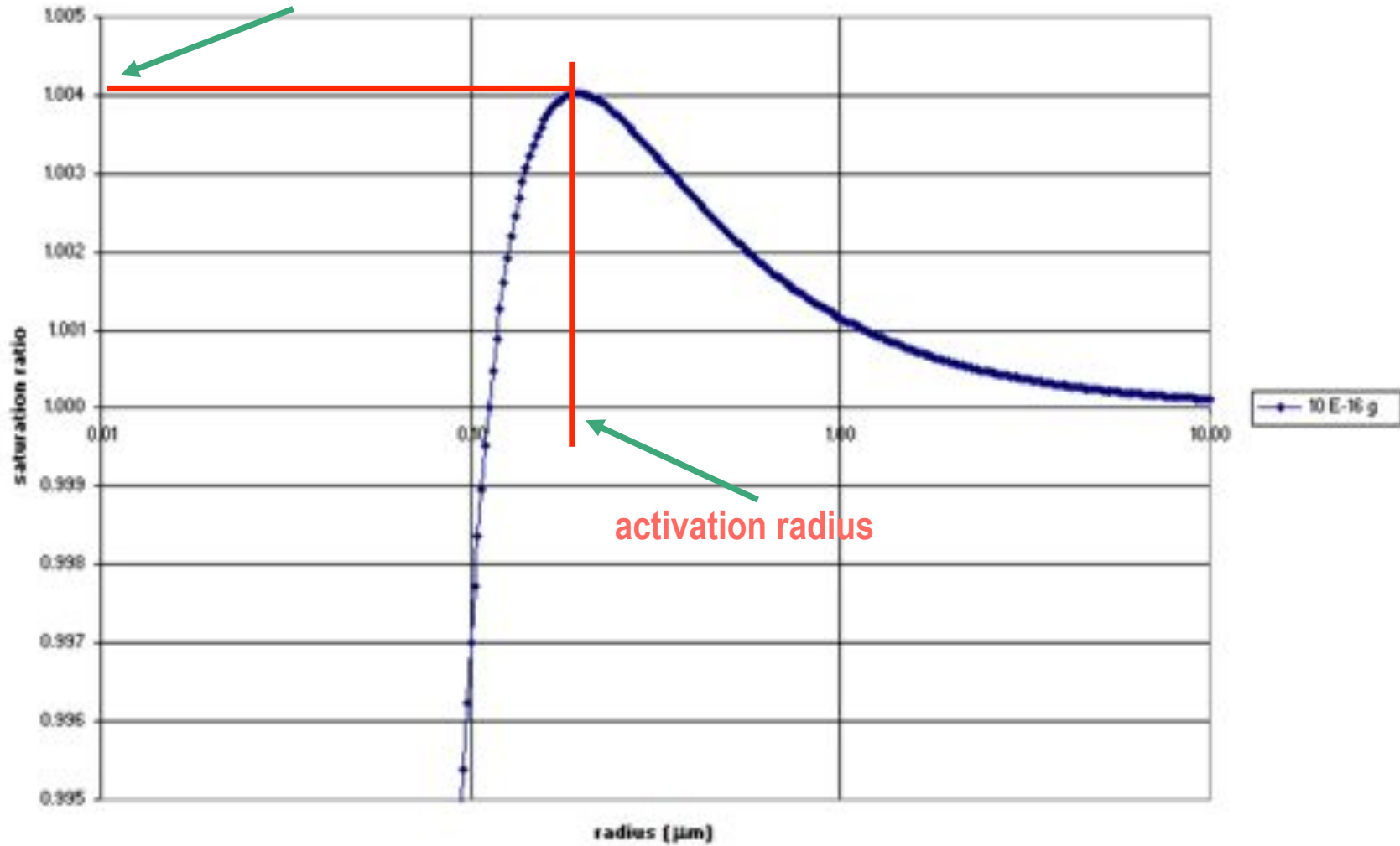
Radius (micrometers)

Kohler Curve for an NaCl CCN at 278 K



Kohler Curve for an NaCl CCN at 278 K

activation saturation ratio (or supersaturation)



CCN, soluble salt particles, have different sizes.

Large CCN are nucleated first, activation of smaller ones follow as the supersaturation builds up.

Once sufficient number of CCN is activated, these keep growing, supersaturation levels off, and activation is completed.

CCN, soluble salt particles, have different sizes.

Large CCN are nucleated first, activation of smaller ones follow as the supersaturation builds up.

Once sufficient number of CCN is activated, supersaturation levels off, and activation is completed.

These processes are typically considered in the context of detailed (bin) microphysics...

Activation of CCN:

N - total concentration of activated droplets

S – supersaturation

$$***N = a S^b***$$

a, b – parameters characterizing CCN

0 < b < 1 (typically, b=0.5)

a~100 cm⁻³ maritime/clean

a~1,000 cm⁻³ continental/polluted

BIN-RESOLVING WARM MICROPHYSICS: CONDENSATION

Introducing *spectral density function* $\phi(r, t)$:

$$\phi(r, t) \equiv \frac{dN(r, t)}{dr}$$

$dN(r, t)$ is the concentration (per unit mass as mixing ratio) of droplets in radius interval $(r, r+dr)$.

Continuity equation for growth by condensation:

$$\frac{\partial \phi(r, t)}{\partial t} + \frac{\partial}{\partial r} \left(\frac{dr}{dt} \phi(r, t) \right) = 0$$

where $\frac{dr}{dt}$ is growth rate of a droplet with radius r :

$$\frac{dr}{dt} = \frac{A(T, p) S}{r}$$

$S = \frac{q_v}{q_{vs}} - 1$ is the supersaturation; q_v is the ambient water vapor mixing ratio; $q_{vs}(p, T)$ is the saturated water vapor mixing ratio.

BIN-RESOLVING WARM MICROPHYSICS: NUCLEATION AND CONDENSATION

Continuity equation for nucleation and growth by condensation:

$$\frac{\partial \phi(r, t)}{\partial t} + \frac{\partial}{\partial r} \left(\frac{dr}{dt} \phi(r, t) \right) = S_{nuc}$$

where S_{nuc} is the source associated with nucleation of cloud droplets (CCN activation).

S_{nuc} adds droplets (typically to the 1st bin) when the concentration of droplets $\int \phi dr$ is smaller than the total concentration for a given supersaturation S , the latter given by aS^b .

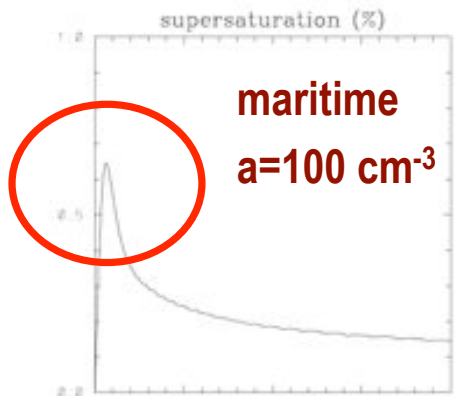
Computational example:

Nucleation and growth of cloud droplets in a parcel of air rising with vertical velocity of 1 m/s;

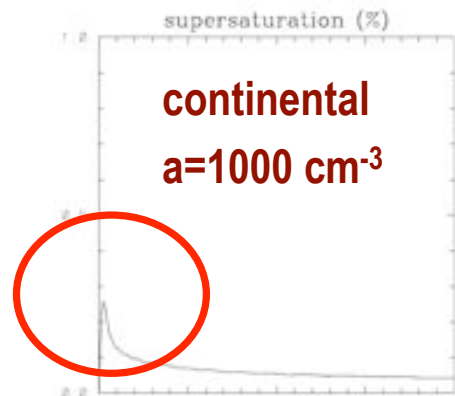
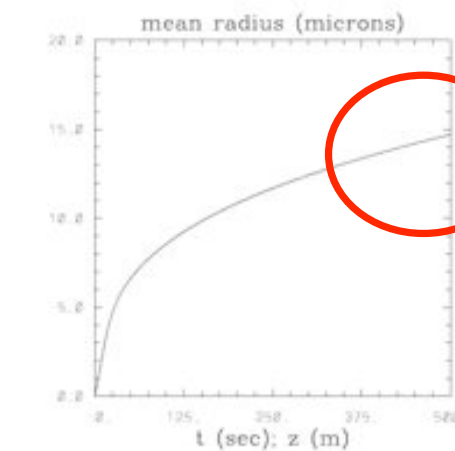
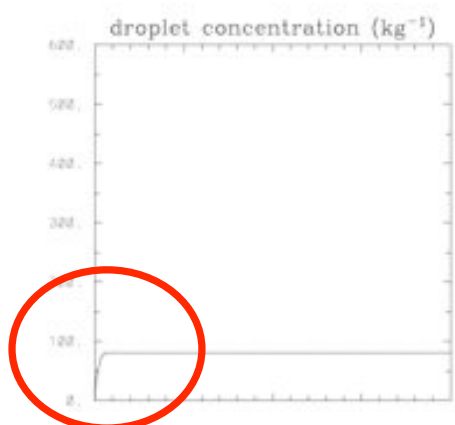
60 bins used;

1D flux-form advection applied in the radius space;

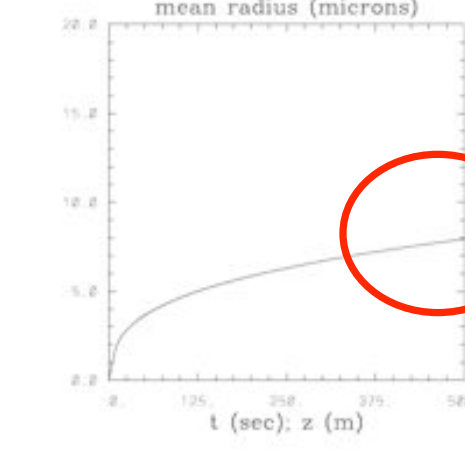
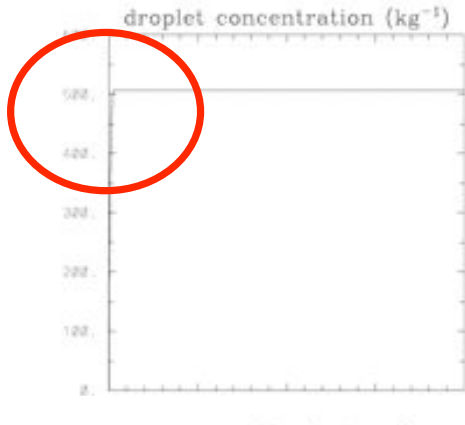
Difference between continental/polluted and maritime/pristine aerosols

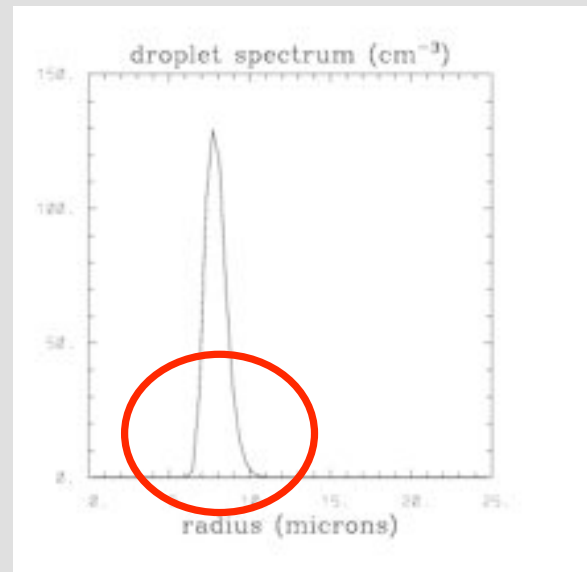
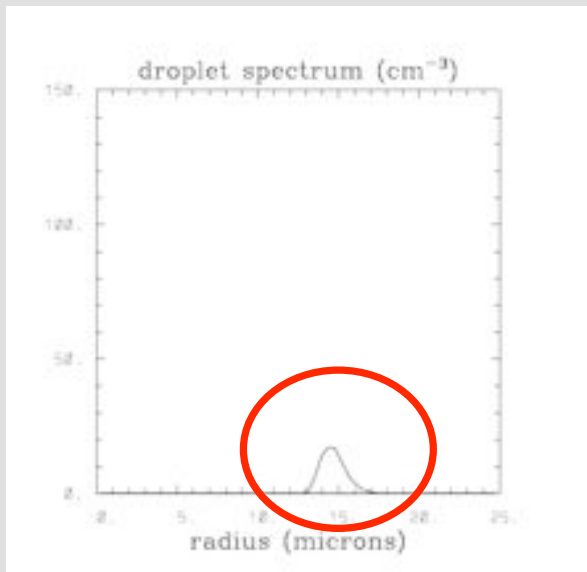
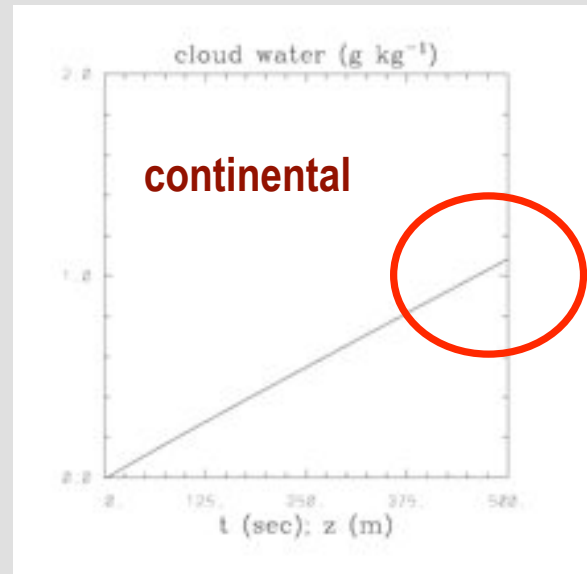
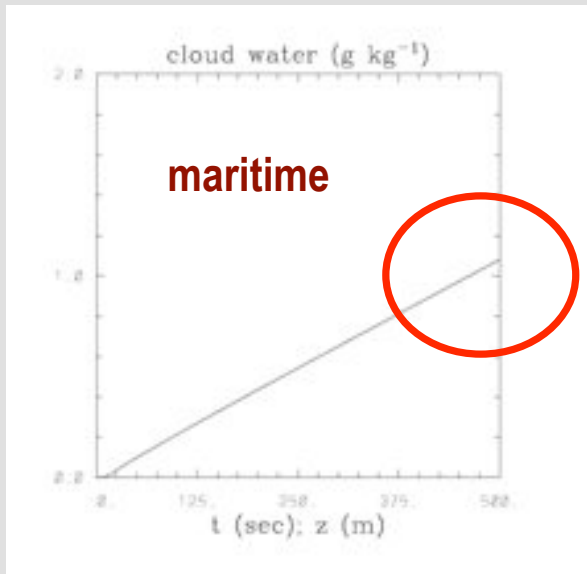


maritime
 $a=100 \text{ cm}^{-3}$

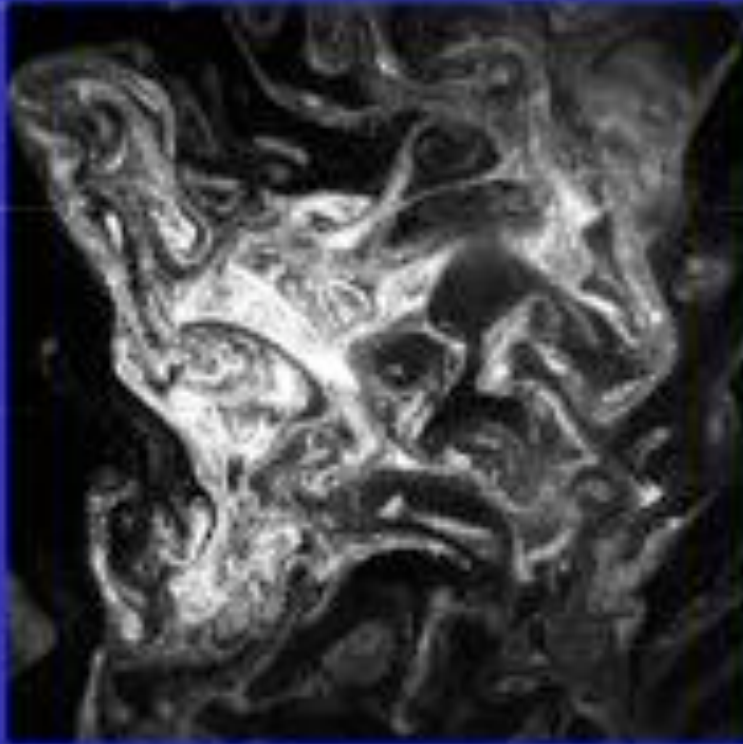


continental
 $a=1000 \text{ cm}^{-3}$





30 cm



Application of the bin-resolving microphysics to the problem of turbulent mixing between cloudy and clear air: cloud chamber mixing versus DNS simulation

Note: DNS 256^3 simulation applies gridlength of about 3 mm !!!

BIN-RESOLVING WARM MICROPHYSICS:

GROWTH BY COLLISION/COALESCENCE

The Smoluchowski equation (aka *kinetic collection equation*, *stochastic coalescence equation*) for the spectral density function $\phi(m, t)$:

$$\begin{aligned}\frac{\partial \phi(m, t)}{\partial t} &= \\ &= \frac{1}{2} \int_0^m \phi(m - M, t) \phi(M, t) K(m - M, M) dM \\ &\quad - \phi(m, t) \int_0^\infty \phi(M, t) K(m, M) dM\end{aligned}$$

m, M - droplet masses

$K(m, M)$ - *collection kernel*; frequency of collisions (per unit volume of air) between droplets with mass m and M

BIN-RESOLVING WARM MICROPHYSICS:

GROWTH BY COLLISION/COALESCENCE

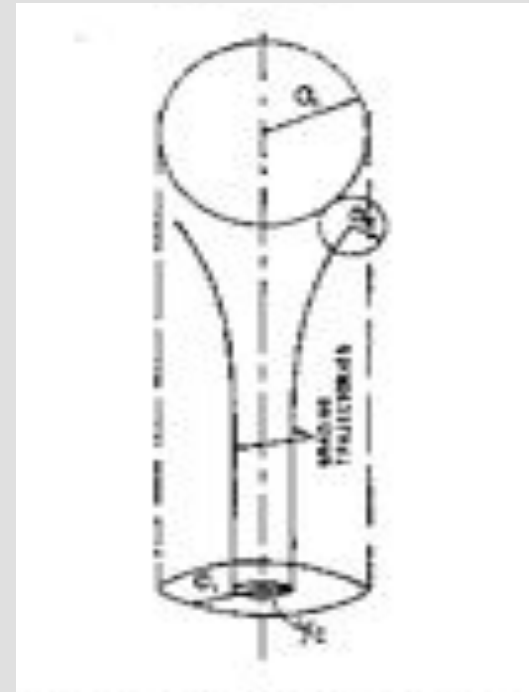
The Smoluchowski equation (aka *kinetic collection equation*, *stochastic coalesce equation*) for the spectral density function $\phi(m, t)$:

$$\begin{aligned} \frac{\partial \phi(m, t)}{\partial t} = & \\ = \frac{1}{2} \int_0^m \phi(m - M, t) \phi(M, t) K(m - M, M) dM & \\ - \phi(m, t) \int_0^\infty \phi(M, t) K(m, M) dM & \end{aligned}$$

m, M - droplet masses

$K(m, M)$ - *collection kernel*, frequency of collisions (per unit volume of air) between droplets with mass m and M

Geometry for gravitational collisions



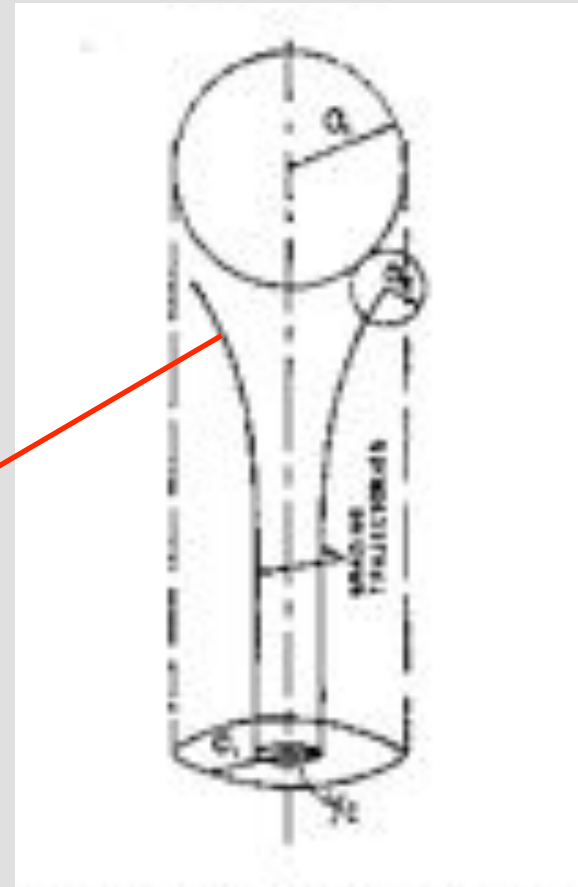
Growth of water droplets by gravitational collision-coalescence:

$$K(m_{a1}, m_{a2}) = E_c \pi (a_1 + a_2)^2 |(V_{a1} - V_{a2})|$$

Collision efficiency:

$$E_c = \frac{y_c^2}{(a_1 + a_2)^2}$$

Grazing trajectory



Droplet inertia is the key; without it, there will be no collisions. This is why collision efficiency for droplets smaller than 10 μm is very small.

TABLE 1. Radius ratio r/R .

Collector drop radius (μm)	0.05	0.10	0.15	0.20	0.25	0.30	0.35	0.40	0.45	0.50	0.55	0.60	0.65	0.70	0.75	0.80	0.85	0.90	0.95	1.00	
300	0.97	1.0	1.0	1.0	1.0	1.0	1.0	1.0	1.0	1.0	1.0	1.0	1.0	1.0	1.0	1.0	1.0	1.0	1.0	1.0	1.0
200	0.87	0.96	0.98	1.0	1.0	1.0	1.0	1.0	1.0	1.0	1.0	1.0	1.0	1.0	1.0	1.0	1.0	1.0	1.0	1.0	1.0
150	0.77	0.93	0.97	0.97	1.0	1.0	1.0	1.0	1.0	1.0	1.0	1.0	1.0	1.0	1.0	1.0	1.0	1.0	1.0	1.0	1.0
100	0.50	0.79	0.91	0.95	0.95	1.0	1.0	1.0	1.0	1.0	1.0	1.0	1.0	1.0	1.0	1.0	1.0	1.0	1.0	1.0	1.0
70	0.20	0.58	0.75	0.84	0.88	0.90	0.92	0.94	0.95	0.95	0.95	0.95	0.95	0.95	0.97	1.0	1.02	1.04	2.3	4.0	
60	0.05	0.43	0.64	0.77	0.84	0.87	0.89	0.90	0.91	0.91	0.91	0.91	0.91	0.92	0.93	0.95	1.0	1.03	1.7	3.0	
50	0.005	0.40	0.60	0.70	0.78	0.83	0.86	0.88	0.90	0.90	0.90	0.90	0.89	0.88	0.88	0.89	0.92	1.01	1.3	2.3	
40	0.001	0.07	0.38	0.50	0.62	0.68	0.74	0.78	0.80	0.80	0.80	0.78	0.77	0.76	0.77	0.77	0.78	0.79	0.95	1.4	
30	0.0001	0.002	0.02	0.04	0.085	0.17	0.27	0.40	0.50	0.55	0.58	0.59	0.58	0.54	0.51	0.49	0.47	0.45	0.47	0.52	
20	0.0001	0.0001	0.005	0.016	0.022	0.03	0.043	0.052	0.064	0.072	0.079	0.082	0.080	0.076	0.067	0.057	0.048	0.040	0.033	0.027	
10	0.0001	0.0001	0.0001	0.014	0.017	0.019	0.022	0.027	0.030	0.033	0.035	0.037	0.038	0.038	0.037	0.036	0.035	0.032	0.029	0.027	

Hall (*J. Atmos. Sci.* 1980)
 (compilation of many theoretical studies and
 laboratory measurements)

TABLE 1. Radius ratio r/R .

Collector drop radius (μm)	0.05	0.10	0.15	0.20	0.25	0.30	0.35	0.40	0.45	0.50	0.55	0.60	0.65	0.70	0.75	0.80	0.85	0.90	0.95	1.00	
300	0.97	1.0	1.0	1.0	1.0	1.0	1.0	1.0	1.0	1.0	1.0	1.0	1.0	1.0	1.0	1.0	1.0	1.0	1.0	1.0	1.0
200	0.87	0.96	0.98	1.0	1.0	1.0	1.0	1.0	1.0	1.0	1.0	1.0	1.0	1.0	1.0	1.0	1.0	1.0	1.0	1.0	1.0
150	0.77	0.93	0.97	0.97	1.0	1.0	1.0	1.0	1.0	1.0	1.0	1.0	1.0	1.0	1.0	1.0	1.0	1.0	1.0	1.0	1.0
100	0.50	0.79	0.91	0.95	0.95	1.0	1.0	1.0	1.0	1.0	1.0	1.0	1.0	1.0	1.0	1.0	1.0	1.0	1.0	1.0	1.0
70	0.20	0.58	0.75	0.84	0.88	0.90	0.92	0.94	0.95	0.95	0.95	0.95	0.95	0.95	0.97	1.0	1.02	1.04	2.3	4.0	
60	0.05	0.43	0.64	0.77	0.84	0.87	0.89	0.90	0.91	0.91	0.91	0.91	0.91	0.92	0.93	0.95	1.0	1.03	1.7	3.0	
50	0.005	0.40	0.60	0.70	0.78	0.83	0.86	0.88	0.90	0.90	0.90	0.90	0.89	0.88	0.88	0.89	0.92	1.01	1.3	2.3	
40	0.001	0.07	0.38	0.50	0.62	0.68	0.74	0.78	0.80	0.80	0.80	0.78	0.77	0.76	0.77	0.77	0.78	0.79	0.95	1.4	
30	0.0001	0.002	0.02	0.04	0.085	0.17	0.27	0.40	0.50	0.55	0.58	0.59	0.58	0.54	0.51	0.49	0.47	0.45	0.47	0.52	
20	0.0001	0.0001	0.005	0.016	0.022	0.03	0.043	0.052	0.064	0.072	0.079	0.082	0.080	0.076	0.067	0.057	0.048	0.040	0.033	0.027	
10	0.0001	0.0001	0.0001	0.014	0.017	0.019	0.022	0.027	0.030	0.033	0.035	0.037	0.038	0.038	0.037	0.036	0.035	0.032	0.029	0.027	

Hall (*J. Atmos. Sci.* 1980)
 (compilation of many theoretical studies and
 laboratory measurements)

TABLE 1. Radius ratio r/R .

Collector drop radius (μm)	0.05	0.10	0.15	0.20	0.25	0.30	0.35	0.40	0.45	0.50	0.55	0.60	0.65	0.70	0.75	0.80	0.85	0.90	0.95	1.00	
300	0.97	1.0	1.0	1.0	1.0	1.0	1.0	1.0	1.0	1.0	1.0	1.0	1.0	1.0	1.0	1.0	1.0	1.0	1.0	1.0	1.0
200	0.87	0.96	0.98	1.0	1.0	1.0	1.0	1.0	1.0	1.0	1.0	1.0	1.0	1.0	1.0	1.0	1.0	1.0	1.0	1.0	1.0
150	0.77	0.93	0.97	0.97	1.0	1.0	1.0	1.0	1.0	1.0	1.0	1.0	1.0	1.0	1.0	1.0	1.0	1.0	1.0	1.0	1.0
100	0.50	0.79	0.91	0.95	0.95	1.0	1.0	1.0	1.0	1.0	1.0	1.0	1.0	1.0	1.0	1.0	1.0	1.0	1.0	1.0	1.0
70	0.20	0.58	0.75	0.84	0.88	0.90	0.92	0.94	0.95	0.95	0.95	0.95	0.95	0.95	0.97	1.0	1.02	1.04	2.3	4.0	
60	0.05	0.43	0.64	0.77	0.84	0.87	0.89	0.90	0.91	0.91	0.91	0.91	0.91	0.91	0.92	0.93	0.95	1.0	1.03	1.7	3.0
50	0.005	0.40	0.60	0.70	0.78	0.83	0.86	0.88	0.90	0.90	0.90	0.90	0.89	0.88	0.88	0.89	0.92	1.01	1.3	2.3	
40	0.001	0.07	0.28	0.50	0.62	0.68	0.74	0.78	0.80	0.80	0.80	0.78	0.77	0.76	0.77	0.77	0.78	0.79	0.95	1.4	
30	0.0001	0.002	0.02	0.04	0.085	0.17	0.27	0.40	0.50	0.55	0.58	0.59	0.58	0.54	0.51	0.49	0.47	0.45	0.47	0.52	
20	0.0001	0.0001	0.005	0.016	0.022	0.03	0.043	0.052	0.064	0.072	0.079	0.082	0.080	0.076	0.067	0.057	0.048	0.040	0.033	0.027	
10	0.0001	0.0001	0.0001	0.014	0.017	0.019	0.022	0.027	0.030	0.033	0.035	0.037	0.038	0.038	0.037	0.036	0.035	0.032	0.029	0.027	

Hall (*J. Atmos. Sci.* 1980)
 (compilation of many theoretical studies and
 laboratory measurements)

TABLE 1. Radius ratio r/R .

Collector drop radius (μm)	0.05	0.10	0.15	0.20	0.25	0.30	0.35	0.40	0.45	0.50	0.55	0.60	0.65	0.70	0.75	0.80	0.85	0.90	0.95	1.00	
100	0.97	1.0	1.0	1.0	1.0	1.0	1.0	1.0	1.0	1.0	1.0	1.0	1.0	1.0	1.0	1.0	1.0	1.0	1.0	1.0	1.0
200	0.87	0.96	0.98	1.0	1.0	1.0	1.0	1.0	1.0	1.0	1.0	1.0	1.0	1.0	1.0	1.0	1.0	1.0	1.0	1.0	1.0
150	0.77	0.93	0.97	0.97	1.0	1.0	1.0	1.0	1.0	1.0	1.0	1.0	1.0	1.0	1.0	1.0	1.0	1.0	1.0	1.0	1.0
100	0.50	0.79	0.91	0.95	0.95	1.0	1.0	1.0	1.0	1.0	1.0	1.0	1.0	1.0	1.0	1.0	1.0	1.0	1.0	1.0	1.0
70	0.20	0.58	0.75	0.84	0.88	0.90	0.92	0.94	0.95	0.95	0.95	0.95	0.95	0.95	0.97	1.0	1.02	1.04	2.3	4.0	
60	0.05	0.43	0.64	0.77	0.84	0.87	0.89	0.90	0.91	0.91	0.91	0.91	0.91	0.92	0.93	0.95	1.0	1.03	1.7	3.0	
50	0.005	0.40	0.60	0.70	0.78	0.83	0.86	0.88	0.90	0.90	0.90	0.90	0.89	0.88	0.88	0.89	0.92	1.01	1.3	2.3	
40	0.001	0.07	0.38	0.50	0.62	0.68	0.74	0.78	0.80	0.80	0.80	0.78	0.77	0.76	0.77	0.77	0.78	0.79	0.95	1.4	
30	0.0001	0.002	0.02	0.04	0.085	0.17	0.27	0.40	0.50	0.55	0.58	0.59	0.58	0.54	0.51	0.49	0.47	0.45	0.47	0.52	
20	0.0001	0.0001	0.005	0.016	0.022	0.03	0.043	0.052	0.064	0.072	0.079	0.082	0.080	0.076	0.067	0.057	0.048	0.040	0.033	0.027	
10	0.0001	0.0001	0.0001	0.014	0.017	0.019	0.022	0.027	0.030	0.033	0.035	0.037	0.038	0.038	0.037	0.036	0.035	0.032	0.029	0.027	

Hall (*J. Atmos. Sci.* 1980)
 (compilation of many theoretical studies and
 laboratory measurements)

Adiabatic parcel model

$$c_p \frac{dT}{dt} = -g w + LC$$

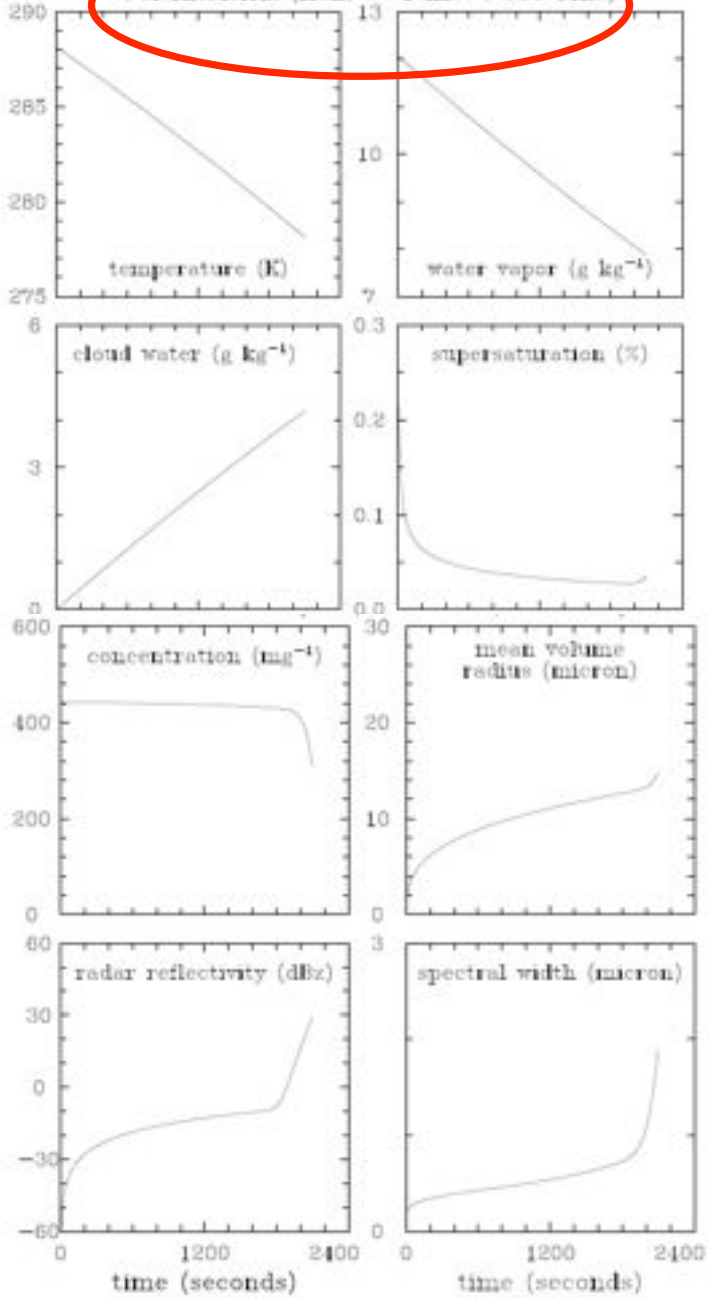
$$\frac{dq_v}{dt} = -C$$

$$\frac{dp}{dt} = -\rho_o w g$$

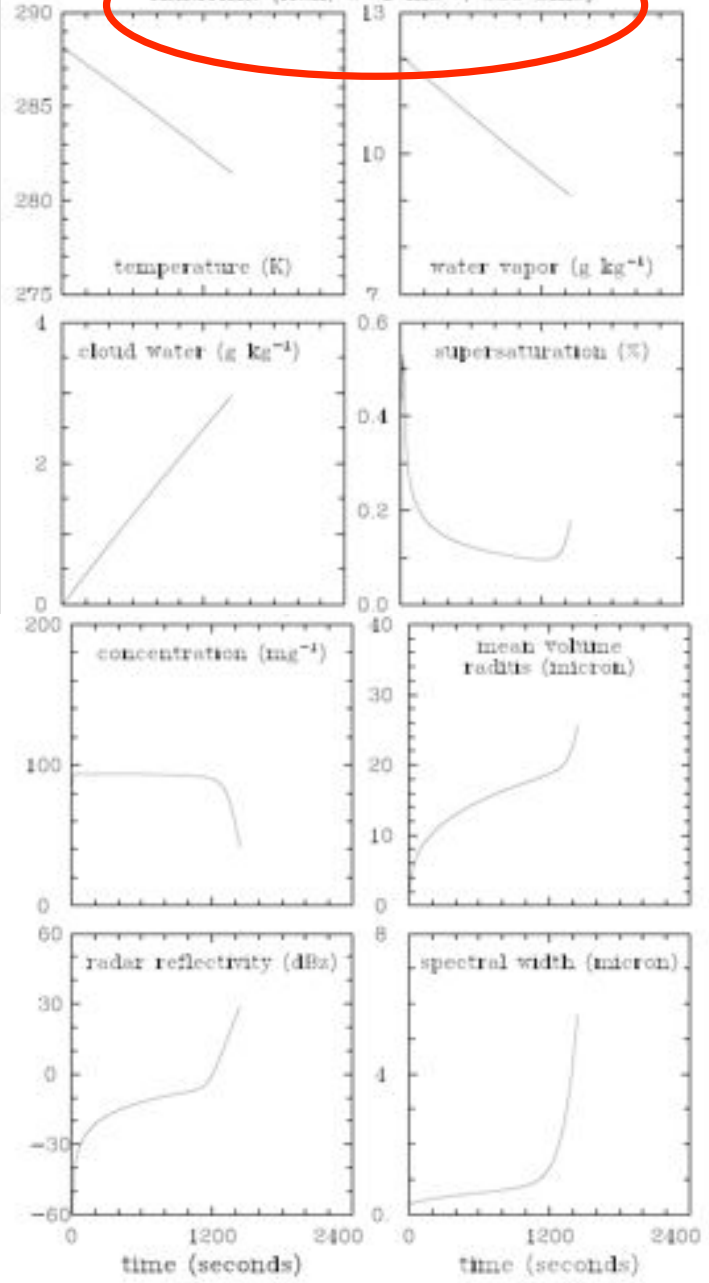
$$\frac{\partial \phi}{\partial t} + \frac{\partial}{\partial r} \left(\frac{dr}{dt} \phi \right) = \left(\frac{\partial \phi}{\partial t} \right)_{\text{act}} + \left(\frac{\partial \phi}{\partial t} \right)_{\text{coal}}$$

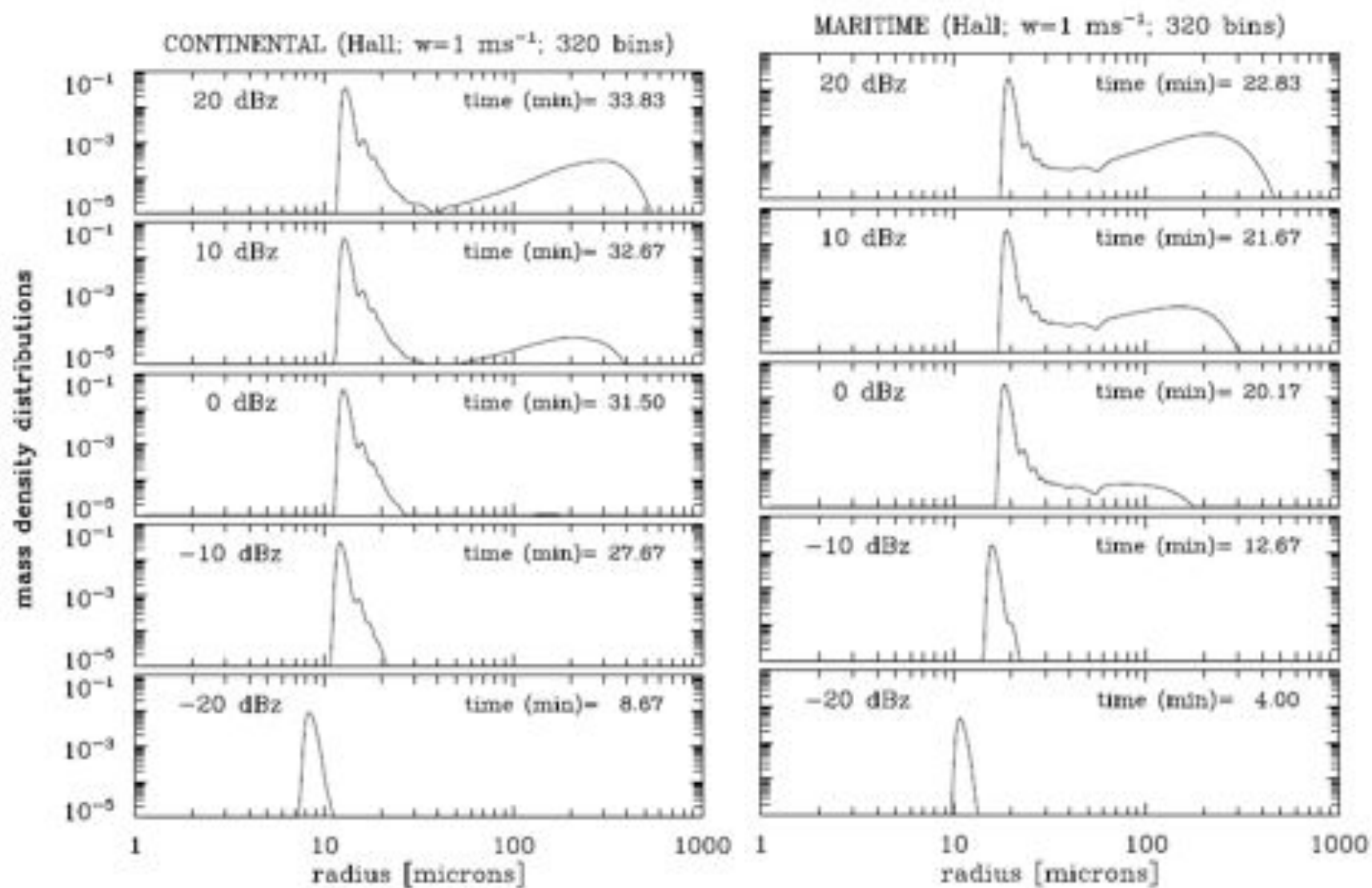
Grabowski and Wang, *Atmos. Chem. Phys.* 2009

CONTINENTAL (Hall, $w=1 \text{ ms}^{-1}$; 320 bins)



MARITIME (Hall, $w=1 \text{ ms}^{-1}$; 320 bins)





Traditional bulk model is computationally efficient (just 2 variables for condensed water).

Traditional bin-resolving (detailed) microphysics is computationally demanding (~100 variables).

Is there anything between?

YES, a two-moment bulk scheme, i.e., predicting mass and number of cloud droplets and rain/drizzle drops (just 4 variables; e.g., Morrison and Grabowski JAS 2007, 2008). This scheme also predicts supersaturation.

WARM-RAIN PHYSICS:

cloud water: q_c, N_c

drizzle/rain water: q_r, N_r

October 1974 EDWIN X BERRY AND RICHARD L. REINHARDT 1527

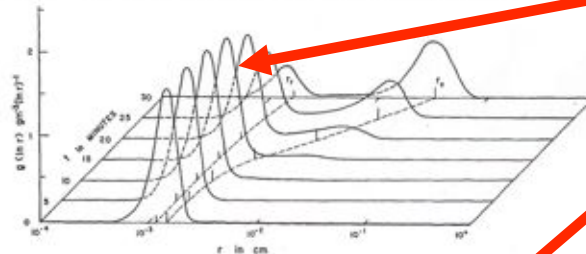


FIG. 3. Time evolution of the initial spectrum for $r_0^3 = 12 \mu\text{m}^3$, var $s = 1$.

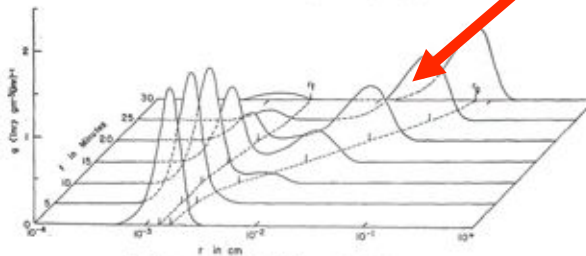


FIG. 4. Time evolution of the initial spectrum for $r_0^3 = 14 \mu\text{m}^3$, var $s = 1$.

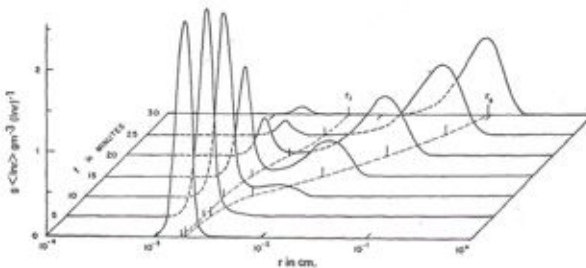


FIG. 5. Time evolution of the initial spectrum for $r_0^3 = 18 \mu\text{m}^3$, var $s = 0.25$.

Nucleation of cloud droplets: link to CCN characteristics

Drizzle/rain development: link to mean droplet size

$$\begin{aligned}
\frac{\partial N}{\partial t} + \frac{1}{\rho_a} \nabla \cdot [\rho_a (\mathbf{u} - V_N \mathbf{k}) N] &= \mathcal{F}_N \\
&= \left(\frac{\partial N}{\partial t} \right)_{\text{act}} + \left(\frac{\partial N}{\partial t} \right)_{\text{cond}} + \left(\frac{\partial N}{\partial t} \right)_{\text{acc}} + \left(\frac{\partial N}{\partial t} \right)_{\text{auto}} \\
&\quad + \left(\frac{\partial N}{\partial t} \right)_{\text{self}} + D(N)
\end{aligned} \tag{3}$$

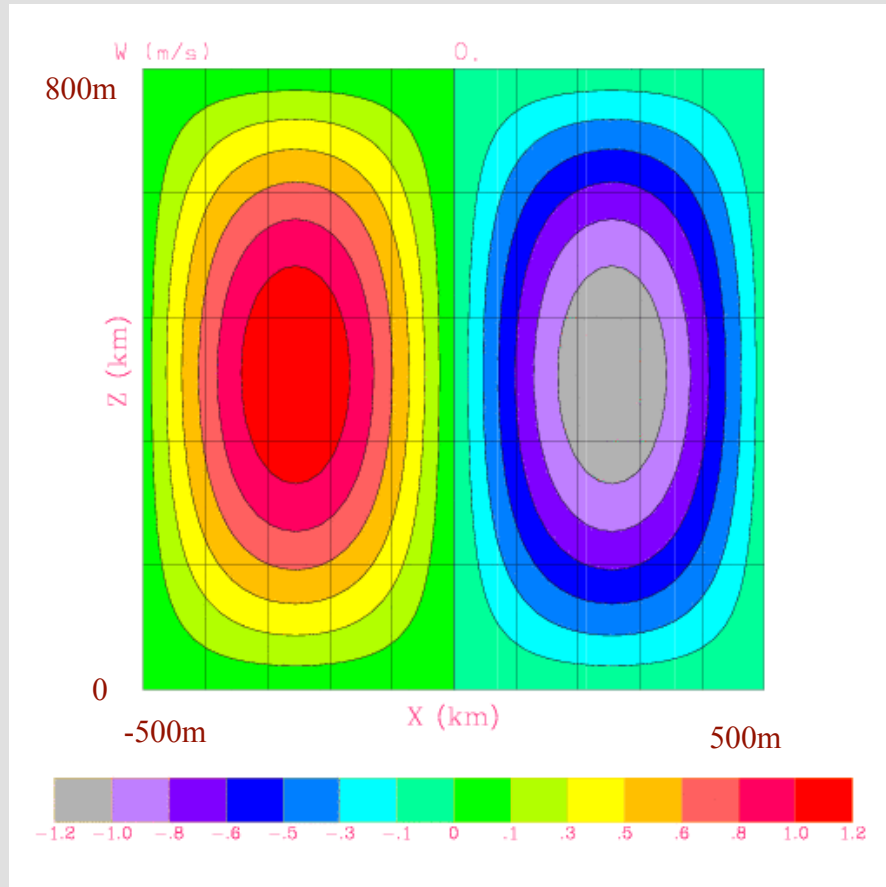
$$\begin{aligned}
\frac{\partial q}{\partial t} + \frac{1}{\rho_a} \nabla \cdot [\rho_a (\mathbf{u} - V_q \mathbf{k}) q] &= \mathcal{F}_q \\
&= \left(\frac{\partial q}{\partial t} \right)_{\text{act}} + \left(\frac{\partial q}{\partial t} \right)_{\text{cond}} + \left(\frac{\partial q}{\partial t} \right)_{\text{acc}} + \left(\frac{\partial q}{\partial t} \right)_{\text{auto}} \\
&\quad + D(q),
\end{aligned} \tag{4}$$

N_c, q_c – cloud water concentration and mixing ratio
 N_r, q_r – drizzle/rain water concentration and mixing ratio

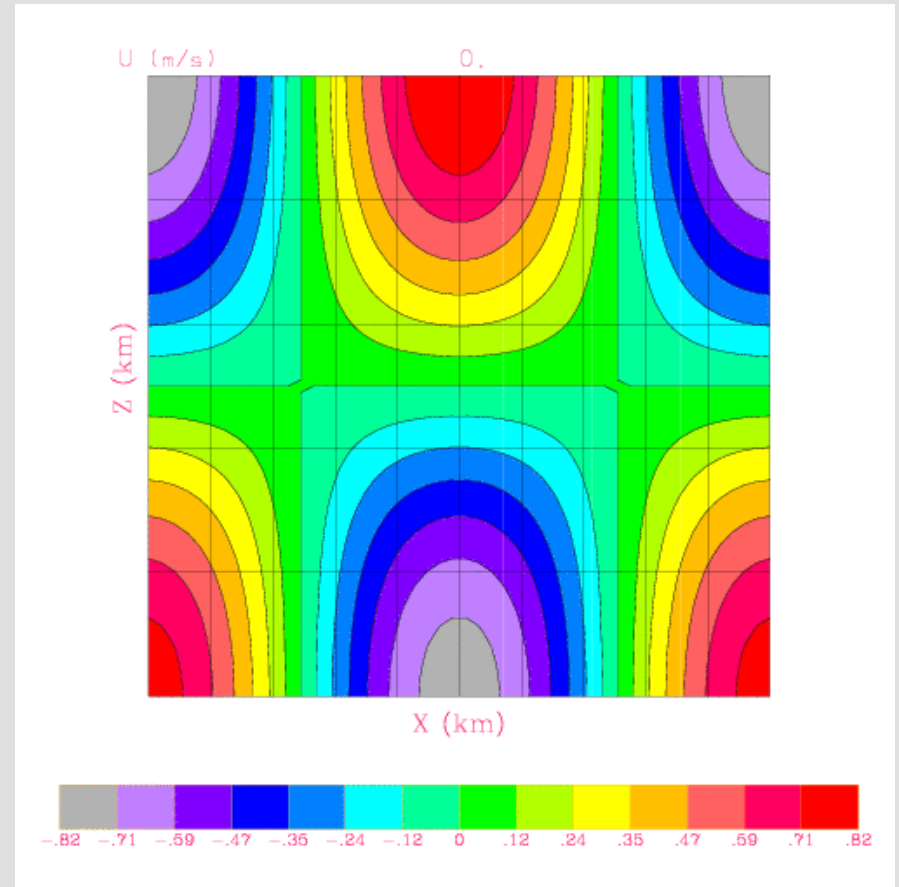
$$\frac{\partial N_{\text{act}}}{\partial t} + \frac{1}{\rho_a} \nabla \cdot (\rho_a \mathbf{u} N_{\text{act}}) = \mathcal{F}_{N_{\text{act}}} \equiv \left(\frac{\partial N_c}{\partial t} \right)_{\text{act}} + D(N_{\text{act}}).$$

concentration of activated CCN

Kinematic (prescribed-flow) model of microphysical processes in Stratocumulus (2D: x-z)



Vertical velocity



Horizontal velocity

Run up to quasi-steady-state is obtained (typically couple hours) ...

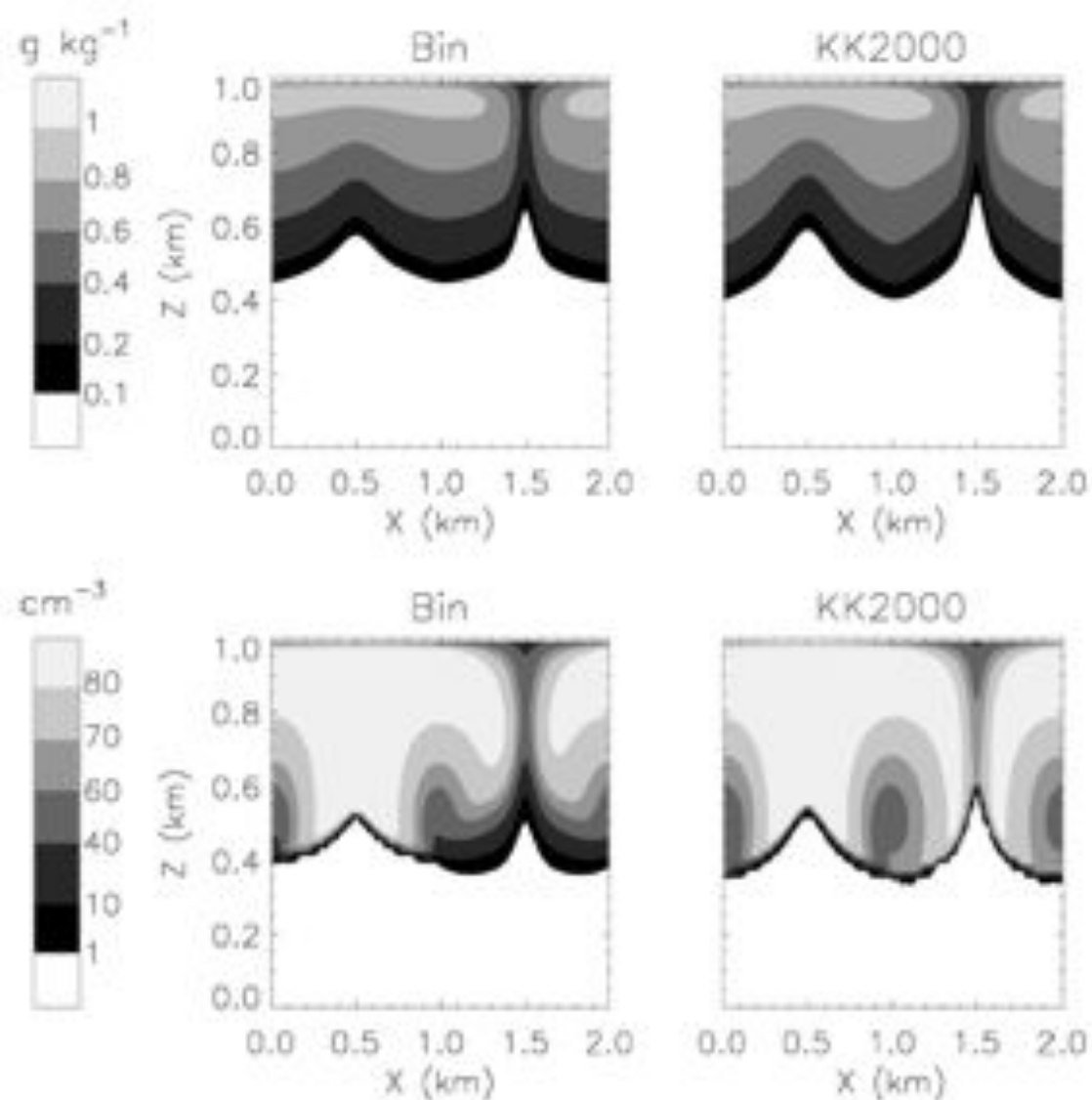


FIG. 4. Plot (x-z) of the (top) equilibrium cloud water mixing ratio and (bottom) droplet number concentration for the bin and bulk (using KK2000) PRISTINE stratocumulus simulations with $LHF = 3\ W\ m^{-2}$. A similar cloud structure is produced by the bulk model using the SB2001 and B1994 parameterizations.

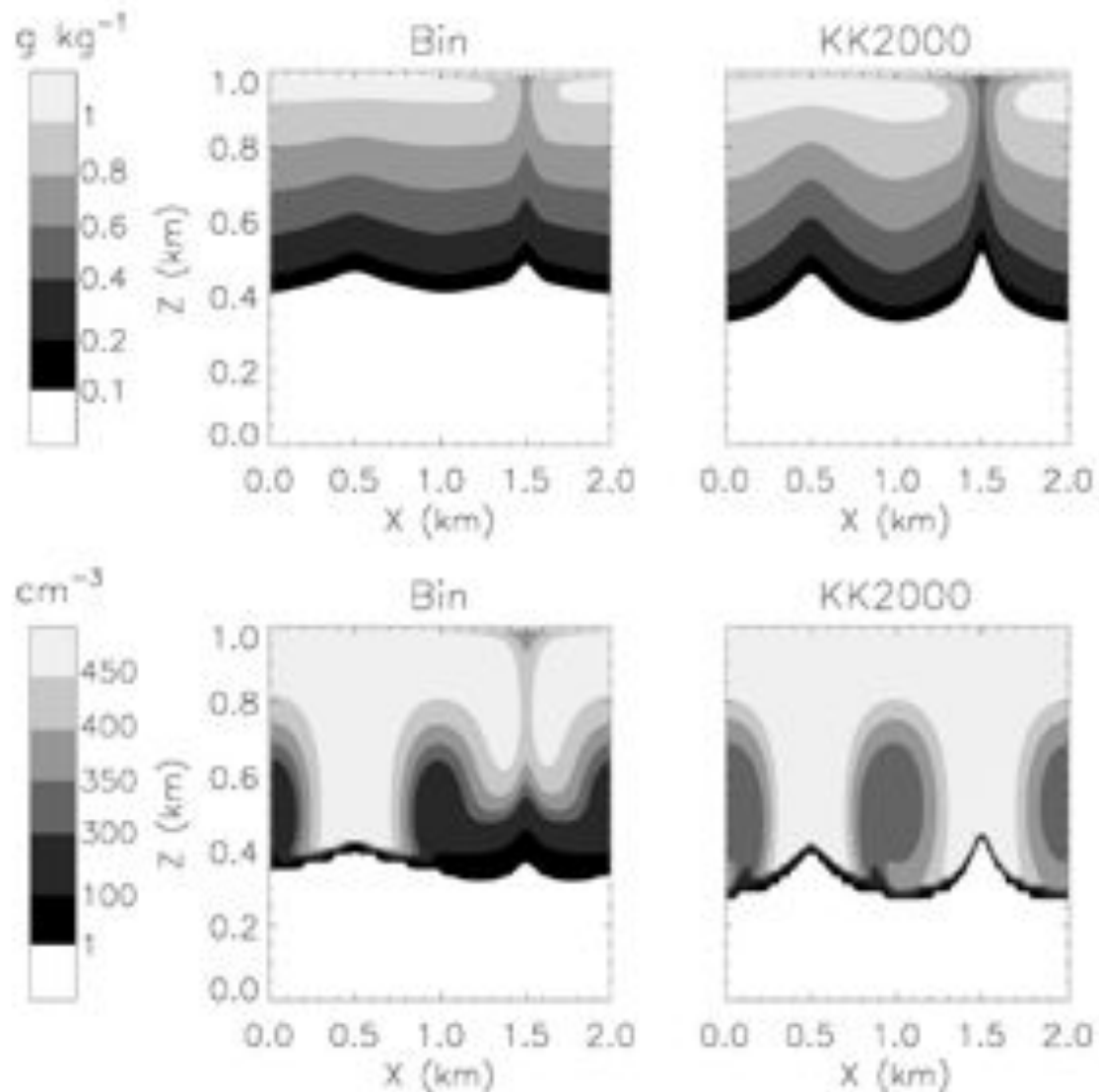


FIG. 5. As in Fig. 4 but for the POLLUTED stratocumulus simulations.

Microphysical transformations during subgrid-scale mixing

- Flexibility to treat any mixing scenario from homogeneous to extremely inhomogeneous.

$$N_f = N_i \left(\frac{q_f}{q_i} \right)^a$$

- $a = 1$: extremely inhomogeneous
- $a = 0$: homogeneous

N – droplet concentration

q – cloud water mixing ratio

N_i, q_i – initial (i.e., after advection and mixing)

N_f, q_f – final (i.e., after advection, mixing, and microphysical adjustment)

Summary:

Warm-rain microphysics: cloud droplet activation, condensational growth, collisional growth.

Entrainment and mixing; impact on cloud microphysics (and connection to indirect aerosol effects).

Modeling warm-rain processes:

- bulk single-moment scheme: mixing ratios for cloud water and drizzle/rain water (activation irrelevant, no information about spectral characteristics, model resolution can be low);

- detailed (bin) microphysics: concentration (per unit mass) of cloud and drizzle/rain drop in each size (mass) category (~100 variables); supersaturation and droplet activation predicted, requires high spatial resolution (especially near cloud base); can be even more complicated if detailed information about aerosols is added;

- double-moment microphysics: mixing ratios and concentrations of cloud and drizzle/rain drops, supersaturation does not have to be predicted (but it can be; e.g., MG scheme), activation either predicted (MG; high resolution needed) or parameterized (low resolution).

...and there is part 2 – ice microphysics...

Cloud droplets and turbulence: a cloud physicist perspective

Wojciech Grabowski

NCAR, Boulder, Colorado, USA

From
“very interesting, but irrelevant”
to
“still interesting and very relevant”

Wojciech Grabowski
NCAR, Boulder, Colorado, USA

Cloud droplets grow by the diffusion of water vapor (i.e., by condensation) and by collision/coalescence.

For both cloud turbulence has thought to play some role...

Turbulent entrainment and mixing affects the spectrum of cloud droplets as well.

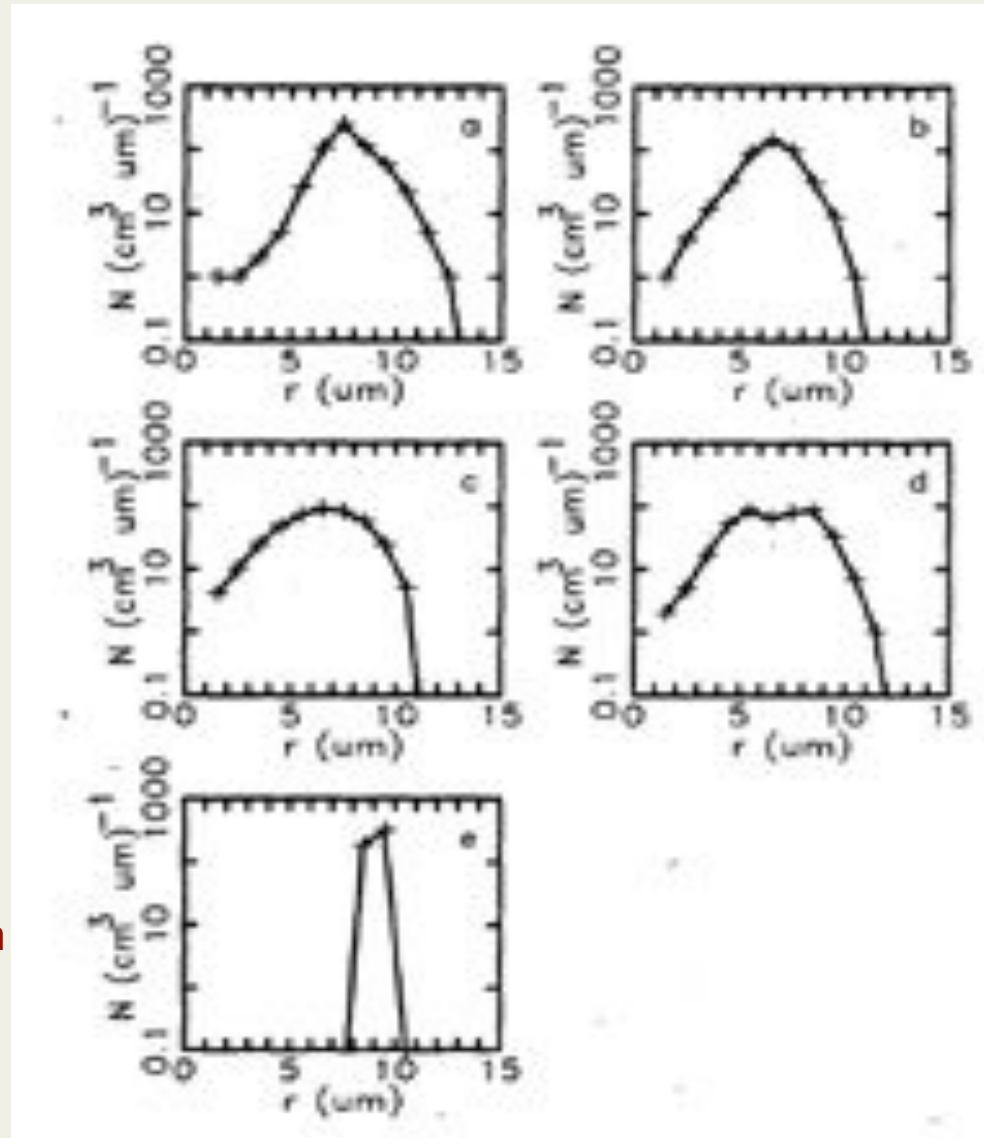
Condensational growth inside “adiabatic cores”: the problem of the width of cloud droplet spectrum.

Observed cloud droplet spectra averaged over ~100m:

observed,
adiabatic fraction
 $AF \approx 1$; $\sigma_r = 1.3 \mu\text{m}$

observed, $AF \approx 0.8$; $\sigma_r = 1.8 \mu\text{m}$

calculated adiabatic
spectrum; $\sigma_r = 0.1 \mu\text{m}$

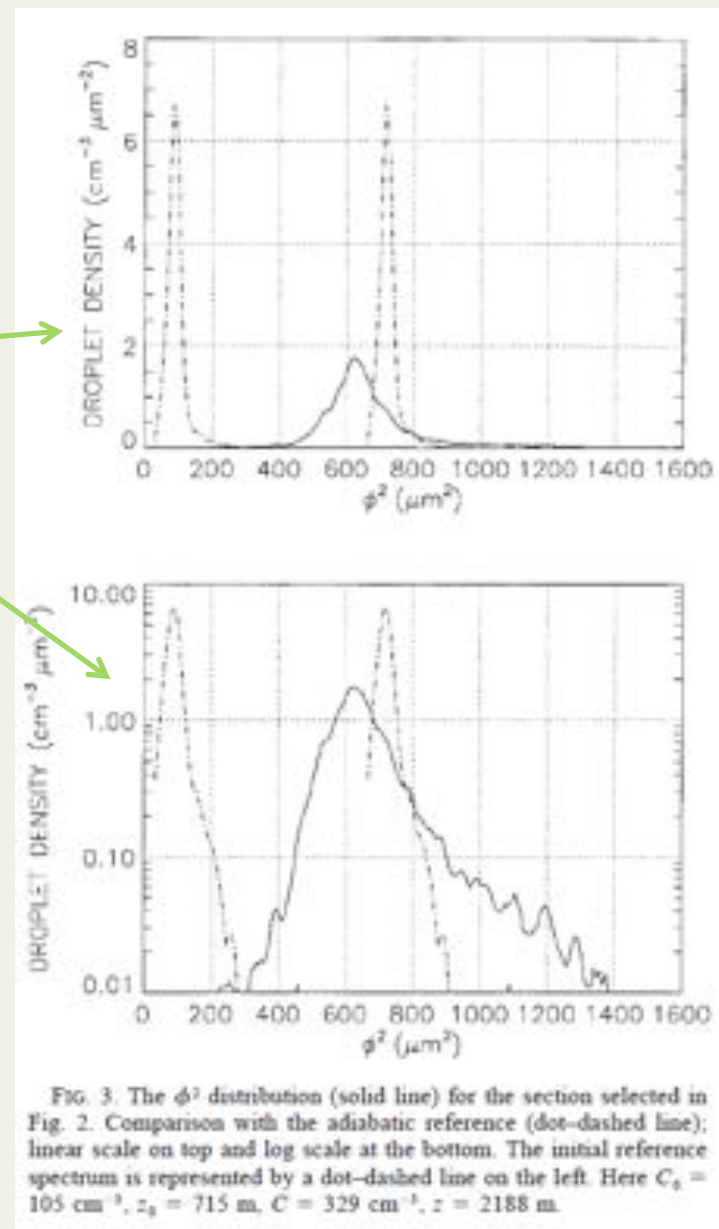
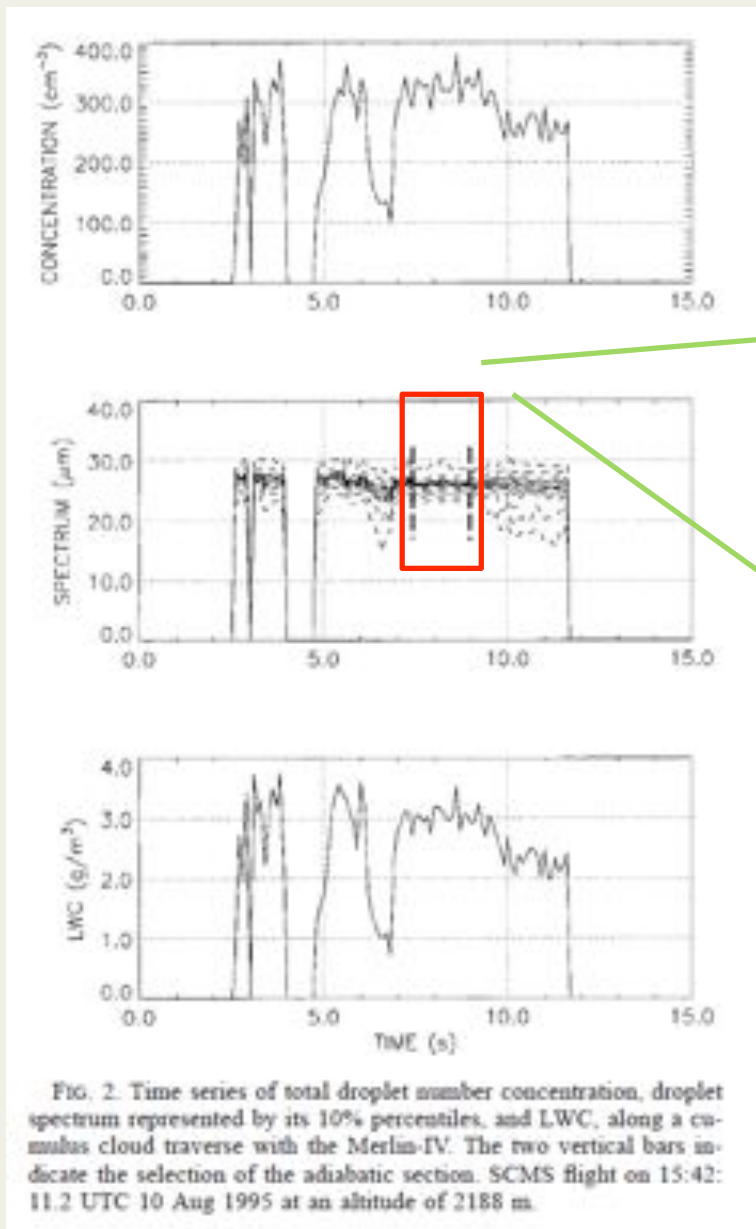


observed, $AF \approx 0.8$;
 $\sigma_r = 1.3 \mu\text{m}$

observed, $AF \approx 1$; bimodal

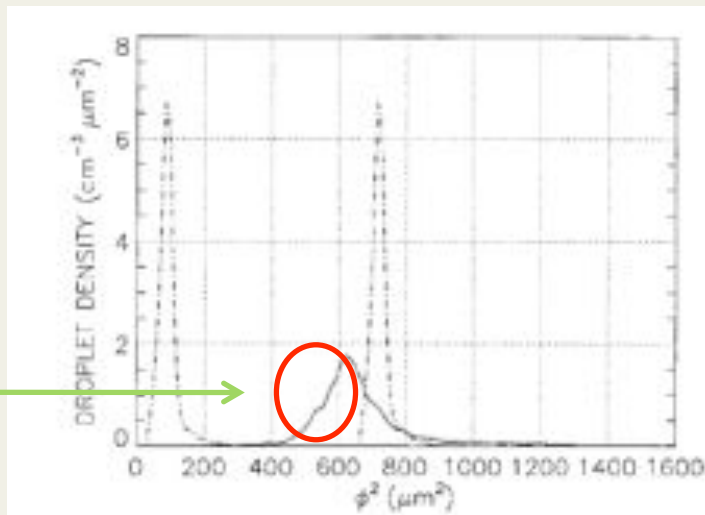
(Jensen et al. JAS 1985)

Cloud droplet spectra in near-adiabatic cores using Fast FSSP



Cloud droplet spectra in near-adiabatic cores using Fast FSSP

Effect of
small
dilution



Instrumental artifacts
(coincidences), possibly
some collisional growth

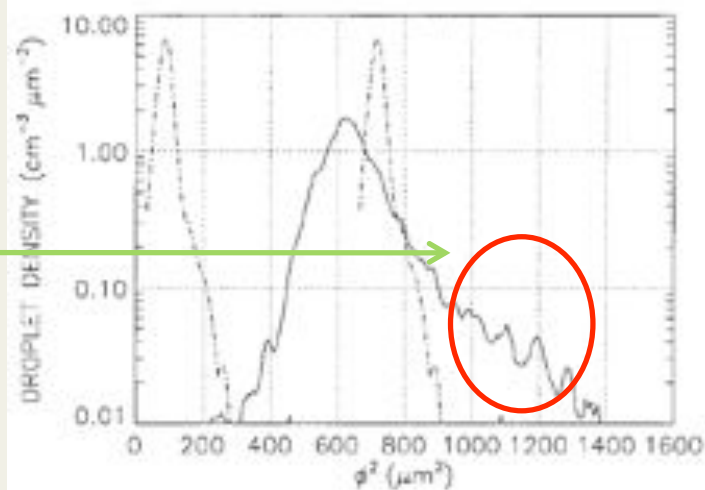
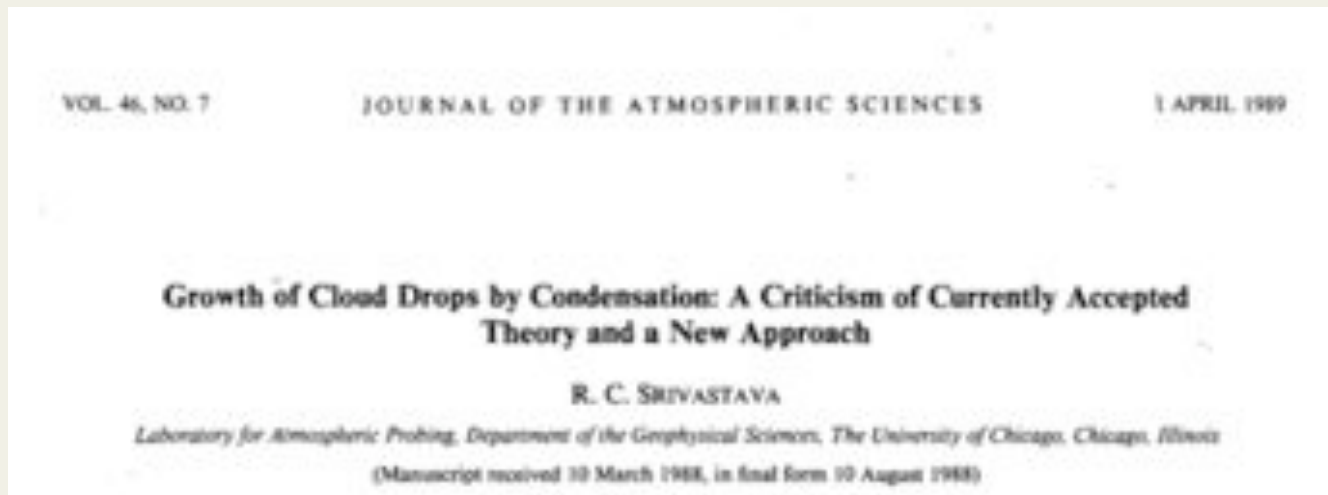


FIG. 3. The ϕ^2 distribution (solid line) for the section selected in Fig. 2. Comparison with the adiabatic reference (dot-dashed line); linear scale on top and log scale at the bottom. The initial reference spectrum is represented by a dot-dashed line on the left. Here $C_0 = 105 \text{ cm}^{-3}$, $z_0 = 715 \text{ m}$, $C = 329 \text{ cm}^{-3}$, $z = 2188 \text{ m}$.

Condensational growth inside “adiabatic cores”: the problem of the width of cloud droplet spectrum.

Srivastava J. Atmos. Sci. 1989.



macroscopic versus microscopic supersaturation

$$\frac{dT}{dt} = -\frac{g}{c_p} w + \frac{L}{c_p} C_d$$

$$\frac{dq_v}{dt} = -C_d$$

$$\frac{dq_c}{dt} = C_d$$

$$q_c \sim Nr^3$$

$$\frac{dq_c}{dt} \sim r^2 \frac{dr}{dt} \sim rS$$

macroscopic
supersaturation

$$S = \frac{q_v}{q_{vs}} - 1$$

$$q_{vs} \sim \frac{e_s(T)}{p}$$

$$\frac{dS}{dt} = \alpha w - \frac{S}{\tau_{qe}}$$

$$\tau_{qe} \sim \frac{1}{Nr}$$

...but the supersaturation can change from one droplet to another locally.

This is concept of *microscopic* supersaturation.

My involvement started in early 1990ies with a PhD student from McGill University, Paul Vaillancourt, together with Peter Yau, a cloud physicist, and Peter Bartello, “a DNS guy”.

The idea was to look at the effects of small-scale turbulence on growth of cloud droplets by the diffusion of water vapor in “an adiabatic core” of a convective cloud using DNS.

The issue: why cloud droplet spectra often appear broader than predicted by the classical theory?

Elementary facts about cloud droplets:

Radius r : 5-30 microns ($r \ll$ Kolmogorov length scale)

Concentration: 50-2,000 cm^{-3} (mean separation distance $\gg r$)

Mass loading: 0.5-5 g kg^{-1} ($\ll 1$; no effects on turbulence)

Can DNS of droplets growing by the diffusion of water vapor be done?

The issue is about the details of droplet growth and small-scale ($\sim 20 r$) temperature and moisture fields that (almost instantaneously, milliseconds) develop near the growing droplet...

Detailed model of droplet growth

$$\frac{\partial T}{\partial t} = k_a \frac{1}{r^2} \frac{\partial}{\partial r} \left(r^2 \frac{\partial T}{\partial r} \right) + F,$$

$$\frac{\partial q}{\partial t} = D_v \frac{1}{r^2} \frac{\partial}{\partial r} \left(r^2 \frac{\partial q}{\partial r} \right) \quad (\text{A1a})$$

with boundary conditions

$$\frac{\partial T}{\partial r} = 0, \quad \frac{\partial q}{\partial r} = 0 \quad \text{for } r = R \quad (\text{A1b})$$

$$T = T_d \quad q = q_s(T_d, p) \quad \text{for } r = R_d, \quad (\text{A1c})$$

where $q_s(T_d, p)$ is the saturated water vapor density, $F = -g/c_p w$ is the external cooling (w is the updraft speed taken as 2 m s^{-1} in both models), and T_d is the droplet temperature predicted from the conservation of heat

$$m_d c_w \frac{dT_d}{dt} = 4\pi L R_d^2 D_v \left(\frac{\partial q}{\partial r} \right)_{r=R_d} + 4\pi \rho_a c_p R_d^2 k_a \left(\frac{\partial T}{\partial r} \right)_{r=R_d} \quad (\text{A2})$$

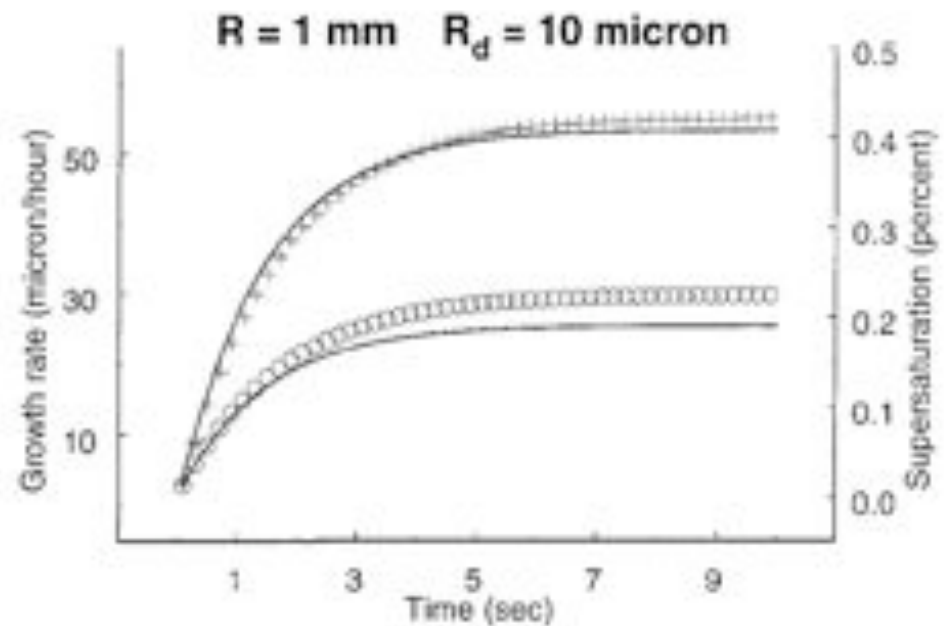


FIG. A1. Evolution of the supersaturation S (bottom curves) from the simple model and the supersaturation at $r = R$ predicted by (A1), as well as the droplet growth rates (top curves) predicted by both models, as a function of time. The symbols (pluses and circles) are for model (A1) and the corresponding solid lines are for the simple model.

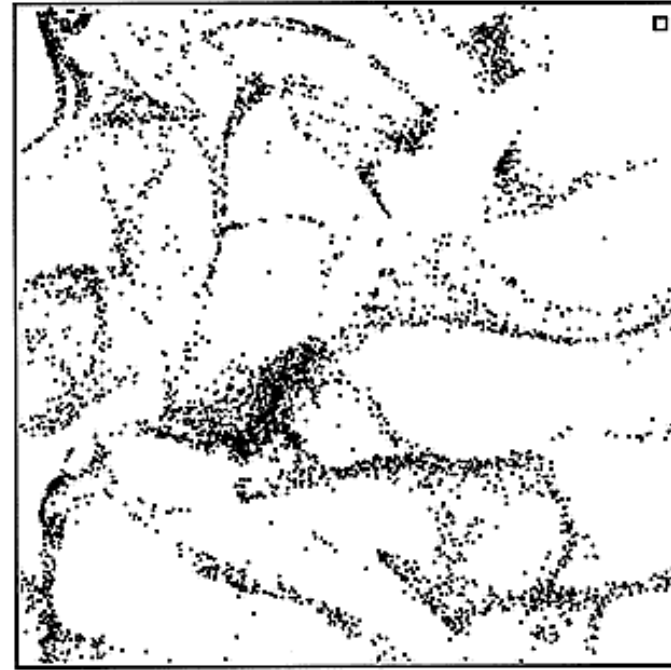
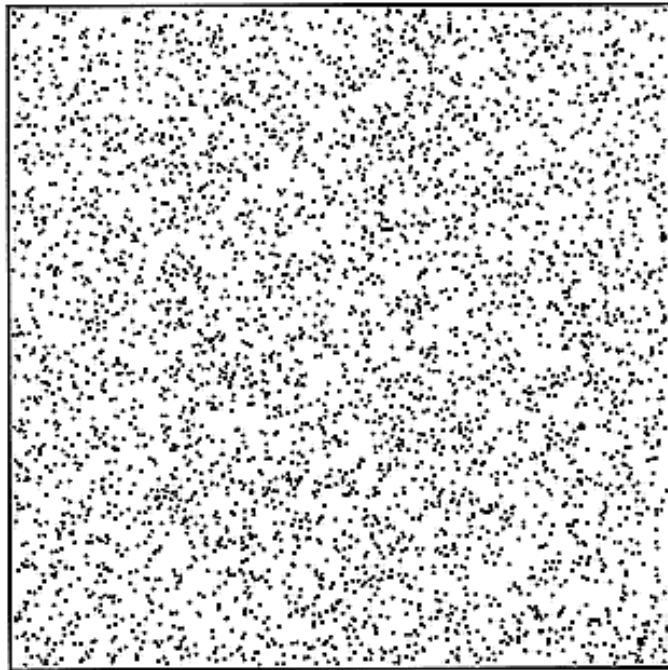
Simple model of droplet growth:
 “macroscopic” model taken to the limit
 of a single droplet in the mean volume
 occupied by a droplet in a cloud.

Vaillancourt et al. 2001

So the answer is YES...

initial conditions

solution at a later time



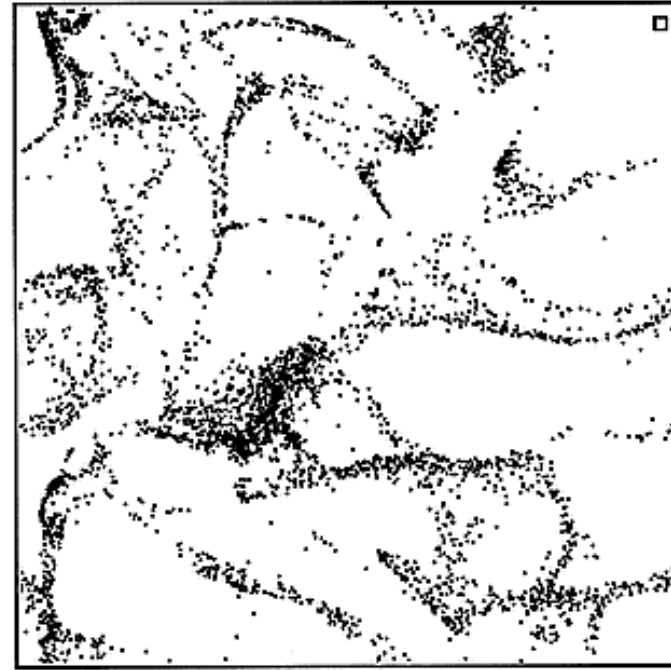
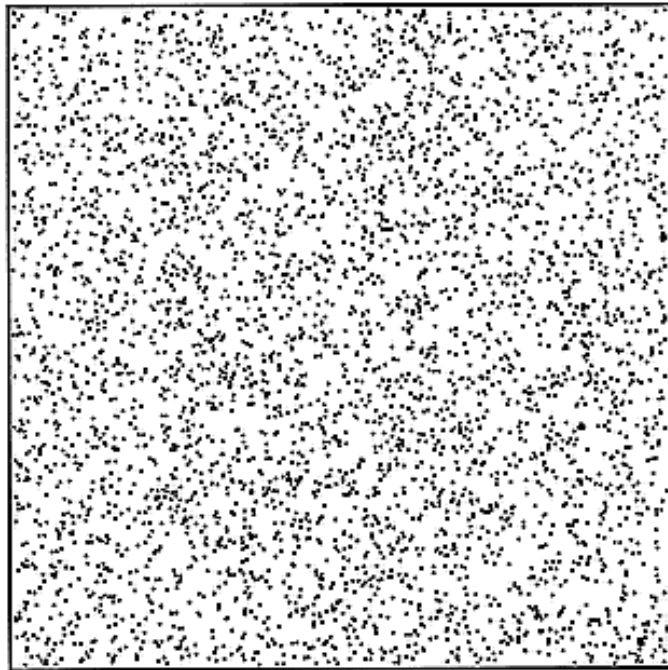
Kolmogorov
scale

Clustering of nonsedimenting particles for $St \sim 1$

Shaw et al. JAS 1998

initial conditions

solution at a later time



Kolmogorov
scale

Clustering of nonsedimenting particles for $St \sim 1$

Is this how cloud microscale looks like?

Not really!....

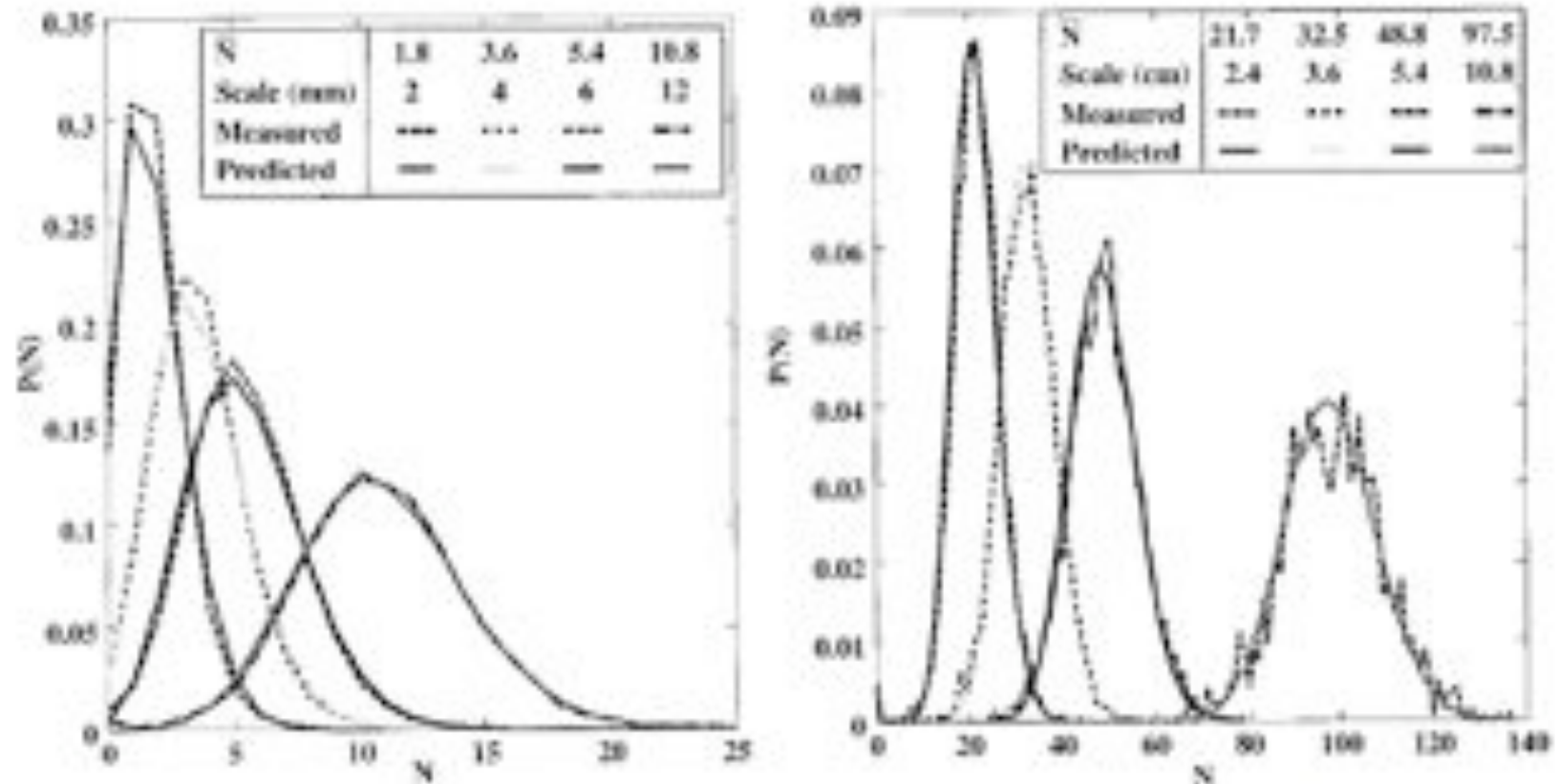


FIG. 1. Probability distribution of the number of counts in actual subsamples (dashed lines), compared to the Poisson distribution (solid lines), for various values of subsample sizes, i.e., of N . The corresponding spatial scale is indicated in the legend. SCMS sample, at 1542-18.6 UTC 10 Aug 1995 (duration: 1.6 s): $z = 2188$ m, $C = 329$ cm⁻², $\bar{\phi} = 25.7$ μ m.

Parameters describing interaction of cloud droplets with turbulence for the case with gravity:

Stokes number: $St = \tau_p / \tau_\eta$

τ_p - droplet response time

τ_η - Kolmogorov timescale

Nondimensional sedimentation velocity: $Sv = v_p / v_\eta$

v_p - droplet sedimentation velocity ($g\tau_p$ for small droplets)

v_η - Kolmogorov velocity scale

Nondimensional parameters (*St* and *Sv*) for typical cloud conditions: *St* \ll *Sv*

<i>R</i> μm	<i>v_t</i> cm s ⁻¹	<i>t_p</i> s	ϵ m ² s ⁻³ <i>v_η</i> cm s ⁻¹ <i>t_η</i> s	Kolmogorov velocity scale		
				<i>St</i>	<i>Sv</i>	<i>St</i>
			10 ⁻⁴	10 ⁻³	10 ⁻²	
			0.64	1.10	2.00	
			0.41	0.13	4.1 × 10 ⁻²	
5	0.32	3.3 × 10 ⁻⁴	<i>St</i>	8.0 × 10 ⁻⁴	2.5 × 10 ⁻³	8.0 × 10 ⁻³
			<i>Sv</i>	0.50	0.28	0.16
15	2.7	2.9 × 10 ⁻³	<i>St</i>	7.0 × 10 ⁻³	2.2 × 10 ⁻²	7.0 × 10 ⁻²
			<i>Sv</i>	4.2	2.4	1.3
25	7.5	8.2 × 10 ⁻³	<i>St</i>	2.0 × 10 ⁻²	6.3 × 10 ⁻²	0.20
			<i>Sv</i>	12	6.6	3.7

Dissipation rate time scale
 Kologorov velocity scale
 Kolmogorov
 droplet radius
 sedimentation velocity
 response time

Nondimensional parameters (*St* and *Sv*) for typical engineering applications: ***St* >> *Sv***

<i>R</i> μm	<i>v_t</i> cm s ⁻¹	<i>t_p</i> s	ϵ m ² s ⁻³	<i>v_η</i> cm s ⁻¹	<i>t_η</i> s
				11.00	1.3 × 10 ⁻³
				10	
5	0.32	3.3 × 10 ⁻⁴	<i>St</i>	0.25	
			<i>S_v</i>	2.8 × 10 ⁻²	
15	2.7	2.9 × 10 ⁻³	<i>St</i>	2.2	
			<i>S_v</i>	0.24	
25	7.5	8.2 × 10 ⁻³	<i>St</i>	6.3	
			<i>S_v</i>	0.66	

$$St / Sv \sim \epsilon^{3/4} \quad (\text{for Stokes limit: } \mathbf{v}_p = g\tau_p)$$

Flow: DNS model

Droplets: position traced in time and space

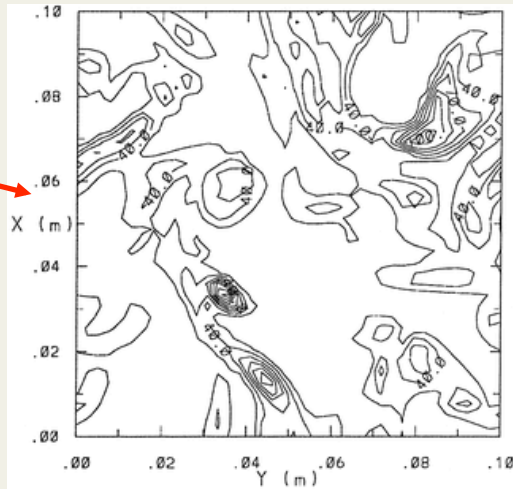
$$\tau_p \frac{d\mathbf{V}(t)}{dt} = \mathbf{U}[\mathbf{X}(t), t] - \mathbf{V}(t) + \mathbf{V}_T,$$
$$\frac{d\mathbf{X}(t)}{dt} = \mathbf{V}(t),$$

Size: growth in local conditions

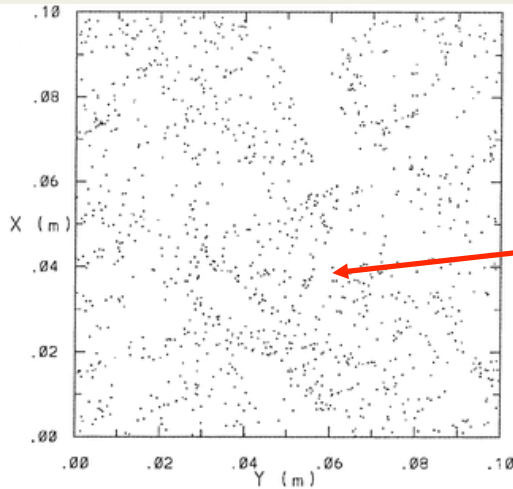
$$\frac{dr}{dt} = A \frac{S}{r} \quad S - \text{local supersaturation}$$

DNS simulations with sedimenting droplets for conditions relevant to cloud physics ($\epsilon=160 \text{ cm}^2\text{s}^{-3}$)

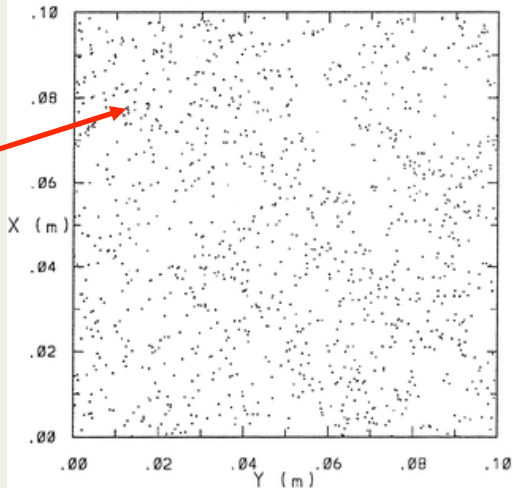
Vorticity
(contour 15 s^{-1})



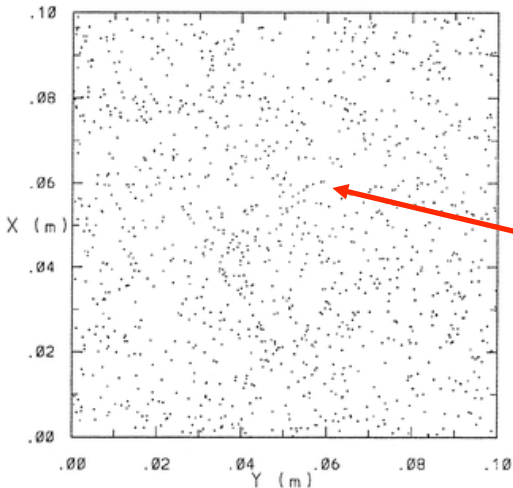
$r=20$ micron

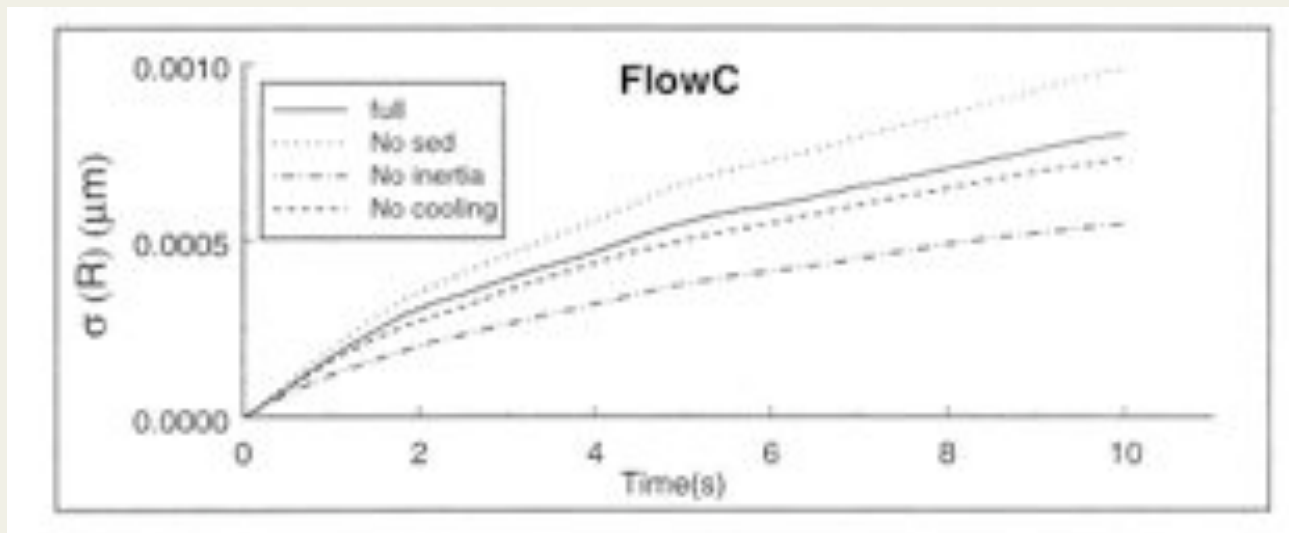


$r=15$ micron



$r=10$ micron





Main conclusion: small-scale turbulence has a very small effect...

For a given flow, it was found that both preferential concentration and the cooling term have a broadening effect on the size distribution. It was also shown that sedimentation of droplets cannot be neglected since it significantly reduces the broadening.

.....

The above results are a consequence of the decrease in decorrelation time and an increase in preferential concentration as the intensity of turbulence increases. In other words, the stronger deviations in droplet concentration from the mean when preferential concentration occurs does result in a wider instantaneous supersaturation perturbation distribution. However, this does not compensate for the fact that, on average, the droplets are exposed to these perturbations for a shorter and shorter time as turbulence intensity increases.

Based on the results obtained, and keeping in mind the limitations of the approach described in the introduction, we now answer the central question posed in the following way. The *microscopic approach*, which takes into account nonuniformity in the spatial distribution of the size and position of droplets and variable vertical velocity in a turbulent medium, does *not* lead to significant broadening of the droplet size distribution.

What about those DNS limitations?

Argument: if Re increases (i.e., the range of scales involved increases), can supersaturation fluctuation increase as well?

Yes, but only to some point...

The brake on supersaturation fluctuations:

$$\frac{dS}{dt} = \alpha w - \frac{S}{\tau_{qe}}$$

$$\tau_{qe} \sim 1 \text{ sec}$$

$$\frac{dS}{dt} \equiv 0 \rightarrow S_{qe} = \alpha w \tau_{qe}$$

TABLE 1. Time constant characterizing supersaturation.
(Values of $\tau = 1/(a_2 I)$ s for $p = 771$ mb, $T = 4.3^\circ\text{C}$)

Radius (μm)	Droplet concentration (cm^{-3})			
	100	300	500	1000
2	14.1	4.7	2.8	1.4
3	8.7	2.9	1.7	0.87
5	4.9	1.6	0.98	0.49
10	2.3	0.77	0.46	0.23

Politovich and Cooper, JAS 1988

For eddies with time-scale larger than τ_{qe} , S is limited to S_{qe} !!!

The break on supersaturation fluctuations:

$$\frac{dS}{dt} = \alpha w - \frac{S}{\tau_{qe}}$$

Latent
heating!!!

$$\tau_{qe} \sim 1\text{sec}$$

$$\frac{dS}{dt} \equiv 0 \rightarrow S_{qe} = \alpha w \tau_{qe}$$

For me, as a cloud physicist, the story is finished.

There might be some minor effects (perhaps worth exploring), but this would contribute little to the cloud physics. Not to mention that more recent observations do not support the broadening controversy concerning spectral broadening in “adiabatic cores”.

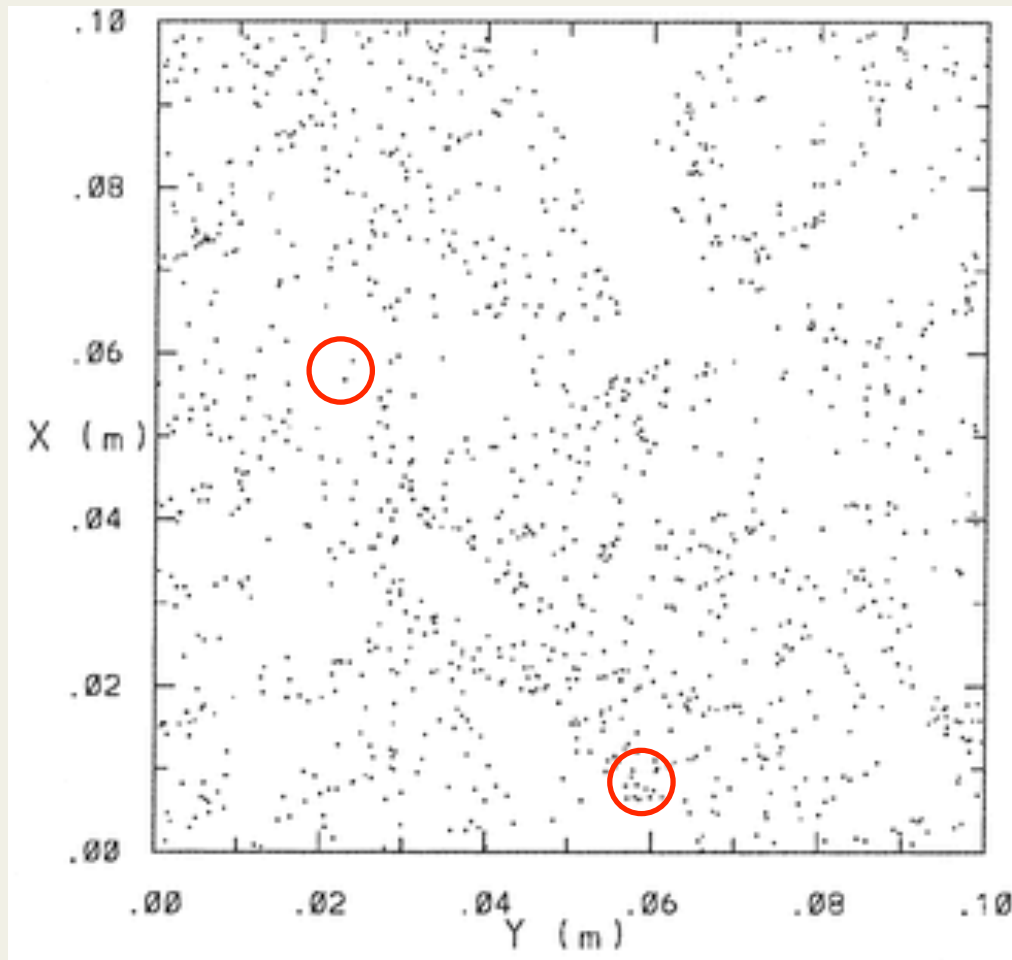
Point that I made but is worth emphasizing here:
studies without gravity and latent heating are irrelevant to cloud physics...

Another way to think about this problem:

Condensational growth is reversible: droplets grow more in higher S , and then less in lower S , and the two situations change rapidly...

But if you think about the collisional growth, then the story is different: growth is not reversible...

Growth by collision/coalescence: nonuniform distribution of droplets in space affects droplet collisions...



Three basic mechanisms of turbulent enhancement of gravitational collision/coalescence:

-Turbulence modifies local droplet concentration (preferential concentration effect)

-Turbulence modifies relative velocity between colliding droplets (e.g., small-scale shears, fluid accelerations)

- Turbulence modifies hydrodynamic interactions when two droplets approach each other

Three basic mechanisms of turbulent enhancement of geometric collisions
gravitational collision/coalescence: (no hydrodynamic interactions)

-Turbulence modifies local droplet concentration (preferential concentration effect)

-Turbulence modifies relative velocity between colliding droplets (e.g., small-scale shears, fluid accelerations)

- Turbulence modifies hydrodynamic interactions when two droplets approach each other

Three basic mechanisms of turbulent enhancement of gravitational collision/coalescence:

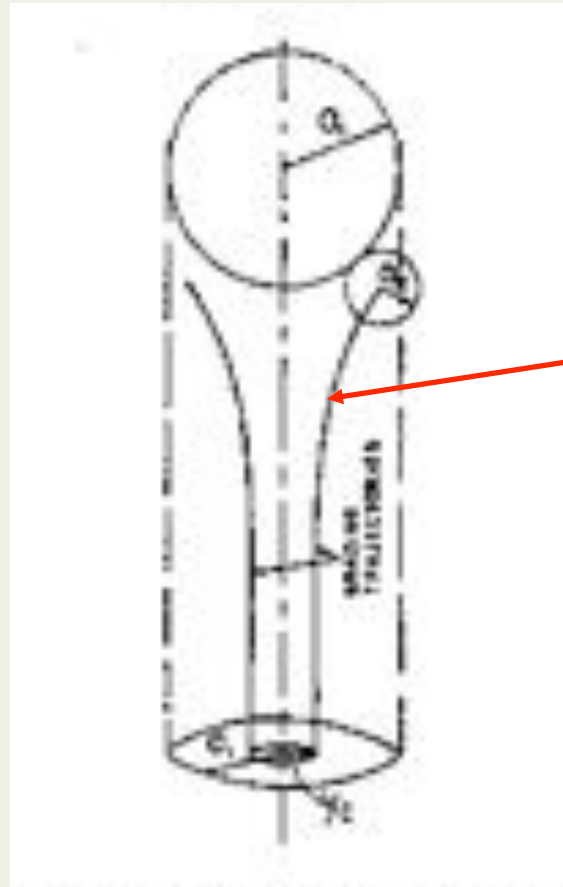
-Turbulence modifies local droplet concentration (preferential concentration effect)

-Turbulence modifies relative velocity between colliding droplets (e.g., small-scale shears, fluid accelerations)

- Turbulence modifies hydrodynamic interactions when two droplets approach each other

collision efficiency

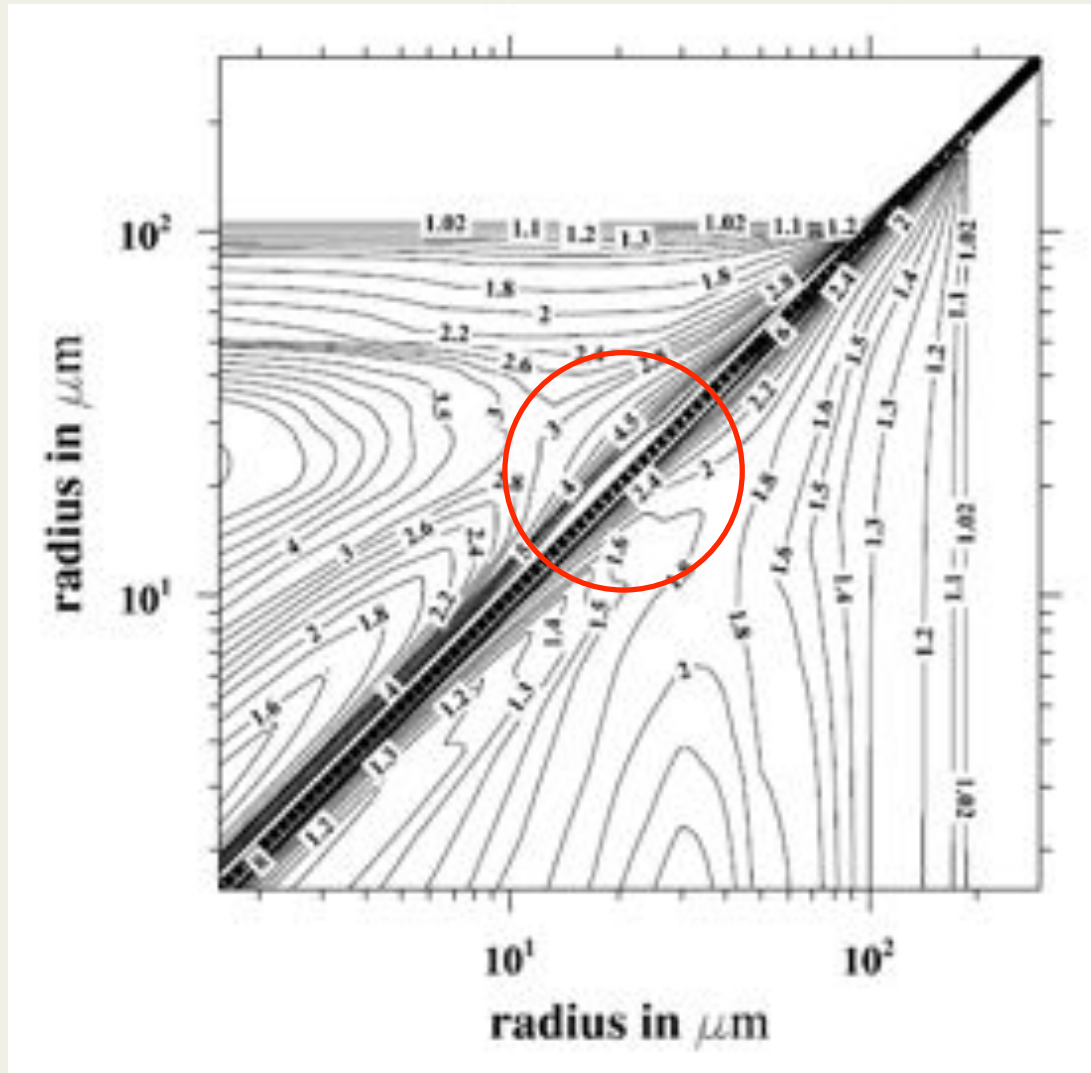
Collision efficiency E_c for the gravitational case:



Grazing trajectory

$$E_c = \frac{y_c^2}{(a_1 + a_2)^2}$$

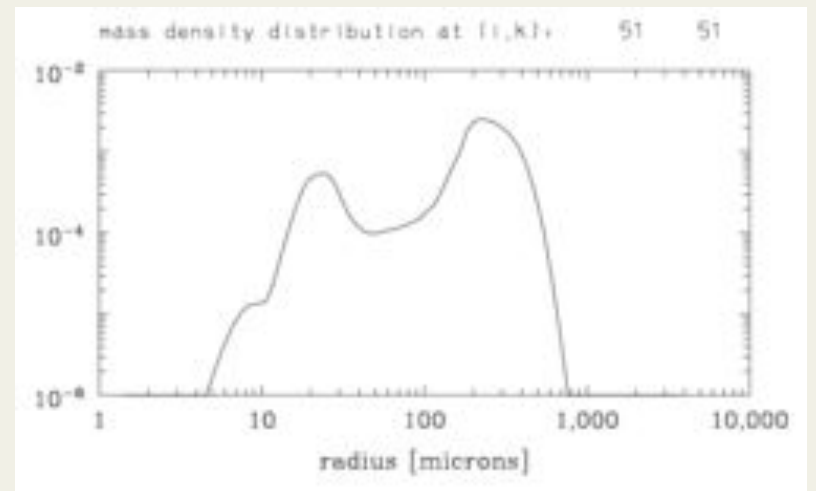
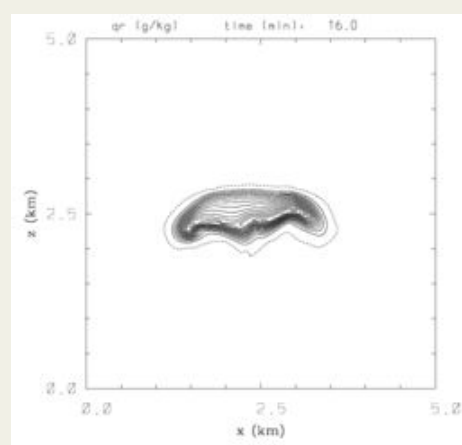
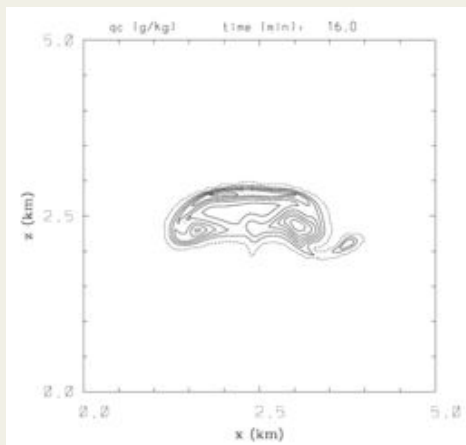
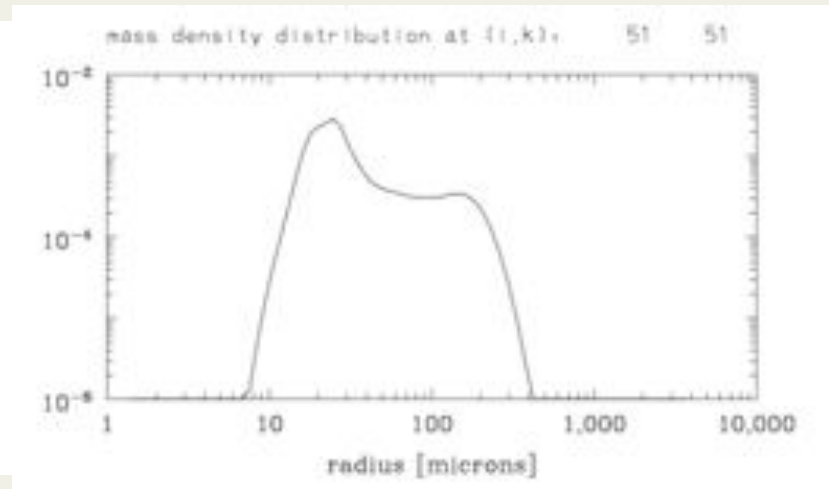
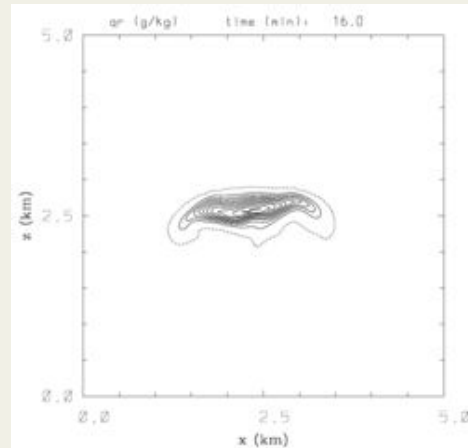
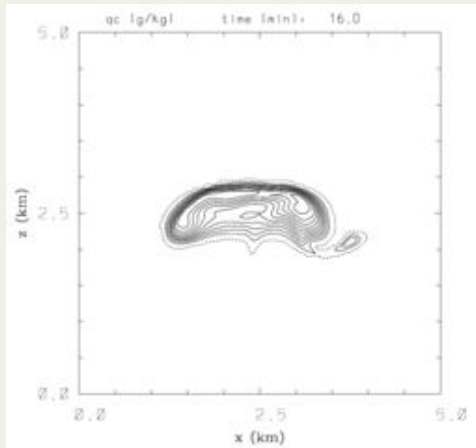
...see Lian-Ping Wang for details how DNS can be extended to guide models of turbulent droplet collision enhancement...



Enhancement factor for the collision kernel (the ratio between turbulent and gravitation collision kernel in still air) including turbulent collision efficiency; $\varepsilon = 100$ and $400 \text{ cm}^2 \text{ s}^{-3}$.

2D simulation of a small precipitating cloud: $t=16$ min

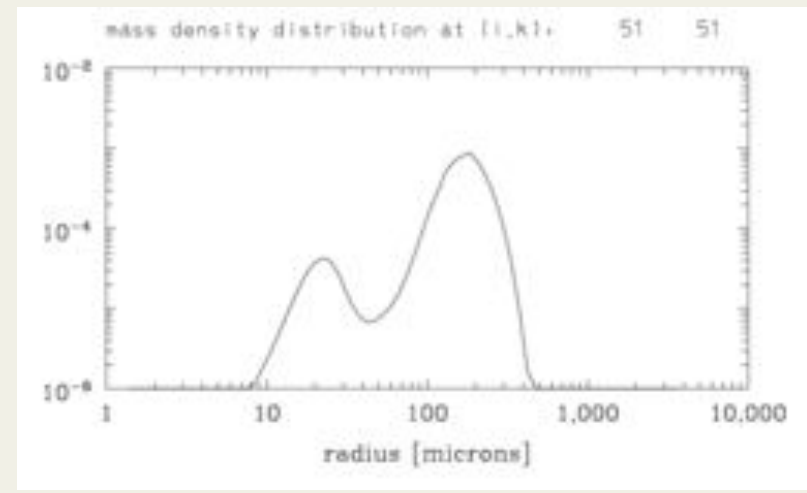
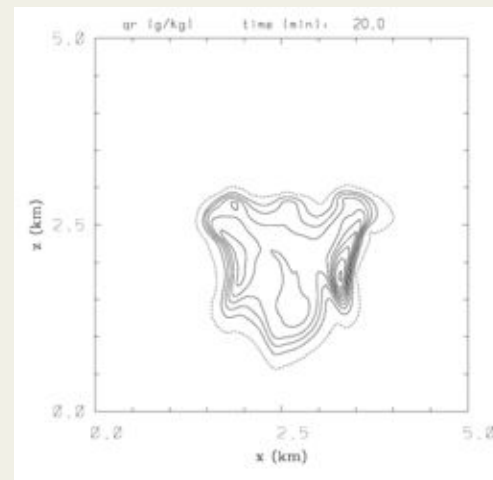
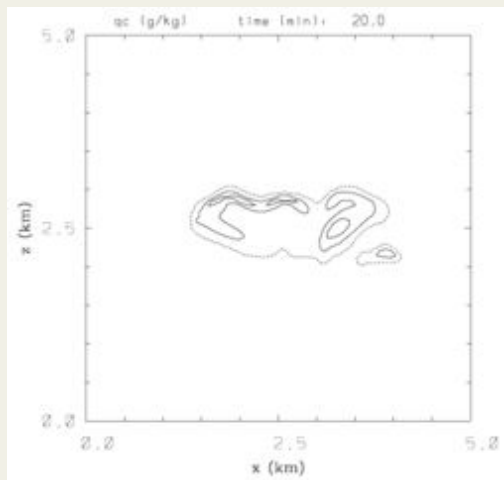
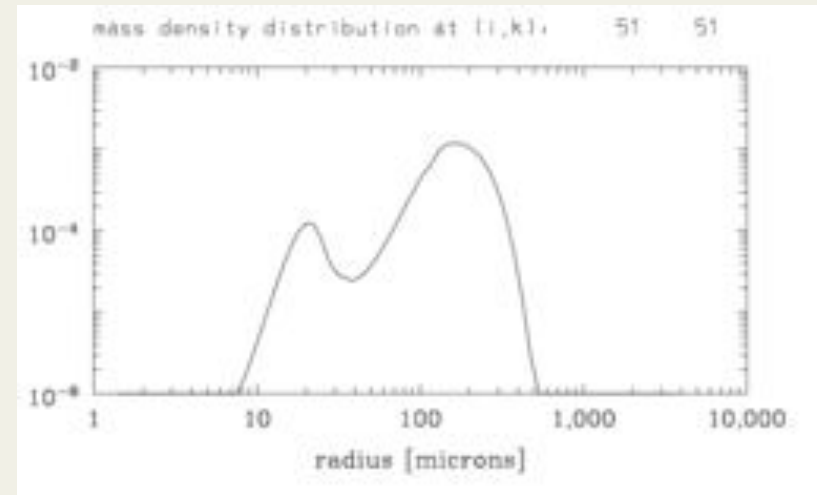
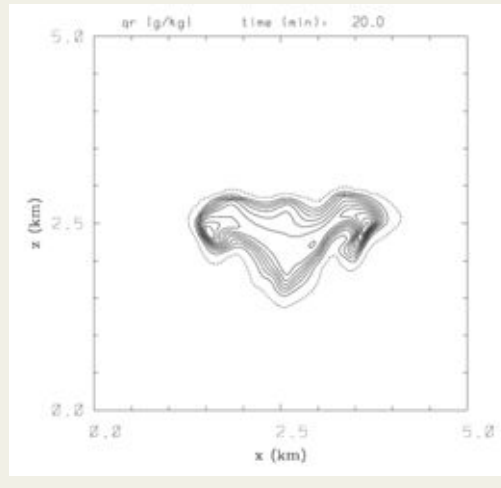
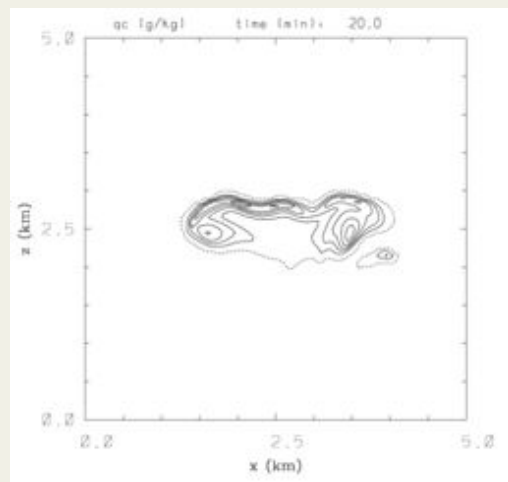
no turbulence



with turbulence – Ayala kernel with $100 \text{ cm}^2\text{s}^{-3}$

2D simulation of a small precipitating cloud: $t=20$ min

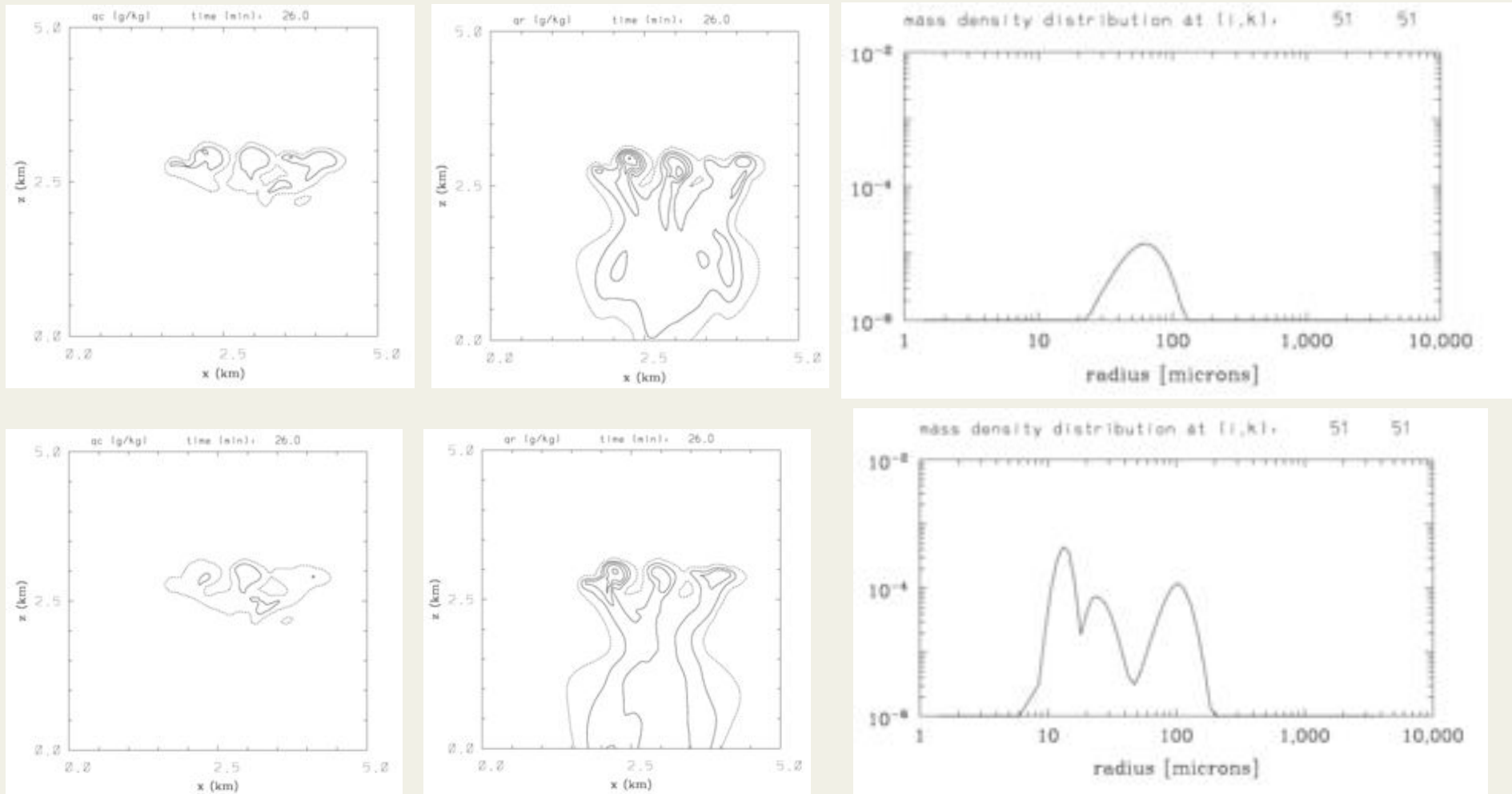
no turbulence



with turbulence – Ayala kernel with $100 \text{ cm}^2\text{s}^{-3}$

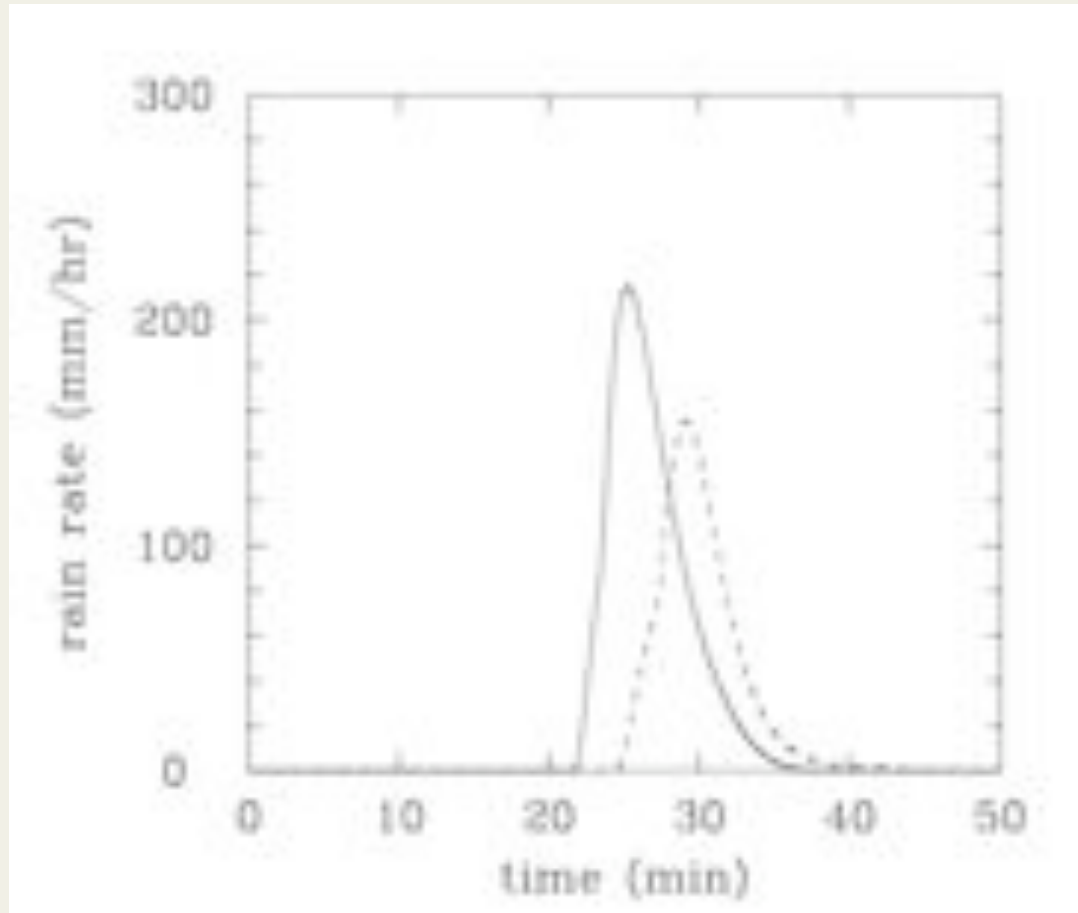
2D simulation of a small precipitating cloud: $t=26$ min

no turbulence

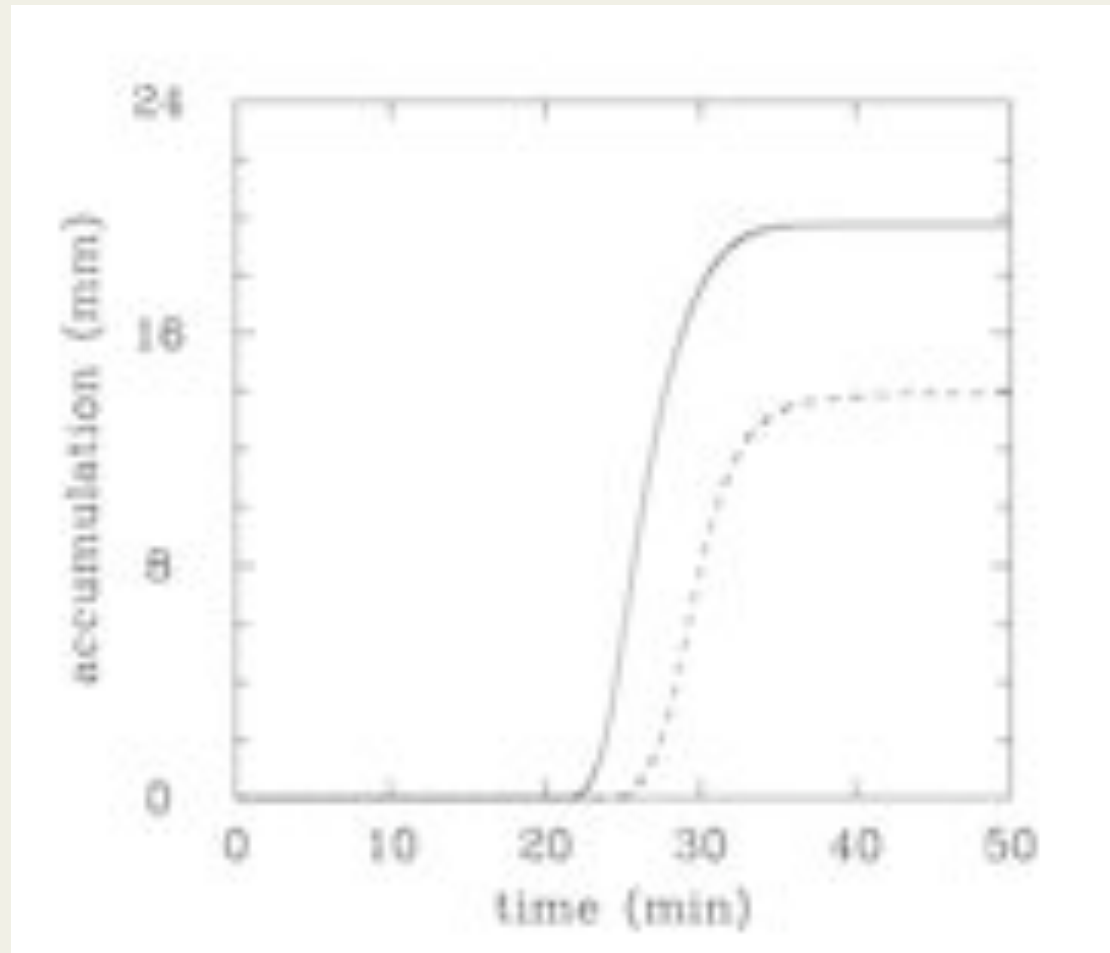


with turbulence – Ayala kernel with $100 \text{ cm}^2 \text{ s}^{-3}$

Surface precipitation intensity evolution: turbulent collisions lead to earlier rain at the ground and higher peak intensity...



...but also to more rain at the surface. This implies higher precipitation efficiency!

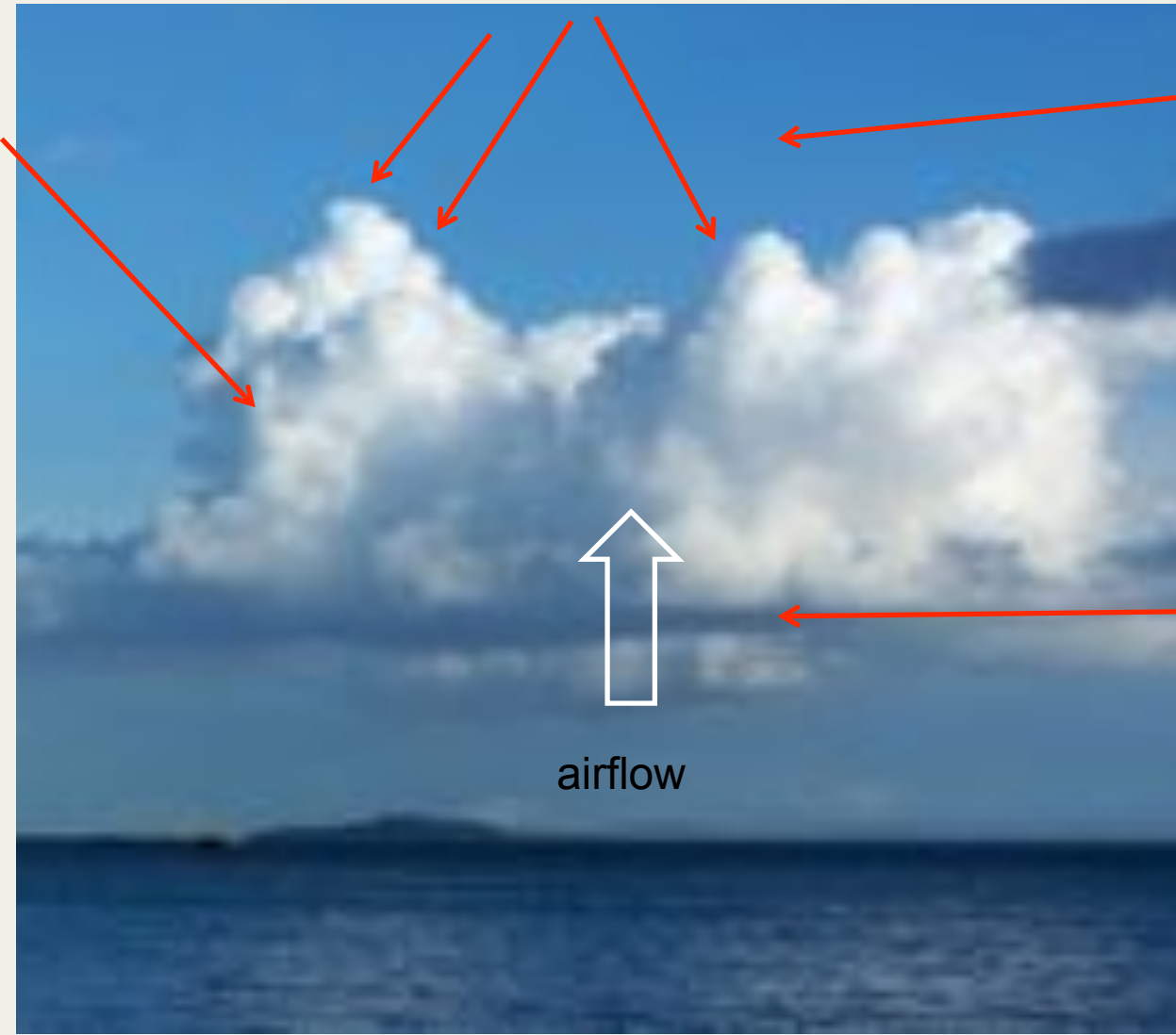


Entrainment/mixing and the cloud droplet spectra

turbulent
cloud

interfacial
instabilities

calm (low-
turbulence)
environment



cloud base
(activation of
cloud droplets)

airflow



droplet
spectra

vertical and
along-track
velocity

liquid water
content

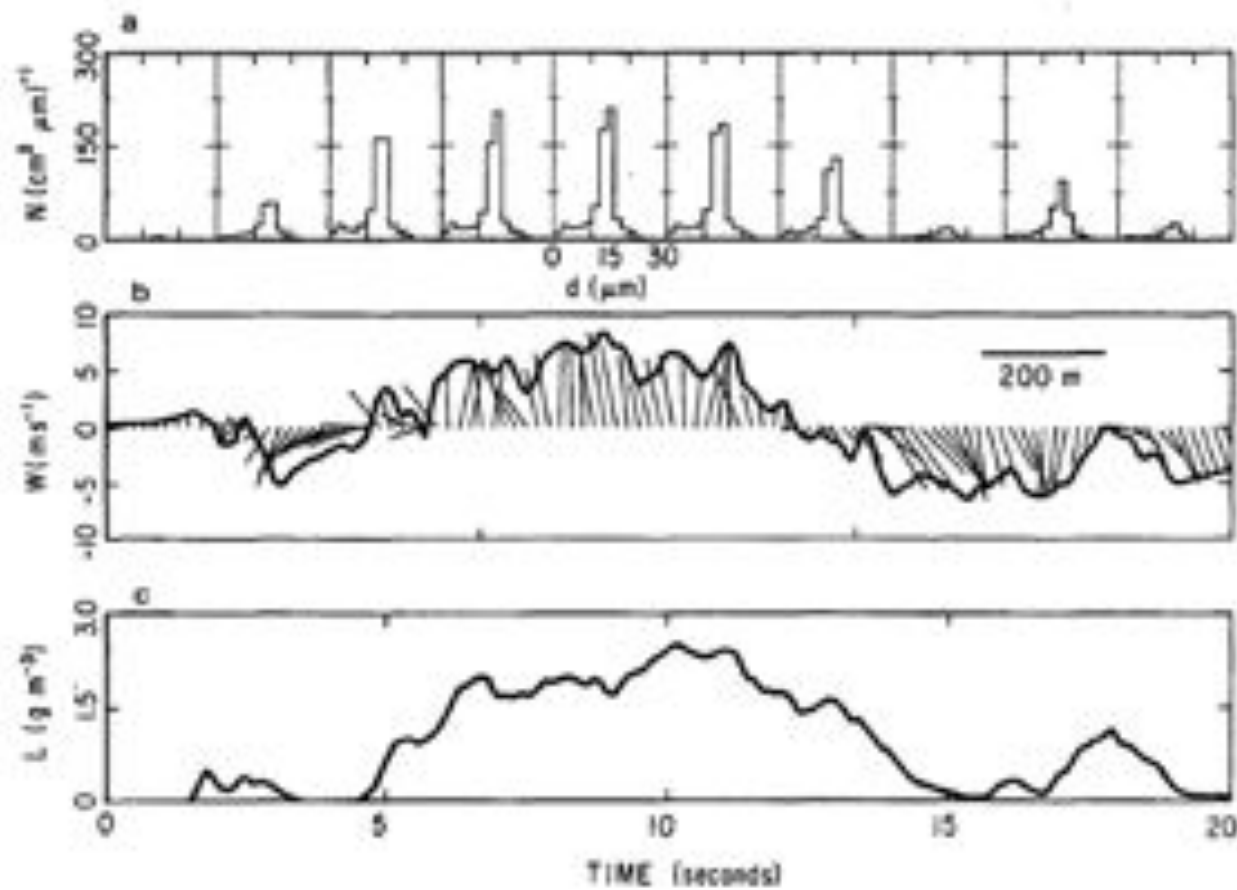


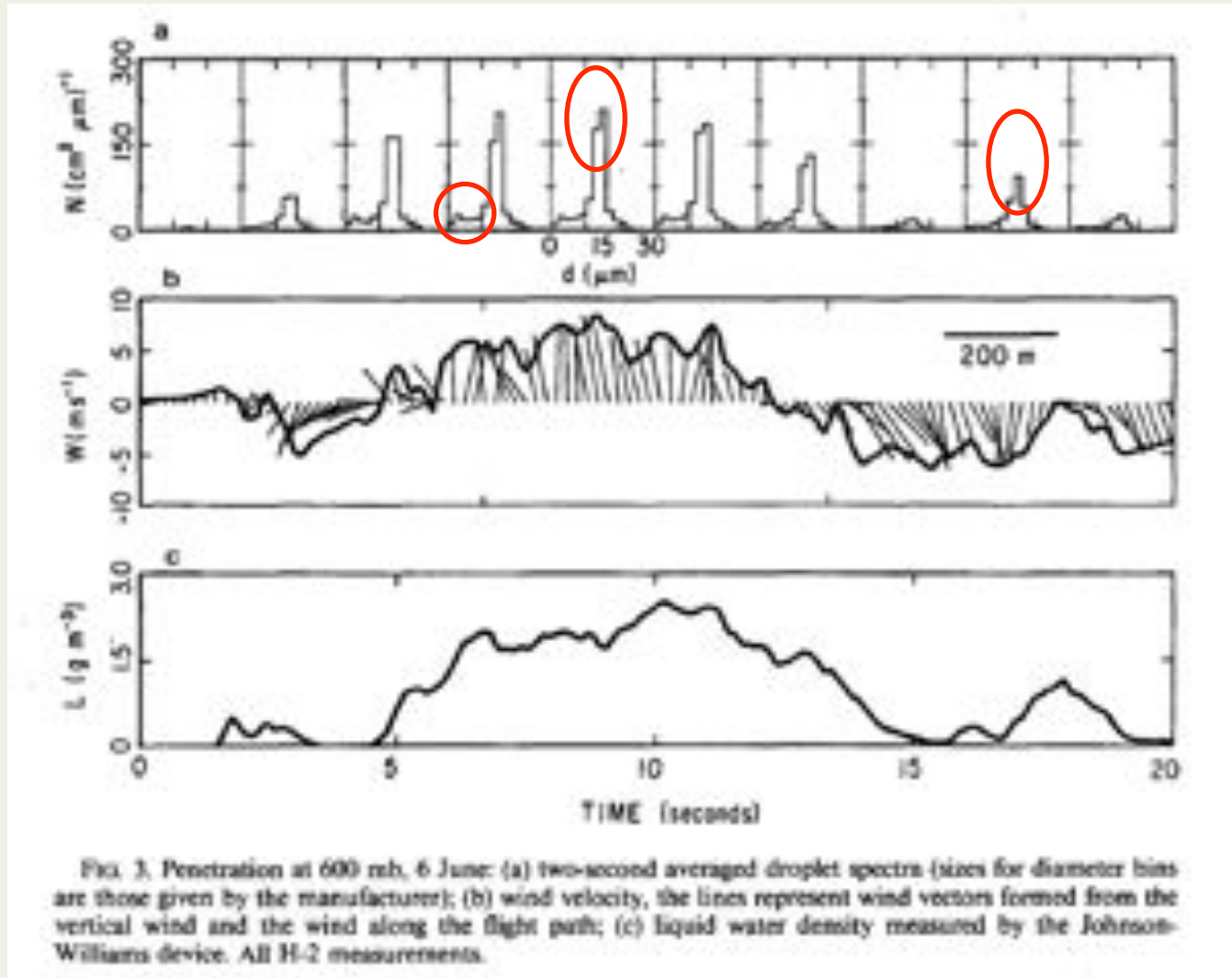
FIG. 3. Penetration at 600 mb, 6 June: (a) two-second averaged droplet spectra (sizes for diameter bins are those given by the manufacturer); (b) wind velocity, the lines represent wind vectors formed from the vertical wind and the wind along the flight path; (c) liquid water density measured by the Johnson-Williams device. All H-2 measurements.

(Austin et al. JAS 1985)

droplet spectra

vertical and along-track velocity

liquid water content



(Austin et al. JAS 1985)

The Water Content of Cumuliform Cloud

By J. WARNER, Radiophysics Laboratory, C.S.I.R.O., Sydney

(Manuscript received April 5, 1955)

Abstract

Measurements have been made of liquid water content throughout many cumuliform clouds. The amount of water present at any level was always less than the adiabatic value, and the ratio of these two quantities decreased with height above cloud base. This ratio was found to be independent of the horizontal extent of the cloud except in the case of very small clouds. The transition between clear air and dense cloud was frequently abrupt.

I. WARNER

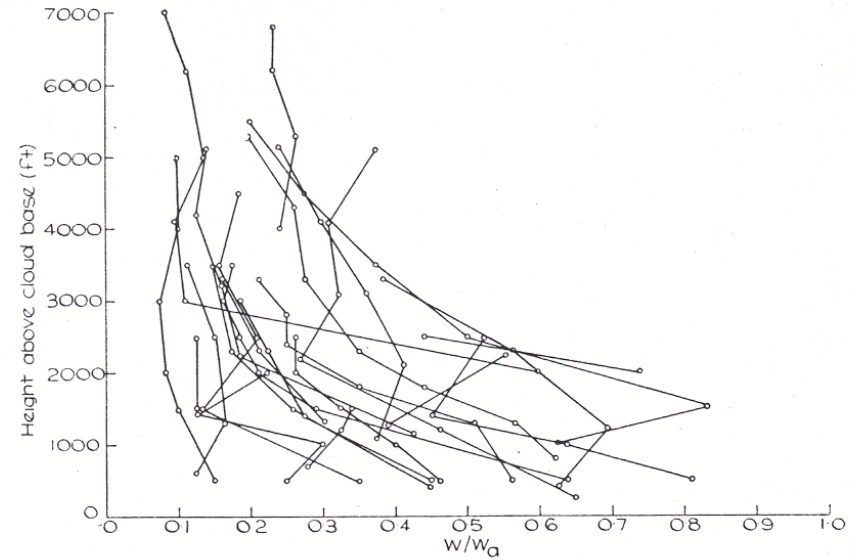


Fig. 7. Ratio of observed liquid water content to adiabatic value versus height above base.

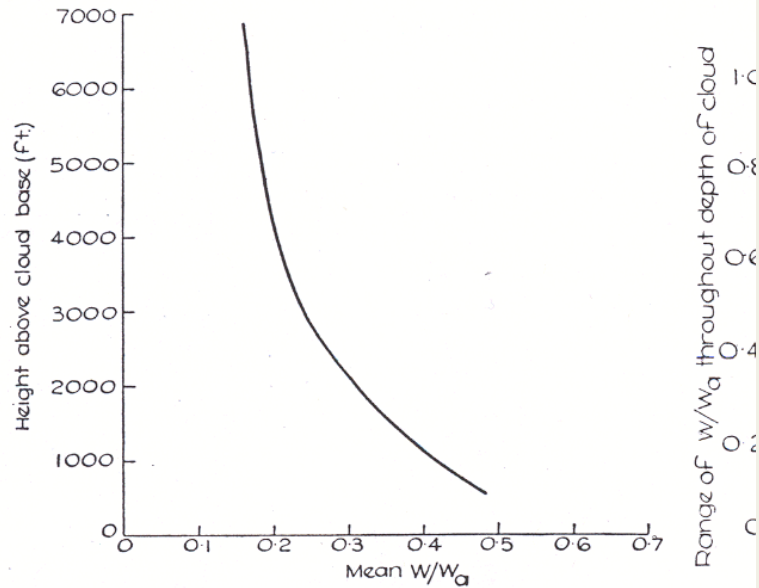
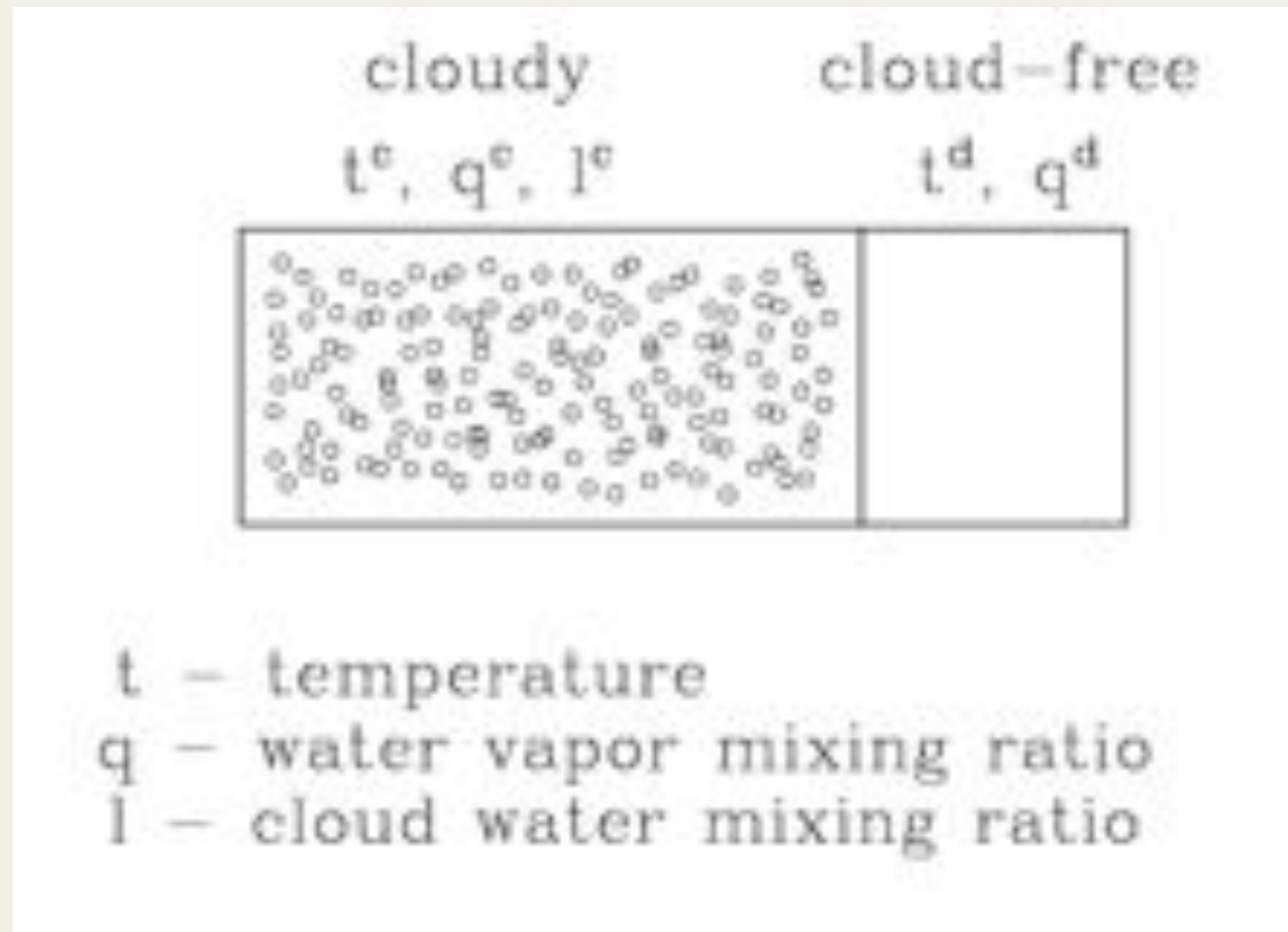


Fig. 8. Mean ratio W/W_a versus height above base.



Fig

Bulk mixing between cloudy and cloud-free air (adiabatic, isobaric)



What is wrong with this picture?

time-scale for cloud droplet evaporation τ_d :

$$\tau_d \equiv r \left(\frac{dr}{dt} \right)^{-1} = \frac{r^2}{A(1 - RH)}$$

r - droplet radius, $A \approx 10^{-10} \text{ m}^2\text{s}^{-1}$, RH - relative humidity

$$\begin{aligned} \tau_d &\approx 1 \text{ s for } RH=0.1 \\ \tau_d &\approx 10 \text{ s for } RH=0.9 \end{aligned}$$

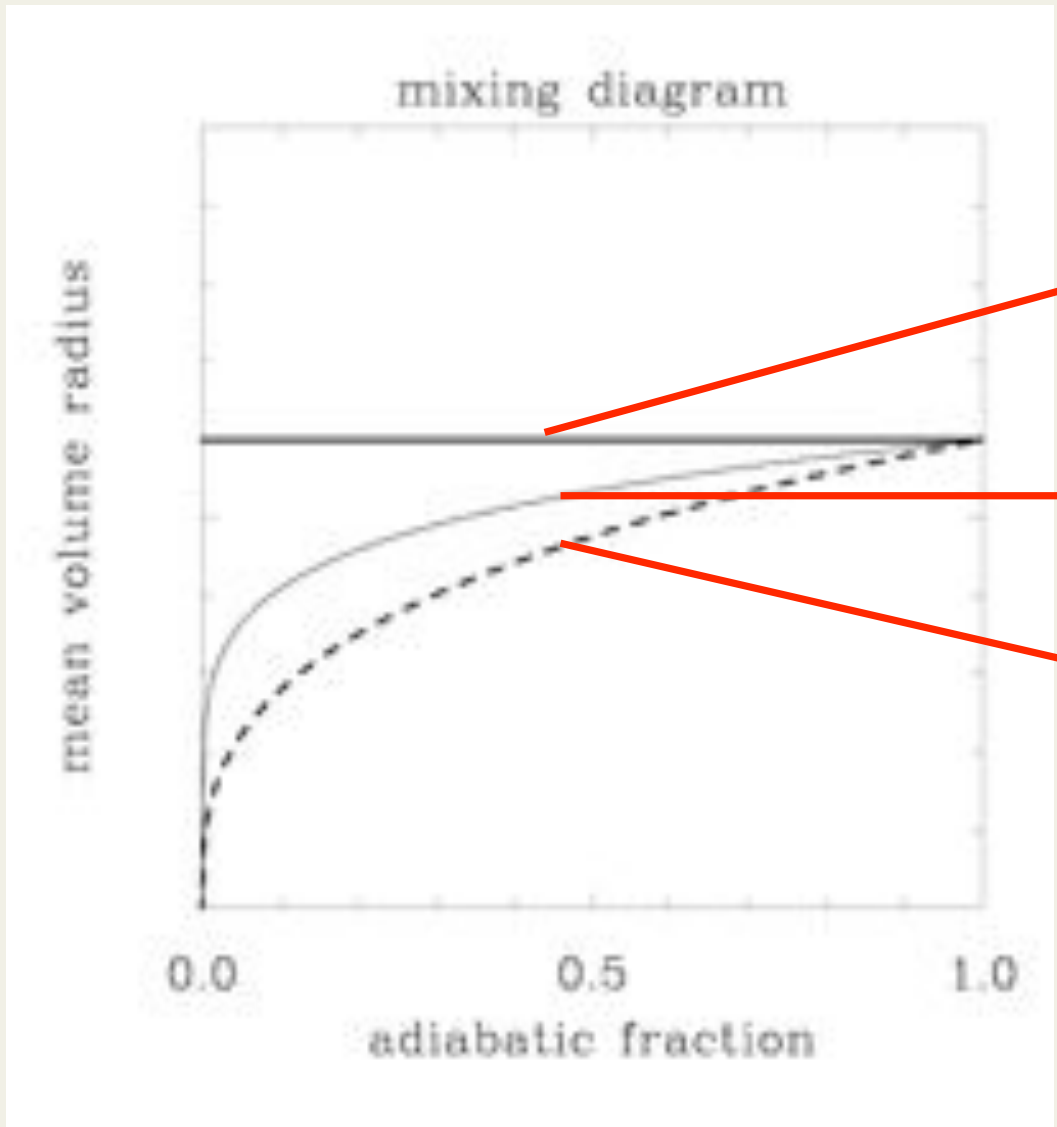
time-scale for turbulent homogenization τ_t :

$$\tau_t \equiv \frac{L}{U} \sim \left(\frac{L^2}{\epsilon} \right)^{1/3}$$

L , U - eddy length scale and velocity, ϵ - turbulence dissipation rate

for $\epsilon = 100 \text{ cm}^2\text{s}^{-3}$:

$$\begin{aligned} \tau_t &\approx 0.2 \text{ s for } L = 1 \text{ cm} \\ \tau_t &\approx 5 \text{ s for } L = 1 \text{ m} \\ \tau_t &\approx 100 \text{ s for } L = 100 \text{ m} \end{aligned}$$

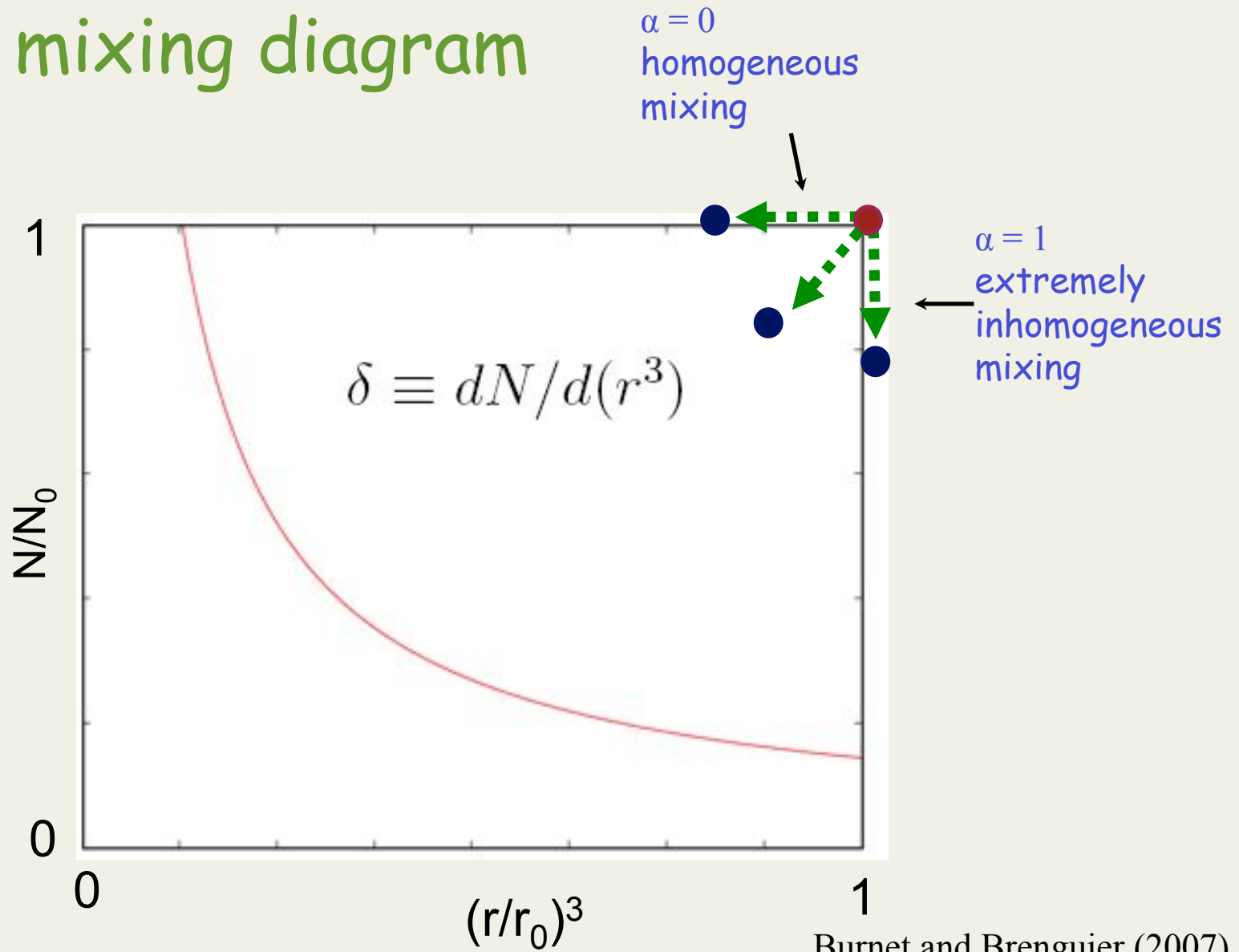


Extremely inhomogeneous: droplet evaporation much faster than turbulent mixing

Inhomogeneous; DNS simulations (Andrejczuk et al JAS 2004, 2006)

Homogeneous: turbulent mixing much faster than droplet evaporation

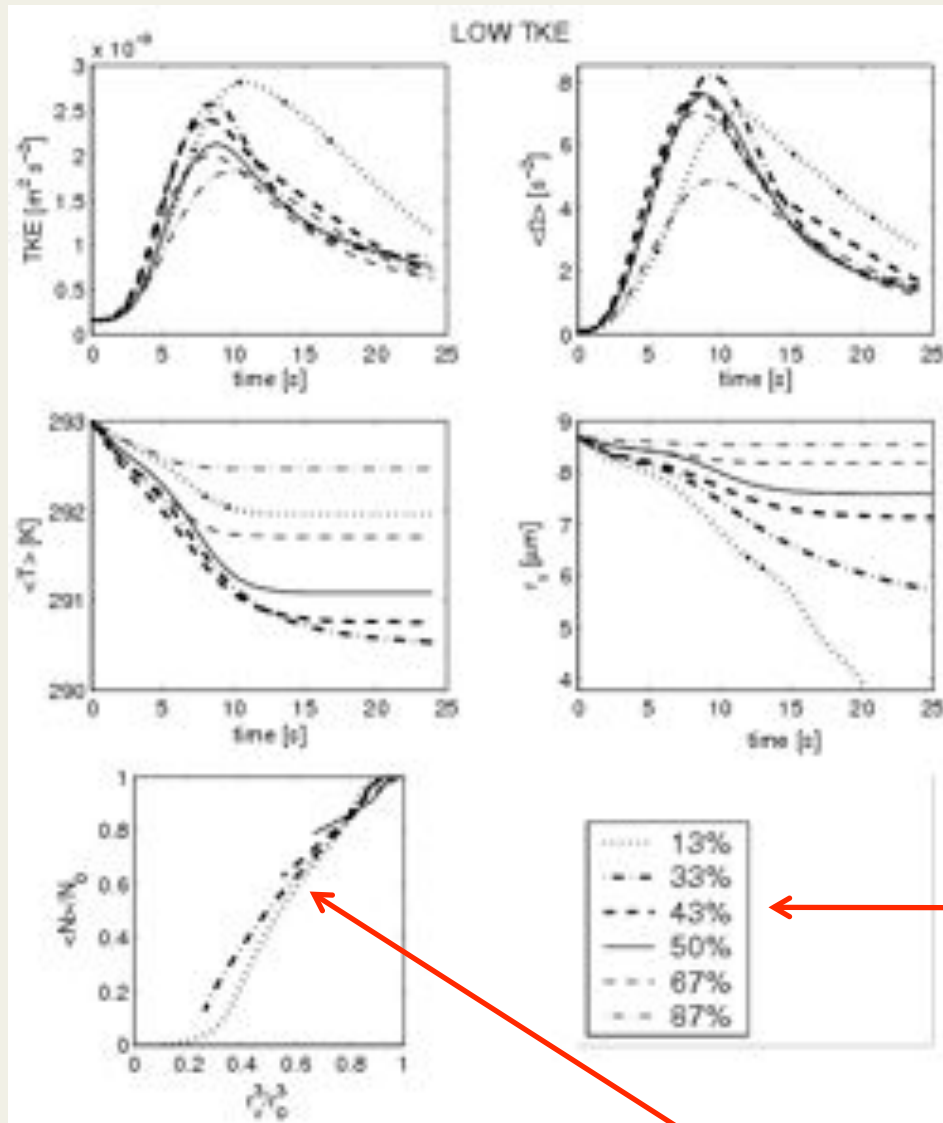
The mixing diagram



Burnet and Brenguier (2007)
Andrejczuk et al. (2006)

DNS simulations of microscale homogenization of initially separate filaments of cloudy and cloud-free air.

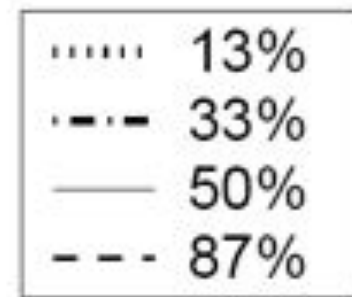
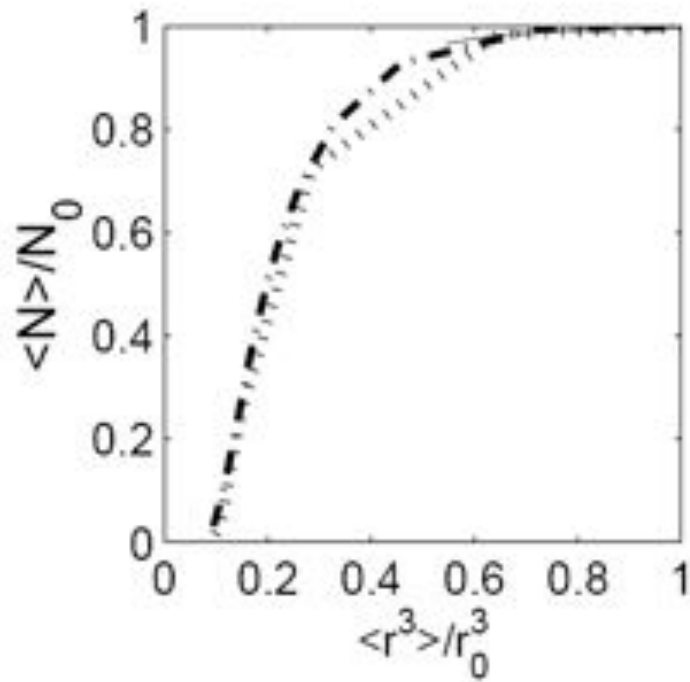
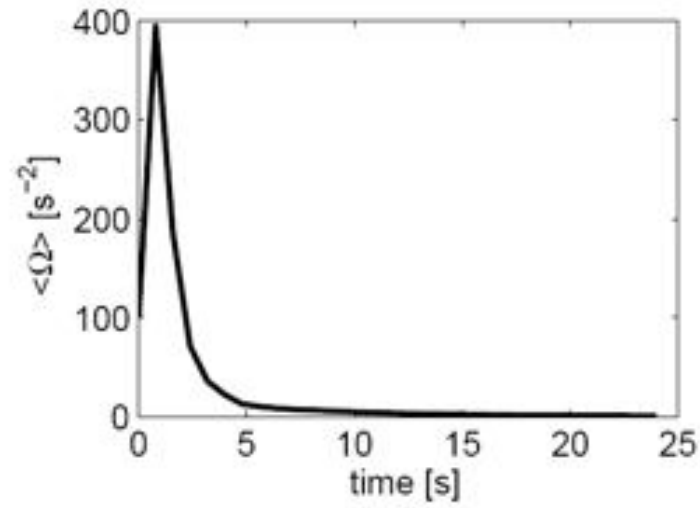
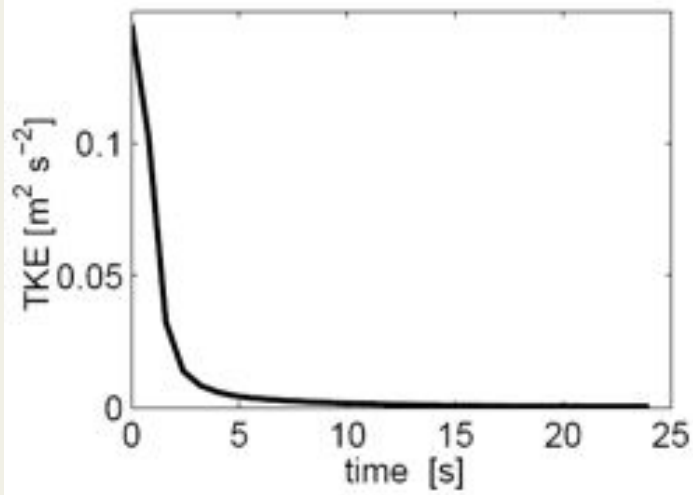
Andrejczuk et al JAS 2006



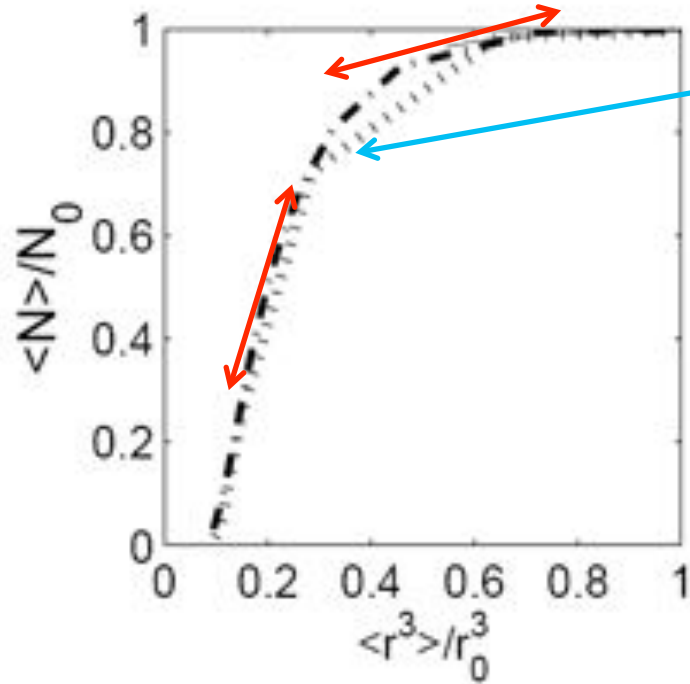
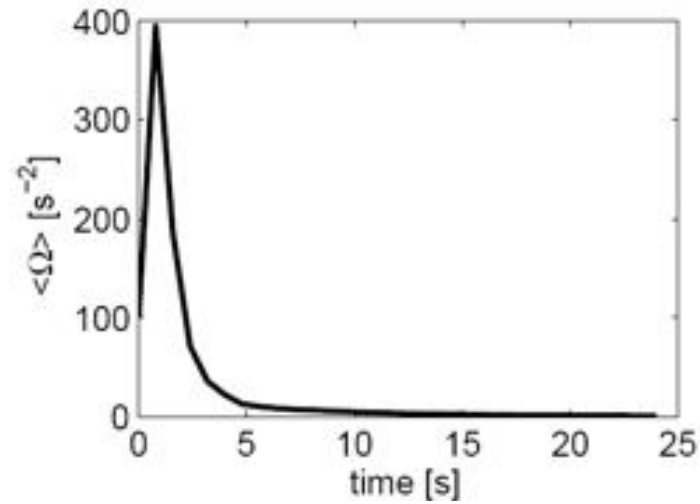
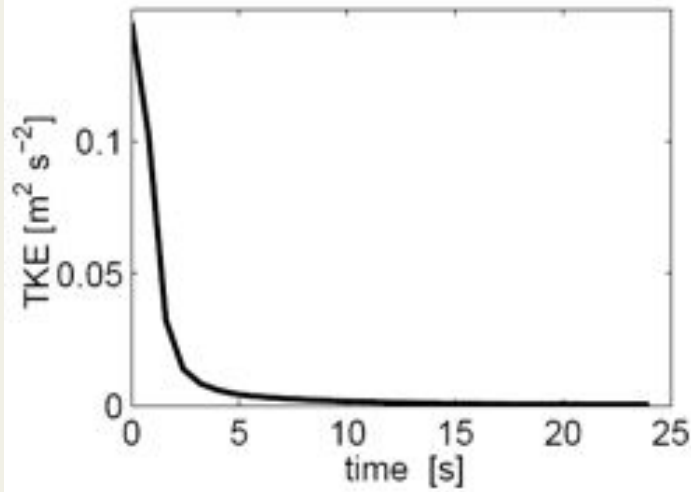
The percentage represents the initial volume fraction of cloudy air.

Evolution of the number of droplets N and their mean volume radius r_v , both normalized by the initial values

HIGH TKE

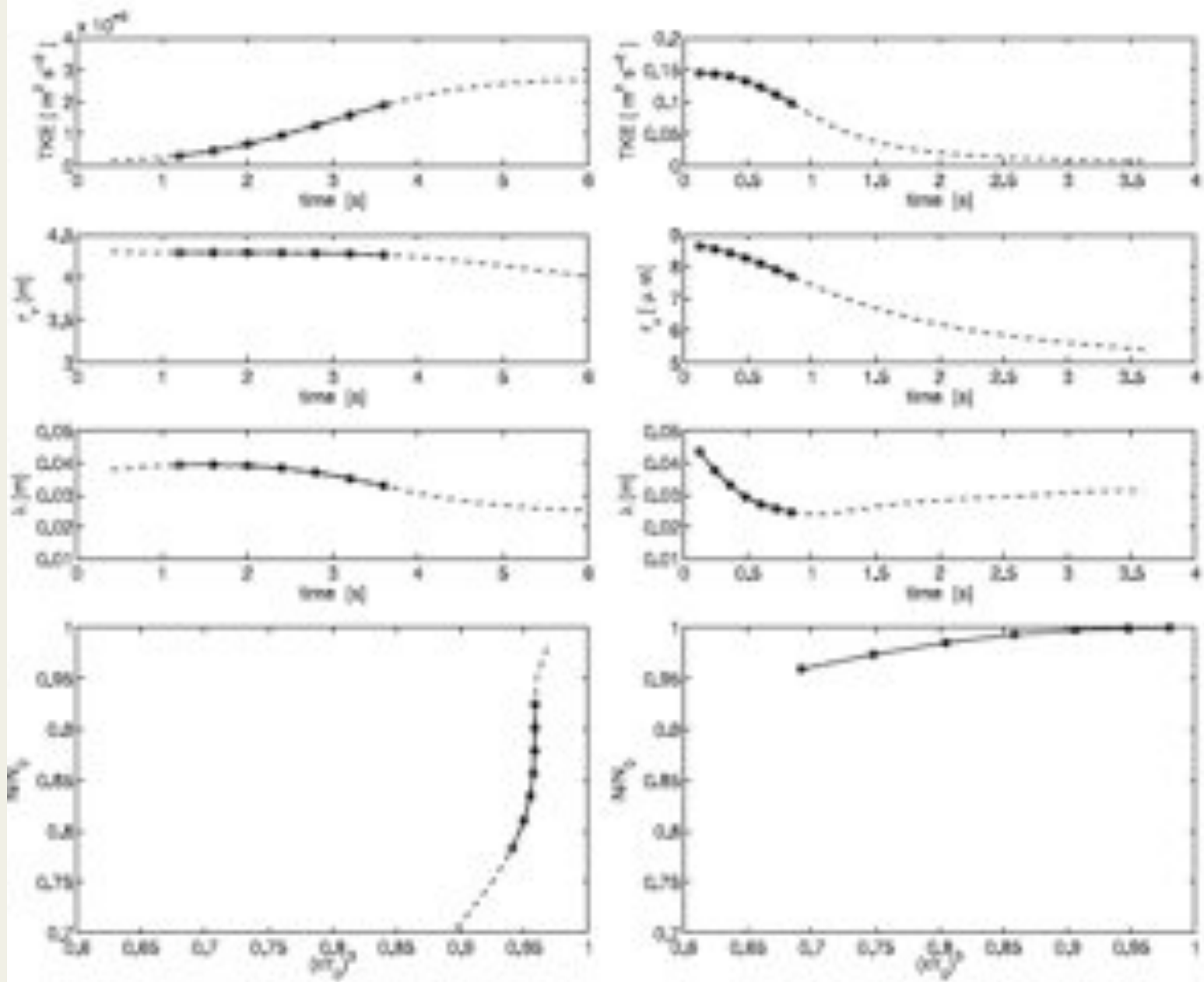


HIGH TKE

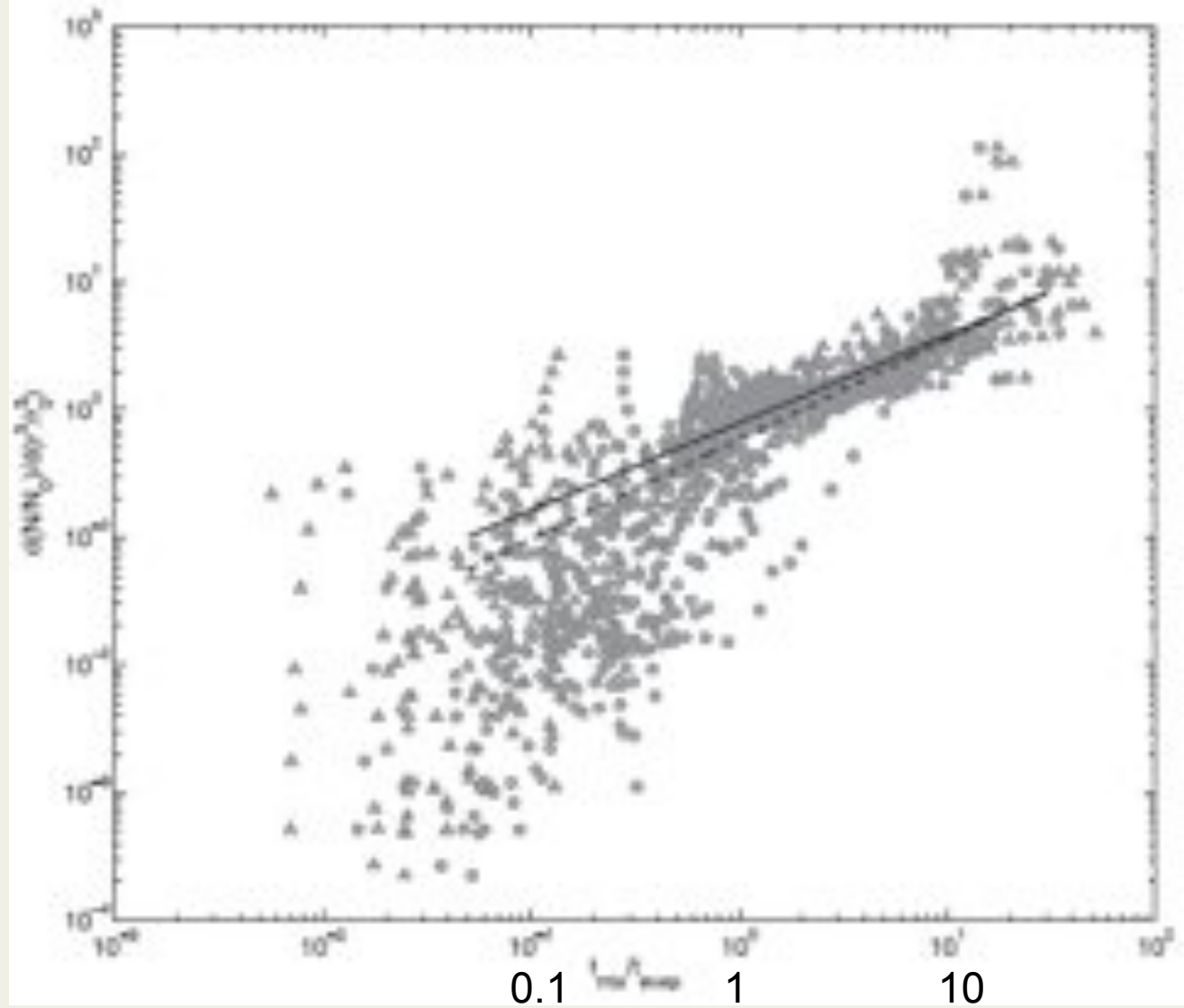


$$\delta = \frac{d(N_*)}{d(r_*^3)}$$

.....	13%
- . - .	33%
—	50%
- - -	87%



↑ slope 10
↓ 0.1



← homogeneous

→ extremely inhomogeneous

$t_{\text{mix}}/t_{\text{evap}}$ (Damkohler number)

Andrejczuk et al. JAS 2009

slope of the mixing line on the $N - r$ diagram:

$$\delta = \frac{d(N_*)}{d(r_*)}$$

$\delta = 0$ - homogeneous mixing

$\delta \rightarrow \infty$ - extremely inhomogeneous mixing

relationship between parameter α (homogeneity of mixing in the two-moment bulk scheme of Morrison and Grabowski 2008) and δ :

$$\alpha = \frac{\delta}{\delta + 1}$$

$\alpha = 0$ - homogeneous mixing

$\alpha = 1$ - extremely inhomogeneous mixing

A Large Eddy Simulation Intercomparison Study of Shallow Cumulus Convection

JAS
2003

A. PIER SIEBESMA,¹ CHRISTOPHER S. BRETHERTON,² ANDREW BROWN,² ANDREAS CHLOND,⁴ JOAN CUXART,⁶
PETER G. DUYNKERKE,^{1*} HONGLI JIANG,² MARAT KHAIROUTDINOV,³ DAVID LEWELLEN,¹ CHIN-HOH MOENG,⁷
ENRIQUE SANCHEZ,⁵ BJORN STEVENS,¹ AND DAVID E. STEVENS^{8*}

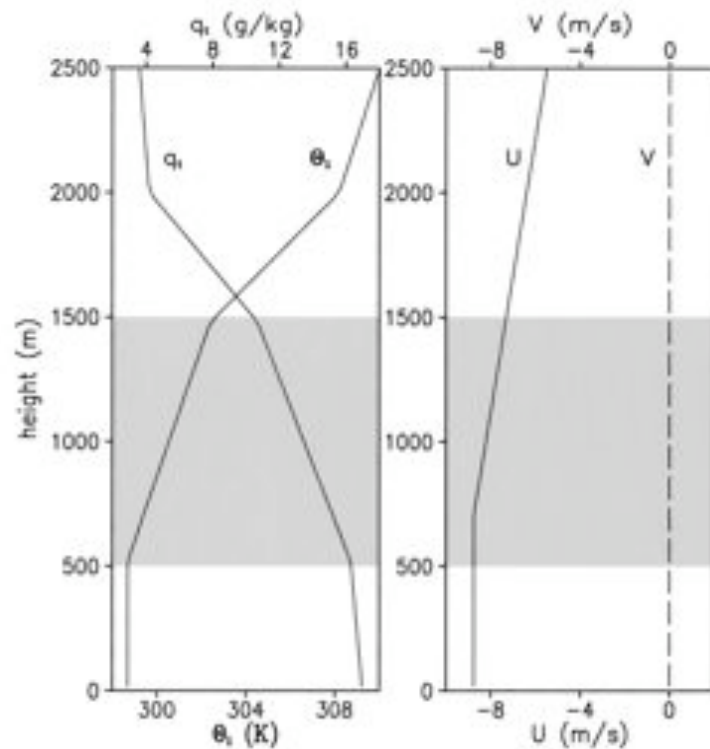
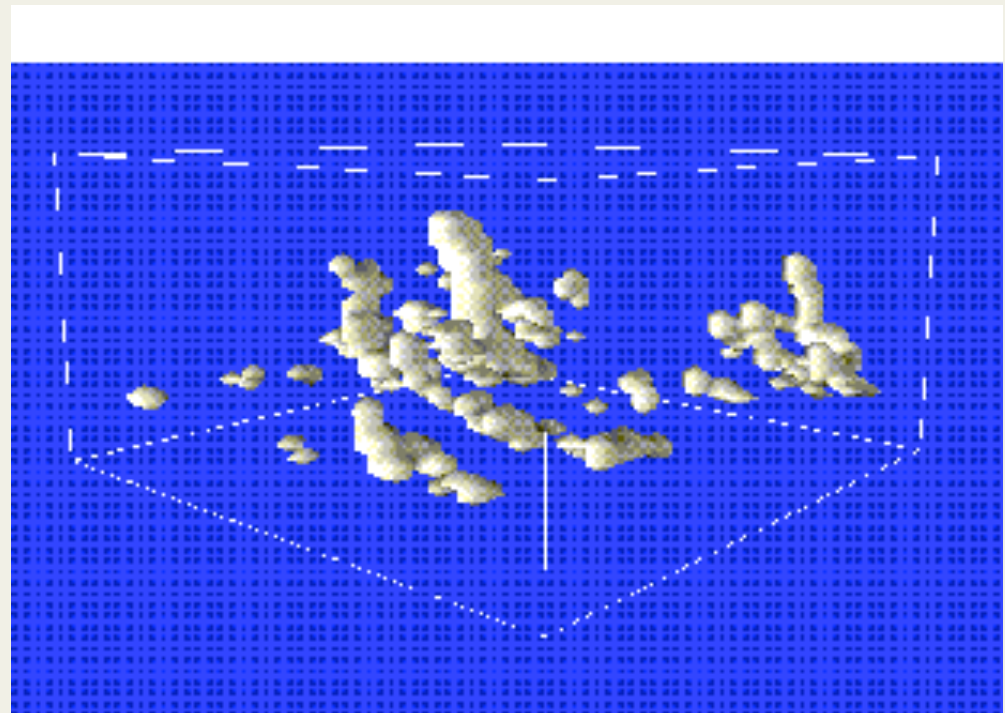
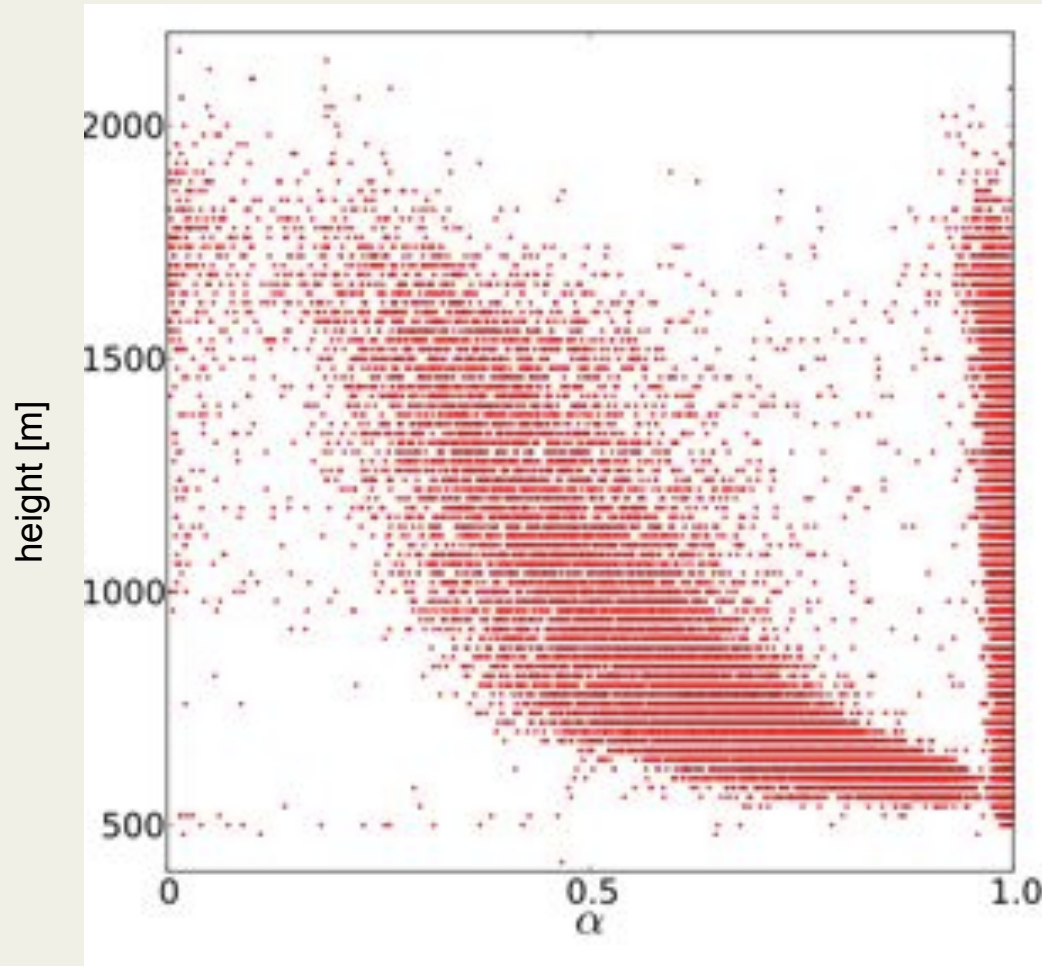


FIG. 1. Initial profiles of the total water specific humidity q_t , the liquid water potential temperature θ_l , and the horizontal wind components u and v . The shaded area denotes the conditionally unstable cloud layer.



Changes of the parameter α with height



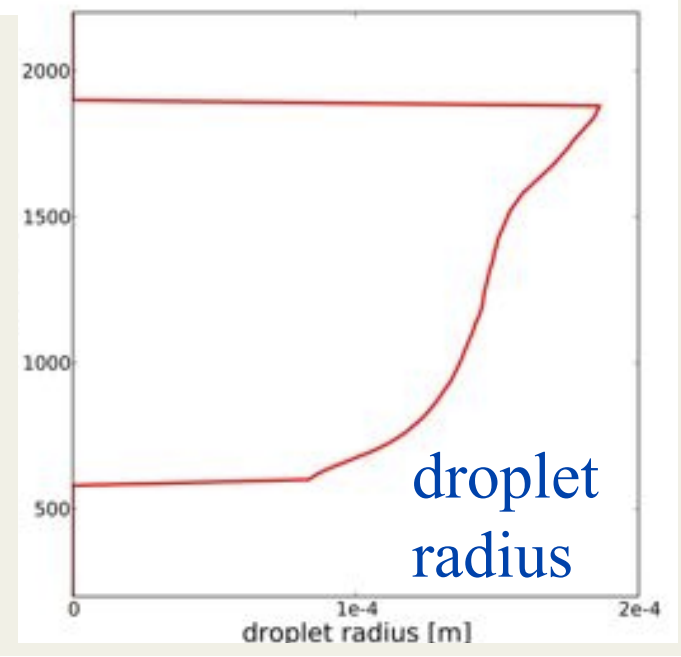
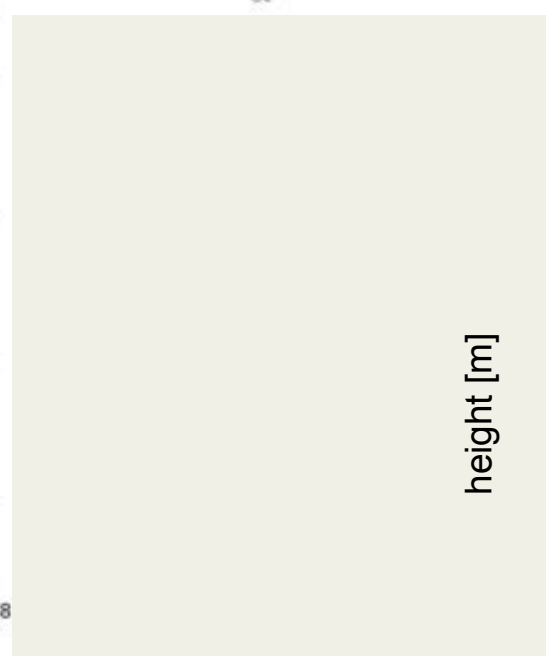
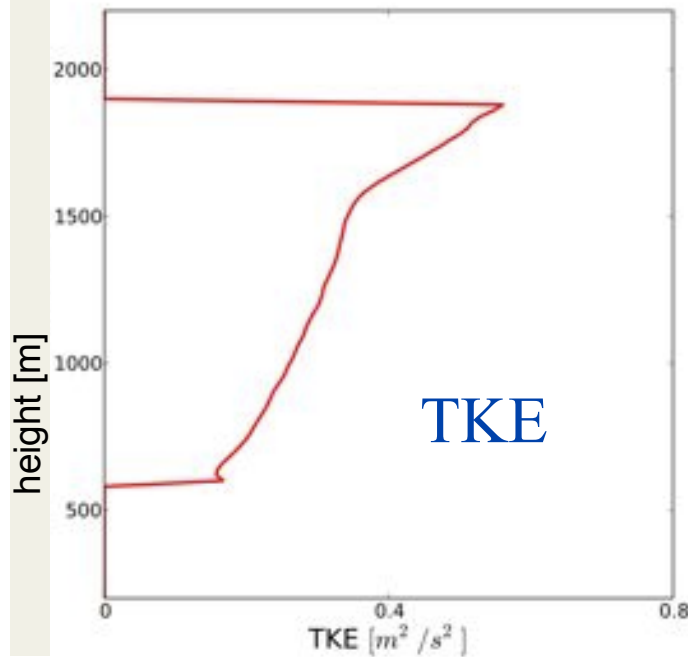
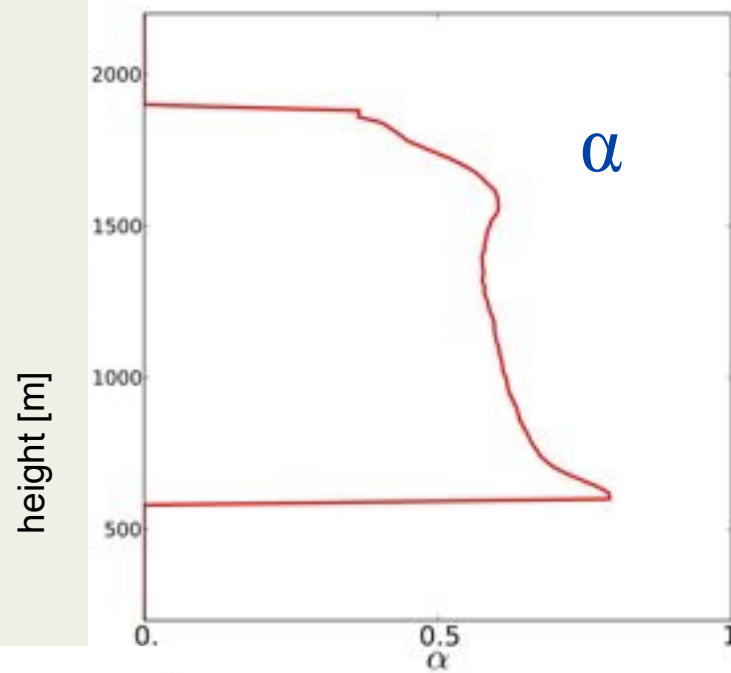
D. Jarecka
(PhD work
in progress)

$\alpha = 0$
homogeneous
mixing

$\alpha = 1$
extremely
inhomogeneous mixing

Vertical profiles of α , droplet radius and TKE

D. Jarecka
(PhD work
in progress)



Summary:

Small-scale turbulence seems to have insignificant effect on diffusional growth of cloud droplets

(It plays some role when entrainment and mixing is considered, a subject I did not address).

Small-scale turbulence appears to have significant effect on collisional growth. Not only rain forms earlier (an aspect emphasized by some...), but also turbulent clouds can rain more. More realistic studies are needed to quantify this aspect.

Effects of entrainment and mixing on evaporation of cloud droplets (homogeneous versus inhomogeneous mixing) - and its effect on albedo on the cloud field – can be quantified using the LES approach with the parameterization developed using DNS simulations.